



Université Libre de Bruxelles  
Faculté des Sciences Appliquées  
Service de Métrologie Nucléaire, C.P. 165/84  
50, Av. F.D.Roosevelt  
B-1050 Bruxelles

## TRACKS - Version 1.0

A non-analog Monte Carlo transport code for  
the risk assessment of radioactive repository sites

---

USER ' S GUIDE

July 2003

---

Author : M. Magolu monga Made

Supervisors : R. Beauwens and A. Dubus

Funded by : NIRAS/ONDRAF , Belgium

---

Industrial Collaborator : O. Smidts (AVN)

Université Libre de Bruxelles  
Faculté des Sciences Appliquées  
Service de Métrologie Nucléaire, C.P. 165/84  
50, Av. F.D.Roosevelt  
B-1050 Bruxelles

**TRACKS - Version 1.0**

**A non-analog Monte Carlo transport code for  
the risk assessment of radioactive repository sites**

---

**User ' s Guide**

July 2003

---

## Abstract

This report describes the transport simulation code TRACKS which stands for “*Transport of RAdionuclide Chains by nonanalog particle tracKings in Stochastic media”. The present version, which is written in standard FORTRAN 77, is a self-contained code that can be run on any platform. It has been elaborated thanks to the financial support of NIRAS/ONDRAF, the Belgian Agency for Radioactive Waste and Enriched Fissile Materials.*

The manual is mainly intended to be a practical guide that shows the user how to introduce the input data, and how to read the results produced by the code. For completeness, a short background on the mathematical foundation of the approach used is included. Then follows a technical description of the code. Illustrative sample problems are provided. The code is designed primarily to handle three-dimensional models. There is however an option for solving one-dimensional problems.

We would like to acknowledge that this work has benefited from the useful discussions with Jan Marivoet and Xavier Xillen from the Research Unit Waste and Disposal of the SCK/CEN, the Belgian Center for Nuclear Research.

---

## Copyright information and disclaimer

TRACKS package (code and manual), and any modified version, may not be distributed or used in a commercial package without the prior explicit written consent of the Head of Nuclear Metrology Department (Service de Métrologie Nucléaire, Université Libre de Bruxelles). The copyright notice must not be removed or altered in any way. The notice must accompany the package in any approved copy.

This software could be used in research applications for comparison purposes or for evaluation. No guarantee is made whatsoever about the accuracy of any results obtained from the code. The code is provided on an “as is” basis, without any warranty of any kind, either expressed or implied. This manual and the software will evolve to address new options, and therefore are subject to change without notice. Comments, bugs and suggestions should be reported to *magolu@ulb.ac.be*.

©

**Université Libre de Bruxelles  
Faculté des Sciences Appliquées  
Service de Métrologie Nucléaire, C.P. 165/84  
50, Av. F.D.Roosevelt  
B-1050 Bruxelles**

---

# Contents

<b>Abstract</b> .....	<b>i</b>
<b>Copyright information and disclaimer</b> .....	<b>ii</b>
<b>List of Figures</b> .....	<b>v</b>
<b>List of Tables</b> .....	<b>vi</b>
<b>1 Introduction</b> .....	<b>1</b>
<b>2 Theoretical Background</b> .....	<b>3</b>
2.1 The governing equations .....	3
2.1.1 The advection-dispersion equations .....	3
2.1.2 The boundary conditions .....	7
2.1.3 The source term .....	7
2.2 The integral formulation .....	8
2.3 The Monte Carlo method .....	11
2.3.1 Monte Carlo calculation of Volterra integral equations .....	11
2.3.2 Examples of pay-off functions .....	13
2.3.3 Sampling from non-uniform densities .....	14
<b>3 Overview of The Simulation Method</b> .....	<b>19</b>
3.1 Transition probabilities .....	19
3.2 Transition densities .....	21
3.3 Random walk methodology .....	22
3.4 Activities at points and on surfaces .....	23
<b>4 Code Structure</b> .....	<b>30</b>
4.1 General information .....	30
4.2 TRACKS package .....	32
4.3 Program description .....	34
4.4 Input data structure .....	37
4.4.1 Description of input variables .....	37
4.4.2 Sample input file .....	45
4.5 Output structure .....	49
4.5.1 The intermediate results files .....	50
4.5.2 The results files .....	53

---

<b>5</b>	<b>Examples of application</b>	<b>55</b>
5.1	A 3D clay-sand geological model	55
5.1.1	A simplified probabilistic risk assessment (PRA)	56
5.1.2	A deterministic analysis	59
5.2	A deterministic 1D transport model	64
5.2.1	Description of the problem	64
5.2.2	Numerical results	67
<b>6</b>	<b>Concluding remarks and Perspectives</b>	<b>76</b>
	<b>References</b>	<b>78</b>
	<b>Appendices</b>	<b>82</b>
<b>A</b>	<b>The adjoint reference equation parameters</b>	<b>82</b>
<b>B</b>	<b>Examples of adjoint reference solution</b>	<b>84</b>
<b>C</b>	<b>Monte Carlo calculation of integrals</b>	<b>87</b>
<b>D</b>	<b>Double randomization technique</b>	<b>90</b>
D.1	Brief description	90
D.2	Implementation in TRACKS	91
D.3	Sampling of retardation factors	92

---

# List of Figures

2.1	Illustration of the rejection method . . . . .	16
3.1	Branchings view of the random walks for one radionuclide. Transition: Position 1 → Position 2. The simulation ends at symbol “×”. . . . .	27
3.2	General flow-chart of the Monte Carlo simulation for the evaluation of local-wise cumulative activities . . . . .	28
4.1	Physical domain . . . . .	31
4.2	Flow-chart of TRACKS main modules . . . . .	38
4.3	Output structure. $ivisUS = 0$ , $ivisPL = 3$ , $ivisPT = 3$ , and $instant = 0$ . . . . .	51
4.4	Output structure. $ivisUS = 0$ , $ivisPL = 0$ , $ivisPT = 3$ , and $instant = 3$ . . . . .	52
5.1	Relative frequency of cumulative activity near the interface between clay and sand layers. $N_p$ values of retardation factors are sampled from log-normal pdfs. Here, $iclass = 0$ and $dclass = 20$ . $M$ denotes the batch size. . . . .	60
5.2	Relative frequency of cumulative activity near the interface between clay and sand layers. $N_p$ values of retardation factors are sampled from log-normal pdfs. Here, $iclass = 0$ and $dclass = 40$ . $M$ denotes the batch size. . . . .	61
5.3	Complementary cumulative (activity) distribution function near the interface between clay and sand layers. $N_p$ values of retardation factors are sampled from log-normal pdfs. $M$ denotes the batch size. . . . .	62
5.4	1D deterministic model. Concentration profile for $^{234}U$ at $z = 10\,000\,m$ . . . . .	69
5.5	1D deterministic model. Concentration profile for $^{230}Th$ at $z = 10\,000\,m$ . . . . .	69
5.6	1D deterministic model. Concentration profile for $^{226}Ra$ at $z = 10\,000\,m$ . . . . .	70
5.7	1D deterministic model. Cumulative concentration profile for $^{234}U$ at $z = 10\,000\,m$ . . . . .	70
5.8	1D deterministic model. Cumulative concentration profile for $^{230}Th$ at $z = 10\,000\,m$ . . . . .	71
5.9	1D deterministic model. Cumulative concentration profile for $^{226}Ra$ at $z = 10\,000\,m$ . . . . .	71
5.10	1D deterministic model. Concentration profile for $^{234}U$ at $z = 1\,000\,m$ . . . . .	72
5.11	1D deterministic model. Concentration profile for $^{230}Th$ at $z = 1\,000\,m$ . . . . .	72
5.12	1D deterministic model. Concentration profile for $^{226}Ra$ at $z = 1\,000\,m$ . . . . .	73
5.13	1D deterministic model. Concentration profile for $^{234}U$ at $z = 100\,m$ . . . . .	73
5.14	1D deterministic model. Concentration profile for $^{230}Th$ at $z = 100\,m$ . . . . .	74
5.15	1D deterministic model. Concentration profile for $^{226}Ra$ at $z = 100\,m$ . . . . .	74
5.16	1D deterministic model. Cumulative concentration profiles for $^{234}U$ , $^{230}Th$ and $^{226}Ra$ at $z = 100\,m$ . Comparison between TRACKS scores and the analytical solutions . . . . .	75

---

# List of Tables

2.1	Parameters system of units. L=length, M=mass, T=time unit. . . . .	6
5.1	Half-life times ( $T_{\frac{1}{2}}$ ) in years and retardation factors ( $R_i$ ) of $^{240}\text{Pu}$ and $^{236}\text{U}$ in the clay and the sand layer. . . . .	64
5.2	Half-life times ( $T_{\frac{1}{2}}$ , in <i>yr</i> ), radioactive decay rates ( $\lambda_i$ , in $\text{yr}^{-1}$ ), and retardation factors ( $R_i$ ) of radionuclides $^{234}\text{U}$ , $^{230}\text{Th}$ , and $^{226}\text{Ra}$ . Darcy velocity, porosity, molecular diffusion and dispersivity. . . . .	66
5.3	1D deterministic model. Comparison between TRACKS scores and analytical solutions (ANASOL) at $z = 1000\text{ m}$ and $t = t_2$ . Instantaneous concentrations and cumulative concentrations. . . . .	68
D.1	Means and standard deviations of the log-normal pdfs for the retardation factors of $^{240}\text{Pu}$ and $^{236}\text{U}$ in clay and sand . . . . .	93



# Chapter 1

## Introduction

---

---

The objective of the disposal of radioactive waste in deep geological media is to isolate medium- and high-level waste from the biosphere until radioactivity has gone under acceptable levels [26,27,30]. This may take thousands of years [3,17,25]. In order to assess the risk for such radioactive particles from waste repositories to contaminate the geological environment with polluted ground-water, the governing (partial differential) advection-dispersion transport equations could be transformed into integral equation, which in turn is solved by means of Monte Carlo method. This results in a so-called non-analog Monte Carlo simulation method. The reason why Monte Carlo integration method is preferred to classical numerical integration methods is that the number of integration variables is large ( $\gg 5$ ), especially when one has to take uncertainty into account. It is well known that in such cases Monte Carlo method is more efficient than classical techniques [18,20].

Non-analog Monte Carlo methods enable to estimate the concentrations of contaminants at specific local areas of the geological medium, for instance at the interface between two different geological layers, without finding the whole solution field [33,34,35,36]. This contrasts with classical numerical (finite element, finite difference, finite volume) methods where one has to handle the whole physical domain, giving rise to both memory and time consuming computations, in particular in the case of three-dimensional models, or when a stochastic uncertainty analysis is required in order to take into account the uncertainty of the parameters involved [8,22,31,45]. In analog Monte Carlo methods, transport mechanisms like advection by ground-water, molecular diffusion, mechanical dispersion, adsorption and desorption by the host rock, radioactive decay, etc ..., undergone by particles, are directly simulated according to the natural process probabilities. This approach suffers not only from unacceptably large statistical uncertainty, but also from very long computing times because of the interactions of all phenomena involved [20].

In this report, we give a description of TRACKS.1.0, a modular and portable self-contained version of the transport simulation code TRACKS. The acronym TRACKS

stands for “*Transport of RAdionuclide Chains by non-analog particle tracKings in Stochastic media”. TRACKS is a three-dimensional transport code written in standard FORTRAN 77 programming language. It has been initially developed by Olivier Smidts within the framework of his Ph.D. thesis in the Service de Métrologie Nucléaire at the Université Libre de Bruxelles [33]. The present version is an improved modular variant that can be run on any platform.*

The manual is organized as follows. In Chapter 2, we summarize the theoretical basis behind the approach followed in the code. This includes the governing equations, its integral formulation and a brief description of the Monte Carlo methodology. Chapter 3 describes how the Monte Carlo method is applied to solve the integral equations involved. In Chapter 4, a general description of the code is provided, as well as the input data format, the output structure, and the instructions for running the code. Illustrative sample problems are discussed in Chapter 5. Some concluding remarks are reported in Chapter 6, which also summarizes some theoretical and numerical aspects that are under investigation. The appendices include information useful to understand the theoretical approach followed in TRACKS.

## Chapter 2

# Theoretical Background

---

We consider the transport of radionuclide chains in a water saturated porous three-dimensional medium. The physical transport mechanisms taken into consideration are advection by ground-water, molecular diffusion, and mechanical dispersion. The chemical reactions modeled are the adsorption and the desorption of particles by the host rock, and the radioactive decay. We assume a linear and instantaneous equilibrium between species in the liquid and the solid phases.

## 2.1 The governing equations

### 2.1.1 The advection-dispersion equations

The transport of radionuclide chains satisfy the following coupled advection-dispersion partial differential equations (PDEs) [4,5,8,10,11]

$$\mathcal{L}_i A(\bar{r}', t'; i) = \tilde{S}(\bar{r}', t'; i) \quad \text{in } \mathcal{D} \subset \mathcal{R}^3 \quad \text{for } i=1, \dots, N_r \quad (2.1)$$

with

$$\mathcal{L}_i = \left\{ \frac{\partial}{\partial t'} [\omega_i(\bar{r}') \cdot] + \bar{\nabla}_{\bar{r}'} [\bar{q}(\bar{r}') \cdot] - \bar{\nabla}_{\bar{r}'} \left[ \bar{D}(\bar{r}') \bar{\nabla}_{\bar{r}'} \cdot \right] + \lambda_i \omega_i(\bar{r}') \cdot \right\} \quad (2.2)$$

$$\tilde{S}(\bar{r}', t'; i) = S(\bar{r}', t'; i) + \sum_{\substack{j=1 \\ j \neq i}}^{N_r} \frac{\lambda_i}{\lambda_j} p(j \rightarrow i) \omega_j(\bar{r}') A(\bar{r}', t'; j) \quad (2.3)$$

$$\omega_i(\bar{r}') = \theta(\bar{r}') R_i(\bar{r}') \quad (2.4)$$

$$A(\bar{r}', t'; i) = \lambda_i C(\bar{r}', t'; i) \quad (2.5)$$

$$\bar{\bar{D}}(\bar{r}') = \theta(\bar{r}') \bar{\bar{D}}_H(\bar{r}') = \theta(\bar{r}') \left( \bar{\bar{D}}_m(\bar{r}') + \bar{\bar{D}}_c(\bar{r}') \right) \quad (2.6)$$

$$\lambda_j = \sum_{i=1}^{N_r} p(j \rightarrow i) \quad (2.7)$$

where (see Table 2.1 for the units of measure)

$\mathcal{D}$  = the geological domain

$\bar{r}'$  = three-dimensional variable ( $x', y', z'$ )

$t'$  = time variable

$N_r$  = number of radionuclides in the chain

$C(\bar{r}', t'; i)$  = concentration of radionuclide  $i$

$A(\bar{r}', t'; i)$  = activity of radionuclide  $i$

$\theta(\bar{r}')$  = porosity

$R_i(\bar{r}')$  = retardation factor of radionuclide  $i$

$\bar{q}(\bar{r}')$  = Darcy velocity ( $\bar{v}(\bar{r}') = \frac{\bar{q}(\bar{r}')}{\theta(\bar{r}')} =$  advection velocity)

$\lambda_i$  = radioactive decay constant of radionuclide  $i$

$\bar{\bar{D}}(\bar{r}')$  = diffusion-dispersion tensor

$\bar{\bar{D}}_H(\bar{r}')$  = hydrodynamic diffusion-dispersion tensor

$\bar{\bar{D}}_m(\bar{r}')$  = molecular diffusion tensor

$\bar{\bar{D}}_c(\bar{r}')$  = cinematic dispersion tensor

$S(\bar{r}', t'; i)$  = source term of radionuclide  $i$

$p(j \rightarrow i)$  = transition rate from radionuclide  $j$  to radionuclide  $i$

The components of the cinematic (or mechanical) dispersion tensor may be approximated as follows [8,17], where  $z$  denotes the vertical axis:

$$\overline{\overline{D}}_c = \begin{bmatrix} D_{xx} & D_{xy} & D_{xz} \\ D_{yx} & D_{yy} & D_{yz} \\ D_{zx} & D_{zy} & D_{zz} \end{bmatrix} \quad (2.8)$$

with

$$\begin{aligned} D_{xx} &= \alpha_L \frac{\nu_x^2}{\|\vec{\nu}\|} + \alpha_{TH} \frac{\nu_y^2}{\|\vec{\nu}\|} + \alpha_{TV} \frac{\nu_z^2}{\|\vec{\nu}\|} \\ D_{yy} &= \alpha_L \frac{\nu_y^2}{\|\vec{\nu}\|} + \alpha_{TH} \frac{\nu_x^2}{\|\vec{\nu}\|} + \alpha_{TV} \frac{\nu_z^2}{\|\vec{\nu}\|} \\ D_{zz} &= \alpha_L \frac{\nu_z^2}{\|\vec{\nu}\|} + \alpha_{TV} \frac{\nu_x^2}{\|\vec{\nu}\|} + \alpha_{TV} \frac{\nu_y^2}{\|\vec{\nu}\|} \\ D_{xy} &= D_{yx} = (\alpha_L - \alpha_{TH}) \frac{\nu_x \nu_y}{\|\vec{\nu}\|} \\ D_{xz} &= D_{zx} = (\alpha_L - \alpha_{TV}) \frac{\nu_x \nu_z}{\|\vec{\nu}\|} \\ D_{yz} &= D_{zy} = (\alpha_L - \alpha_{TH}) \frac{\nu_y \nu_z}{\|\vec{\nu}\|} \end{aligned} \quad (2.9)$$

where

$\alpha_L$  = longitudinal dispersivity

$\alpha_{TH}$  = horizontal transverse dispersivity

$\alpha_{TV}$  = vertical transverse dispersivity

$\bar{v}$  =  $(v_x, v_y, v_z)$  = pore velocity

$\|\bar{v}\|$  =  $\sqrt{v_x^2 + v_y^2 + v_z^2}$

Table 2.1: Parameters system of units. L=length, M=mass, T=time unit. 1 Bq = 1 dps. The abbreviation dps (dpy) means disintegrations per second (year).

SYMBOLS	MEANING	UNITS		
		GENERIC	SYSTEM OF UNITS	OTHER
$\bar{r} = (x, y, z)$	distance along the axes	L	m	-
$t$	temporal variable (time)	T	s	yr (year)
$C(\dots)$	concentration	$M L^{-3}$	$kg/m^3$	$mol/m^3$
$A(\dots)$	activity	$M L^{-3} T^{-1}$	$kg/(m^3 s)$	$Bq/m^3$
$\theta(\bar{r})$	porosity	-	-	-
$R_i(\dots)$	retardation factor	-	-	-
$\bar{q} (\bar{v})$	Darcy (pore) velocity	$L T^{-1}$	$m/s$	$m/yr$
$\lambda_i$	radioactive decay constant	$T^{-1}$	$1/s$	$/yr$
$D_{i,j}$	diffusion or dispersion coefficients	$L^2 T^{-1}$	$m^2/s$	$m^2/yr$
$S(\dots)$	source term	$M L^{-3} T^{-1}$	$kg/(m^3 s)$	$kg/(m^3 yr)$
$\alpha_L, \alpha_{TH}, \alpha_{TV}$	dispersivity coefficients	$L$	$m$	-

## 2.1.2 The boundary conditions

We assume that the total (normal) flux of radionuclides crossing the surface  $\mathcal{S}$  (bounding the geological domain  $\mathcal{D}$ ) is known and represented by a specified function  $\beta(\bar{r}', t'; i)$ . This means that Equations (2.1)-(2.7) are submitted to the following conditions on  $\mathcal{S}$ :

$$\bar{n} \left\{ -\overline{D}(\bar{r}') \overline{\nabla}_{\bar{r}'} A(\bar{r}', t'; i) + \bar{q}(\bar{r}') A(\bar{r}', t'; i) \right\} = \beta(\bar{r}', t'; i) \quad \forall \bar{r}' \in \mathcal{S} \quad \forall i, 1 \leq i \leq N_r \quad (2.10)$$

where  $\bar{n}$  denotes the outward normal on  $\mathcal{S}$ .

## 2.1.3 The source term

We consider a point source located at  $\bar{r}_s = (x_s, y_s, z_s)$  inside  $\mathcal{D}$  with either a pulse release of radionuclides at time  $t_s$ , or a band release of radionuclides from time  $t_s$  to time  $t_s + T$ . The corresponding source term for radionuclide  $i$  is given by:

$$S(\bar{r}', t'; i) = \begin{cases} s_i \delta(\bar{r}' - \bar{r}_s) \delta(t' - t_s) & \text{if pulse release} \\ B_i(t') [H(t' - t_s) - H(t' - t_s - T)] \delta(\bar{r}' - \bar{r}_s) & \text{if band release} \end{cases} \quad (2.11)$$

with

$s_i$  = intensity of radionuclide  $i$  in the source

$T$  = duration of the release

$\delta$  = Dirac function

$H$  = Heaviside step function ( $H(t) = 1 \quad \forall t \geq 0$  and  $H(t) = 0 \quad \forall t < 0$ )

$B_i$  = Bateman functions

One has [13]

$$B_i(t') = \sum_{j=1}^i b_{ji} e^{-\lambda_j t'} \quad (2.12)$$

where the coefficients  $b_{ji}$  are constants depending on the radioactive decay constants and the initial activities of radionuclides in the source. For the first three elements of a radionuclide chain, we have the following definitions of  $b_{ji}$ :

$$\left\{ \begin{array}{l} b_{11} = A_1^0 \\ b_{12} = \frac{\lambda_2 A_1^0}{\lambda_2 - \lambda_1} \\ b_{13} = \frac{\lambda_2 \lambda_3 A_1^0}{(\lambda_3 - \lambda_1)(\lambda_2 - \lambda_1)} \\ b_{22} = A_2^0 - \frac{\lambda_2 A_1^0}{\lambda_2 - \lambda_1} \\ b_{23} = \frac{\lambda_3}{\lambda_3 - \lambda_2} \left( A_2^0 - \frac{\lambda_2 A_1^0}{\lambda_2 - \lambda_1} \right) \\ b_{33} = A_3^0 - \frac{\lambda_3}{\lambda_3 - \lambda_2} \left( A_2^0 - \frac{\lambda_2 A_1^0}{\lambda_2 - \lambda_1} \right) - \frac{\lambda_2 \lambda_3 A_1^0}{(\lambda_3 - \lambda_1)(\lambda_2 - \lambda_1)} \end{array} \right. \quad (2.13)$$

where  $A_j^0$  is the initial activity of the  $j$ th element in the radionuclide source. In the case of band release, the expression used accounts for a constant leaking of solute radionuclides from the repository. During the release time  $T$ , the isotopic composition of the radionuclides injected in the porous medium is evolving according to radioactive decay laws.

## 2.2 The integral formulation

The mathematical transformations have some similarities with those done in [29, pages 206-209] in a different context. One needs the following *adjoint reference equations*

$$\mathcal{L}_i^* C^*(\bar{r}', t'; i) = \delta(\bar{r}' - \bar{r}) \delta(t' - t) \quad \text{for } i=1, \dots, N_r \quad (2.14)$$

with

$$\mathcal{L}_i^* = -\omega_i^*(\bar{r}') \frac{\partial}{\partial t'} - \bar{q}^*(\bar{r}') \bar{\nabla}_{r'} \cdot - \bar{\nabla}_{r'} \cdot \left[ \bar{D}^*(\bar{r}') \bar{\nabla}_{r'} \cdot \right] + \lambda_i \omega_i^*(\bar{r}'). \quad (2.15)$$

where  $\delta$  denotes the Dirac function. Eqs. (2.14-2.15) is the adjoint of Eq. (2.1) with the following modifications:

1. The coefficients  $\omega_i(\bar{r}')$ ,  $\bar{q}(\bar{r}')$  and  $\bar{D}(\bar{r}')$  are replaced by  $\omega_i^*(\bar{r}')$ ,  $\bar{q}^*(\bar{r}')$  and  $\bar{D}^*(\bar{r}')$ , respectively. The choice of these latter functions of position  $\bar{r}'$ , which is guided by efficiency reasons of the Monte Carlo simulation [34,35,36], is briefly discussed in Appendix A.

2. The source, which is located at  $\bar{r}' = \bar{r}$ , is a unit pulse at time  $t' = t$ .

We assume that the *adjoint reference solutions*  $C^*$  of Eq. (2.14-2.15) in an infinite medium are known and written as  $C^*(\bar{r}', t'; i | \bar{r}, t; i)$  (see Appendix B for illustrative examples). On this basis, an integral formulation of the advection-dispersion boundary value problem (2.1)-(2.10) has been obtained in [33] (see also, [35, Appendix B and Eq. (19)]). The one-dimensional case is treated in detail in [34, Appendix B]. In our case, one gets a Volterra integral equation of the second kind, which may be written as follows:

$$u_S(\bar{r}) A(\bar{r}, t; i) = Q(\bar{r}, t; i) + \sum_{j=1}^{N_r} \int_{t-T_0}^t dt' \int_{\bar{D}} d\bar{r}' \mathcal{K}(\bar{r}', t'; j | \bar{r}, t; i) u_S(\bar{r}') A(\bar{r}', t'; j) \quad (2.16)$$

with

$$u_S(\bar{r}) = \begin{cases} \frac{1}{2} & \bar{r} \in \mathcal{S} \\ 1 & \bar{r} \in \mathcal{D} \end{cases} \quad (2.17)$$

and

$$\bar{D} = \mathcal{D} \cup \mathcal{S}$$

$$T_0 = \text{total simulation time}$$

$$\delta_{j,i} = \text{Kronecker symbol}$$

$$Q(\bar{r}, t; i) = \int_{t-T_0}^t \frac{T_0 - (t - t')}{T_0} dt' \int_{\bar{D}} C^*(\bar{r}', t'; i | \bar{r}, t; i) \{S(\bar{r}', t'; i) - \delta_2(\bar{r}' - \bar{r}'_S) \beta(\bar{r}', t'; i)\} d\bar{r}' \quad (2.18)$$

$$\mathcal{K}(\bar{r}', t'; j | \bar{r}, t; i) = K^{j \rightarrow j}(\bar{r}', t'; j | \bar{r}, t; i) \delta_{j,i} + K^{j \rightarrow i}(\bar{r}', t'; j | \bar{r}, t; i) (1 - \delta_{j,i}) \quad (2.19)$$

The symbol  $\delta_2$  denotes a two-dimensional Dirac function associated to the surface  $\mathcal{S}$ , while

$$K^{j \rightarrow j}(\bar{r}', t'; j | \bar{r}, t; i) = K_{\mathcal{D}}(\bar{r}', t'; j | \bar{r}, t; j) + \delta_2(\bar{r}' - \bar{r}'_{\mathcal{S}}) K_{\mathcal{S}}(\bar{r}', t'; j | \bar{r}, t; j) \quad (2.20)$$

$$K^{j \rightarrow i}(\bar{r}', t'; j | \bar{r}, t; i) = \omega_j(\bar{r}') \frac{\lambda_i}{\lambda_j} p(j \rightarrow i) \frac{T_0 - (t - t')}{T_0} C^*(\bar{r}', t'; i | \bar{r}, t; i) \frac{1}{u_{\mathcal{S}}(\bar{r}')$$

with

$$K_{\mathcal{D}}(\bar{r}', t'; j | \bar{r}, t; j) = \frac{1}{u_{\mathcal{S}} T_0} \left\{ \omega_j(\bar{r}') C^*(\bar{r}', t'; j | \bar{r}, t; j) + [T_0 - (t - t')] \right. \\ \left. \left[ \Delta \omega_j \frac{\partial C^*}{\partial t'} + \Delta \bar{q} \bar{\nabla}_{r'} C^* + \bar{\nabla}_{r'} \left( \Delta \bar{D} \bar{\nabla}_{r'} C^* \right) - \lambda_j \Delta \omega_j C^* \right] \right\} \quad (2.21)$$

$$K_{\mathcal{S}}(\bar{r}', t'; j | \bar{r}, t; j) = \frac{1}{T_0} [T_0 - (t - t')] \left[ -\bar{n} \bar{D}(\bar{r}') \bar{\nabla}_{r'} C^* \right] \frac{1}{u_{\mathcal{S}}(\bar{r}')} \quad (2.22)$$

where

$$\begin{aligned} \Delta \omega_j &= \omega_j(\bar{r}') - \omega_j^* \\ \Delta \bar{q} &= \bar{q}(\bar{r}') - \bar{q}^* \\ \Delta \bar{D} &= \bar{D}(\bar{r}') - \bar{D}^* \end{aligned} \quad (2.23)$$

We have the following observations:

1. The mathematical argument used in deriving the above integral formulation is valid only if both  $c(\bar{r}', t'; i)$  and  $C^*(\bar{r}', t'; i)$  are twice derivable. In the case of (strong) discontinuities, care should be taken to provide some appropriate treatment like in the classical finite difference approach.
2. We have to integrate both over the geological domain  $\mathcal{D}$  and over the surface  $\mathcal{S}$ . This will give rise to two types of particle trackings: a random walk inside the domain and another one over the boundary.
3. Let us interpret the sum  $\sum_{j=1}^{N_r}$  as a discretized version of a one-dimensional integral. Then, thanks to the integral formulation, the somewhat time- and memory-consuming problem of solving a system of coupled PDEs for the transport of a radionuclide chain

is reduced to solving one integral equation by Monte Carlo simulations in a continuous-discrete space  $(\bar{r}, t; i)$ .

4. The adjoint reference solution  $C^*(\bar{r}', t'; j | \bar{r}, t; j)$  appears explicitly in the second member of Eq. (2.16). A natural question that arises is how to interpret the role this solution plays in the simulation. Let us assume that the porous medium is a heterogeneous medium in which the retardation factor  $R_j$  and the Darcy velocity  $\bar{q}$  are random spatial variables. Assume further that we choose constant values for the coefficients  $R_j^*$  and  $\bar{q}^*$  involved in the adjoint reference equation. If these constant values correspond to, for instance, the spatial average of  $R_j$  and  $\bar{q}$  in the domain  $\mathcal{D}$ , then the procedure amounts to defining an adjoint reference solution  $C^*$  for the transport in an approximately equivalent homogeneous medium. The difference between the real heterogeneous medium and the approximately equivalent homogeneous medium are taken into account through the correction terms  $\Delta\omega_j$ ,  $\Delta\bar{q}$  and  $\Delta\bar{D}$ . The adjoint reference solution may be viewed as a guide for the Monte Carlo simulations like the importance function in neutrons transport [20]. In practice,  $C^*$  summarizes, between two successive positions of the random walker, the physico-chemical processes at the microscopic scale. This allows efficient simulations.
5. The source term  $Q(\bar{r}, t; i)$  includes the contributions of the independent source  $S(\bar{r}, t; j)$  and the normal incoming radionuclide flux  $-\delta_2(\bar{r}' - \bar{r}_S) \beta(\bar{r}', t'; j)$  on the outer surface  $\mathcal{S}$ . The integral kernels  $K^{j \rightarrow i}(\bar{r}', t'; j | \bar{r}, t; i)$  and  $K^{j \rightarrow j}(\bar{r}', t'; j | \bar{r}, t; i)$  clearly reflect the radionuclides undergoing a radioactive decay and those not undergoing a radioactive decay, respectively.
6. We stress that the radioactive transition between elements of the chain is not determined by exponential laws as for analog Monte Carlo methods. It is determined by the expressions of the integral kernels involved.

## 2.3 The Monte Carlo method

### 2.3.1 Monte Carlo calculation of Volterra integral equations

For simplicity, we consider the following Volterra integral equation:

$$c(\bar{r}, t) = Q(\bar{r}, t) + \int dt' \int d\bar{r}' K(\bar{r}', t' | \bar{r}, t) c(\bar{r}', t') \quad (2.24)$$

where  $\bar{r}$  is the position vector and  $t$  is time,  $c$  is the unknown function.  $Q$  is a given source term and  $K$  denotes the integral kernel of interest. We assume that a functional of the form of a weighted integral of  $c(\bar{r}, t)$  is the quantity to be determined. In other words, the task is to evaluate the functional [20]

$$J = \int dt \int d\bar{r} f(\bar{r}, t) c(\bar{r}, t) \quad (2.25)$$

where  $f(\bar{r}, t)$  is called the *pay-off function* of the functional.

We summarize briefly below how the quantity  $J$  is evaluated in practice by Monte Carlo simulations. The integral equation (2.24) is rewritten formally as

$$c = Q + \kappa c \quad (2.26)$$

where  $\kappa = \int dt' \int d\bar{r}' K(\bar{r}', t' | \bar{r}, t)$  is the integral operator of (2.24). We have from (2.26) that

$$c = (I - \kappa)^{-1} Q = Q + \kappa Q + \kappa^2 Q + \kappa^3 Q + \dots \quad (2.27)$$

where  $I$  stands for the identity operator. The third member of (2.27) is obtained by an expansion into a Neumann series which is assumed to converge. We may thus write

$$c(\bar{r}, t) = \sum_{j=0}^{\infty} c_j(\bar{r}, t) \quad (2.28)$$

with

$$\begin{aligned} c_0(\bar{r}, t) &= Q(\bar{r}, t) \\ c_j(\bar{r}, t) &= \kappa c_{j-1}(\bar{r}', t') \\ &= \int dt' \int d\bar{r}' K(\bar{r}', t' | \bar{r}, t) c_{j-1}(\bar{r}', t') \end{aligned} \quad (2.29)$$

Therefore, the functional (2.25) is also expandable into an infinite sum

$$J = \sum_{j=0}^{\infty} J_j \quad (2.30)$$

where

$$J_j = \int dt \int d\bar{r} f(\bar{r}, t) c_j(\bar{r}, t) \quad (2.31)$$

In order to evaluate each quantity  $J_j$  in (2.30),  $c_j(\bar{r}, t)$  is interpreted as a multivariate probability density function (pdf) of  $\bar{r}$  and  $t$ . Hence, each integral (2.31) is computed by classical Monte Carlo schemes (see Appendix C), that is, the position vectors  $\bar{r}$  and times  $t$  distributed according to  $c_j(\bar{r}, t)$  are first selected and then the respective values of the pay-off function are averaged.

It can be proved [20] that the successive sampling from  $c_0, c_1, \dots$  to evaluate each term  $J_0, J_1, \dots$  of the infinite sum (2.30) is equivalent to a particle tracking. Let us assume here

that  $K(\bar{r}', t' | \bar{r}, t)$  is a non-negative integral kernel. Each  $i$ th particle tracking begins with the sampling of  $\bar{r}_{i,0}$  and  $t_{i,0}$  from the source term, i.e. from the following pdf:

$$s(\bar{r}, t) = \frac{c_0(\bar{r}, t)}{w_{i,0}} = \frac{Q(\bar{r}, t)}{w_{i,0}} \quad (2.32)$$

with  $w_{i,0} = \int dt \int d\bar{r} Q(\bar{r}, t)$ . Then the simulation continues with the sampling of  $\bar{r}_{i,1}$  and  $t_{i,1}$  from

$$k(\bar{r}_{i,0}, t_{i,0} \rightarrow \bar{r}, t) = \frac{K(\bar{r}_{i,0}, t_{i,0} | \bar{r}, t)}{w_{i,1}(\bar{r}_{i,0}, t_{i,0})}$$

with  $w_{i,1} = \int dt \int d\bar{r} K(\bar{r}_{i,0}, t_{i,0} | \bar{r}, t)$ . For the sampling of the  $(j+1)$ st step, we use the pdf

$$k(\bar{r}_{i,j}, t_{i,j} \rightarrow \bar{r}, t) = \frac{K(\bar{r}_{i,j}, t_{i,j} | \bar{r}, t)}{w_{i,j+1}(\bar{r}_{i,j}, t_{i,j})} \quad (2.33)$$

where  $w_{i,j+1} = \int dt \int d\bar{r} K(\bar{r}_{i,j}, t_{i,j} | \bar{r}, t)$  is called the  $(j+1)$ st weight factor. After  $N$  particle trackings, the quantity

$$\tilde{J}_j = \frac{1}{N} \sum_{i=1}^N W_{i,j} f(\bar{r}_{i,j}, t_{i,j}) \quad (2.34)$$

is an unbiased estimate of  $J_j$  and the weight  $W_{i,j}$  is defined as

$$W_{i,j} = \prod_{\ell=0}^j w_{i,\ell} \quad (2.35)$$

The Monte Carlo estimation of  $J$  in (2.25) is finally obtained from the following development, limited to  $N_L + 1$  terms:

$$\tilde{J} = \sum_{j=0}^{N_L} \tilde{J}_j \quad (2.36)$$

where  $\tilde{J}_j$  is given by (2.34) and where  $N_L$  is chosen such as  $|\tilde{J}_{N_L+1}| \ll |\tilde{J}|$ . The Monte Carlo estimation  $\tilde{J}$  is called “score” of the simulation.

## 2.3.2 Examples of pay-off functions

Various physical quantities may be computed locally by means of Monte Carlo simulation provided that an appropriate pay-off function is selected. We first report below two examples of pay-off functions which play a key role in hydrogeology and in the risk assessment of radioactive waste disposals.

- $f(\bar{r}, t) = H_\Omega(\bar{r} - \bar{r}_E) \delta(t - t_E)$  where  $H_\Omega(\bar{r}) = 1$  inside a domain  $\Omega$  (whose centroid is located at the origin), and 0 everywhere else;  $\delta$  is the Dirac function. The functional  $J$  represents then the contaminant concentration at time  $t_E$  around an extraction well located at  $\bar{r}_E$ .

- $f(\bar{r}, t) = \delta_2(\bar{r} - \bar{r}_S) H_{[0, T_0]}(t)$  where  $\delta_2$  is a two-dimensional Dirac function associated to the surface  $\mathcal{S}$ , while  $H_{[0, T_0]}(t) = 1$  inside  $[0, T_0]$  and 0 outside  $[0, T_0]$ . Now,  $J$  is proportional to the dose due to radionuclides accumulated on the surface  $\mathcal{S}$  during the time interval  $[0, T_0]$ .  $\mathcal{S}$  could be, for instance, the interface between two layers of the geological domain).

Other physical quantities of interest are the scores:

$$J_{\mathcal{S}_\ell} = \int_{t_s}^{T_0} dt \int_{\mathcal{S}_\ell} d\bar{r} c(\bar{r}, t; i) \quad (2.37)$$

$$J_{\bar{P}_k} = \int_{t_s}^{T_0} dt c(\bar{P}_k, t; i) \quad (2.38)$$

where  $\mathcal{S}_\ell$  denotes the plan of equation  $z = z_\ell$  while  $\bar{P}_k$  stands for the point of spatial coordinates  $\bar{P}_k = (x_k, y_k, z_k)$ . the functionals  $J_{\mathcal{S}_\ell}$  and  $J_{\bar{P}_k}$  represent the cumulative concentrations of radionuclide  $i$ , from time  $t_s$  to time  $T_0$ , on the surface  $\mathcal{S}$  and at the point  $\bar{P}_k$ , respectively. The corresponding pay-off functions are given by [34]

$$\varphi(\bar{r}, t; j) = \delta(z - z_\ell) \delta_{j,i} \quad (2.39)$$

$$\varphi(\bar{r}, t; j) = \delta(\bar{r} - \bar{P}_k) \delta_{j,i} \quad (2.40)$$

respectively. The instantaneous concentration of radionuclide  $j$  at  $\bar{P}_k$  at time  $t = t_\mu$  may be computed by using the following pay-off function:

$$\varphi(\bar{r}, t; j) = \delta(\bar{r} - \bar{P}_k) \delta(t - t_\mu) \delta_{j,i} \quad (2.41)$$

which gives rise to the following functional

$$J'_{\bar{P}_k} = c(\bar{P}_k, t_\mu; i) . \quad (2.42)$$

### 2.3.3 Sampling from non-uniform densities

Sampling from any probability density function is based on sampling one or more random number(s) uniformly distributed over the interval  $[0, 1]$ . In TRACKS.1.0 , the pseudo-random numbers generator DLARAN from LAPACK [2] has been used. Once random numbers are sampled in  $[0, 1]$ , some appropriate transformation is applied to sample the target pdf. One may find in [12,18,20] various interesting transformation techniques. We report below only the transformation techniques used in TRACKS.

### 2.3.3.1 Sampling method for discrete univariate distributions

Assume that the random variable  $x$  may take discrete values  $x_i$  with known probabilities  $p_i$ ,  $i = 1, 2, \dots, n$ , with  $\sum_{i=1}^n p_i = 1$ . In order to select one of the discrete values  $x_i$ , one first selects a random number  $\xi$  uniformly distributed on  $(0, 1)$ . Then  $x_j$  is selected if the following inequality holds

$$\sum_{i=1}^{j-1} p_i < \xi \leq \sum_{i=1}^j p_i \quad (2.43)$$

### 2.3.3.2 Decomposition method

Assume that the pdf  $f(\bar{x})$  to be sampled may be written as

$$f(\bar{x}) = \sum_{i=1}^n p_i f_i(\bar{x}) \quad (2.44)$$

where the  $f_i$ 's denote given pdfs and the  $p_i$ 's ( $i = 1, 2, \dots, n$ ) form a probability vector:  $p_i > 0 \forall i$  and  $\sum_{i=1}^n p_i = 1$ . Then, the density  $f(\bar{x})$  may be sampled as follows:

- determine the integer  $j$  such that (2.43) is satisfied for the  $p_i$ 's;
- sample a random variable  $\bar{\xi}$  according to  $f_j(\bar{x})$ .

The decomposition (2.44) is frequently applied to partitioning the definition domain of a density into sub-domains, that is

$$f(\bar{x}) = \sum_{i=1}^n f(\bar{x}) H_{A_i}(\bar{x}) \quad (2.45)$$

where the  $A_i$ 's are disjoint sub-domains and  $H_{A_i}(\bar{x})$  is the indicator function of the sub-domain  $A_i$ . If we can more or less easily sample the densities  $f_i(\bar{x}) = \frac{f(\bar{x})}{p_i} H_{A_i}(\bar{x})$  where  $p_i = \int_{A_i} f(\bar{x}) d\bar{x}$ , then the decomposition method could be applied. The decomposition in sub-domains may be used to increase the efficiency of a rejection method (see below).

### 2.3.3.3 Inversion method

Let  $f(x)$  be a pdf of a variable  $x$ ,  $a \leq x < b$ . Let  $\rho$  denote a random variable uniformly distributed on  $(0, 1)$ . Then an  $x$  value is determined by means of the relations:

$$\begin{aligned} \rho = F(x) &= \int_a^x f(x) dx \\ x &= F^{-1}(\rho) \quad . \end{aligned} \quad (2.46)$$

If  $\rho_i$ ,  $i = 1, 2, \dots, N$ , are independent random numbers uniformly distributed on  $(0, 1)$ , then the  $x_i = F^{-1}(\rho_i)$  values are independent realizations of the  $x$  random variable.

The trouble with this method is that it requires to calculate the inverse  $F^{-1}$  of the cumulative distribution function (CDF)  $F$ , which could be rather intricate or even impossible in practical applications. The method is easy to apply for some important univariate densities like the exponential density and the triangular density [12].

### 2.3.3.4 Rejection method

Let us consider a univariate pdf  $f(x)$  defined on the interval  $[a, b]$ . Let  $M$  a positive real number such that  $f(x) \leq M$  (see Fig. 2.1).

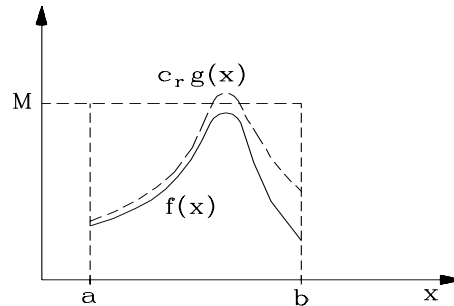


Figure 2.1: Illustration of the rejection method

The method consists simply in first choosing randomly a point in the rectangle whose base is equal to  $b - a$  and its height is equal to  $M$ . If the chosen point falls below the graph of  $f(\xi)$ , then its abscissa is accepted as a sample, if not, it is rejected and a new sampling is performed. Thus, if  $\rho_1$  and  $\rho_2$  are two independent random numbers uniformly distributed on  $(0, 1)$ , then

$$x = a + \rho_1(b - a) \quad (2.47)$$

is accepted if and only if

$$\rho_2 M \leq f(x) \quad (2.48)$$

The validity of this algorithm is proven in [12,20]. It also derives intuitively from Fig. 2.1. An important parameter of this algorithm is the rejection constant  $C_r$  which characterizes the efficiency of the method. It is defined as the ratio between the total mean number of trials and the mean number of random values generated. Here,  $C_r$  is the ratio of the area of the rectangle and the area below the graph of  $f(x)$ , that is

$$C_r = \frac{(b - a)M}{\int_a^b f(x)dx} = (b - a) M. \quad (2.49)$$

A good rejection method has a rejection constant  $C_r \geq 1$  but close to 1. Many improvements of the method are possible. For instance, by combining a rejection method with a decomposition method: the interval  $[a, b]$  is decomposed in sub-intervals and in each sub-interval the rejection method is applied by defining lower and upper bounds of the pdf  $f(x)$ . The rejection method is also readily transposed for a multivariate pdf if the domain definition is simple. If a multivariate pdf  $g(\bar{x})$  easy to sample may be found such that

$$f(\bar{x}) \leq C_r g(\bar{x}) \quad \forall \bar{x} \in \mathcal{D} \quad (2.50)$$

where  $\mathcal{D}$  is the definition domain of the multivariate pdf  $f(\bar{x})$  and  $C_r$  is a constant (a rejection constant), then one can proceed as following:

1. Generate two independent random variables  $\bar{\xi}$  (with density  $g$ ) and  $U$  (uniformly distributed on  $(0, 1)$ );
2. Set  $T = \frac{C_r g(\bar{\xi})}{f(\bar{\xi})}$ ;
3. If  $UT \leq 1$ , accept  $T$ ; if not, reject  $T$  and go back to step 1.

The rejection method is practicable if it is possible to find a “good” overestimating density  $g(\bar{x})$ .

### 2.3.3.5 Conditional distribution method

Consider a multivariate pdf  $f(\bar{x})$  where  $\bar{x} = (x_1, x_2, \dots, x_d)$ . Assume that  $f(\bar{x})$  may be written as

$$f(x_1, x_2, \dots, x_d) = f_1(x_1) f_2(x_2|x_1) \dots f_d(x_d|x_1, \dots, x_{d-1})$$

where the  $f_i$  are conditional pdfs. The generation may be achieved by sampling firstly  $x_1$  from  $f_1$  then  $x_2$  from  $f_2$  with  $x_1$  given and so on. This method allows to reduce a problem of multivariate generation to  $d$  problems of univariate generation. It is clearly easy to use only if the conditional densities are simple. If the multivariate pdf  $f(\bar{x})$  cannot be separated for the variables, one generally resorts to some rejection technique: let the  $d$ -dimensional domain involved be defined by the analytical relation  $G(\xi_1, \xi_2, \dots, \xi_d) \leq 0$ ; the  $d$  values sampled  $(x_1, x_2, \dots, x_d)$  are accepted if and only if  $G(x_1, x_2, \dots, x_d) \leq 0$ .

### 2.3.3.6 The table lookup method

Here, midpoints of equally probable intervals of the variable(s) to be selected are picked up randomly from a table. The table generally contains the coordinates of the finite number midpoints from which an actual value is selected with equal probabilities. One may improve the accuracy of this method by increasing the number of intervals. Another

improvement could be achieved if the midpoints are not just the middle of the intervals, say,

$$\tilde{x}_m = \frac{1}{2} (x_{m+1} - x_m)$$

but the most probable value

$$\tilde{x}_m = \frac{\int_{x_m}^{x_{m+1}} x p(x) dx}{\int_{x_m}^{x_{m+1}} p(x) dx}$$

In case of complicate density functions, the determination of the limits of equal probability intervals themselves may be both intricate and time consuming.

## Chapter 3

# Overview of The Simulation Method

---

The source term  $Q(\bar{r}, t; i)$  and, in particular, the integral kernels  $K_{\mathcal{D}}$  and  $K_{\mathcal{S}}$  are in general intricate and may be not positive. We assume therefore that simple (modified) source term  $\tilde{Q}$  and positive kernels  $\tilde{K}_{\mathcal{D}}$  and  $\tilde{K}_{\mathcal{S}}$  have been derived from the original quantities. This will enable us to compute probability density functions easy to sample. We would like to stress that, in doing so, we simply replace

$$Q, K_{\mathcal{D}}, K_{\mathcal{S}}, K^{j \rightarrow i}, K^{j \rightarrow j}, \dots$$

by identical quantities

$$\frac{Q}{\tilde{Q}} \tilde{Q}, \frac{K_{\mathcal{D}}}{\tilde{K}_{\mathcal{D}}} \tilde{K}_{\mathcal{D}}, \frac{K_{\mathcal{S}}}{\tilde{K}_{\mathcal{S}}} \tilde{K}_{\mathcal{S}}, \frac{K^{j \rightarrow i}}{\tilde{K}^{j \rightarrow i}} \tilde{K}^{j \rightarrow i}, \frac{K^{j \rightarrow j}}{\tilde{K}^{j \rightarrow j}} \tilde{K}^{j \rightarrow j}, \dots$$

We will next describe how the random walks are constructed in the TRACKS code from the integral equation. More specific expressions of the modified quantities depend explicitly on the adjoint reference solution  $C^*$ . Some examples are given in Appendix B.

## 3.1 Transition probabilities

The transition probabilities are obtained by simple quadratures. For instance, for one radionuclide we have for the probability that a single radionuclide  $i$  moves from the source to  $\mathcal{D}$  ( $p_{Q \rightarrow \mathcal{D}}(i)$ ) or to  $\mathcal{S}$  ( $p_{Q \rightarrow \mathcal{S}}(i)$ ) and so on:

$$p_{Q \rightarrow \mathcal{D}}(i) = \frac{\int_{t_s}^{T_0} dt \int_{\mathcal{D}} d\bar{r} \tilde{Q}(\bar{r}, t; i)}{\int_{t_s}^{T_0} dt \int_{\mathcal{D}} d\bar{r} \tilde{Q}(\bar{r}, t; i) + \int_{t_s}^{T_0} dt \oint_{\mathcal{S}} d\bar{r} \tilde{Q}(\bar{r}, t; i)} = 1 - p_{Q \rightarrow \mathcal{S}}(i) \quad (3.1)$$

$$\begin{aligned} p_{\mathcal{D} \rightarrow \mathcal{S}}(z', t'; i) &= \frac{\int_{t'}^{T_0} dt \oint_{\mathcal{S}} d\bar{r} \tilde{K}_{\mathcal{D}}(\bar{r}', t'; i | \bar{r}, t; i)}{\int_{t'}^{T_0} dt \int_{\mathcal{D}} d\bar{r} \tilde{K}_{\mathcal{D}}(\bar{r}', t'; i | \bar{r}, t; i) + \int_{t'}^{T_0} dt \oint_{\mathcal{S}} d\bar{r} \tilde{K}_{\mathcal{D}}(\bar{r}', t'; i | \bar{r}, t; i)} \\ &= 1 - p_{\mathcal{D} \rightarrow \mathcal{D}}(z', t'; i) \end{aligned} \quad (3.2)$$

$$\begin{aligned} p_{\mathcal{S} \rightarrow \mathcal{S}}(t'; i) &= \frac{\int_{t'}^{T_0} dt \oint_{\mathcal{S}} d\bar{r} \tilde{K}_{\mathcal{S}}(\bar{r}', t'; i | \bar{r}, t; i)}{\int_{t'}^{T_0} dt \int_{\mathcal{D}} d\bar{r} \tilde{K}_{\mathcal{S}}(\bar{r}', t'; i | \bar{r}, t; i) + \int_{t'}^{T_0} dt \oint_{\mathcal{S}} d\bar{r} \tilde{K}_{\mathcal{S}}(\bar{r}', t'; i | \bar{r}, t; i)} \\ &= 1 - p_{\mathcal{S} \rightarrow \mathcal{D}}(t'; i) \end{aligned} \quad (3.3)$$

The quantities  $p_{\mathcal{S} \rightarrow \mathcal{S}}$  and  $p_{\mathcal{S} \rightarrow \mathcal{D}}$  are functions of  $t'$  only, whereas  $p_{\mathcal{D} \rightarrow \mathcal{S}}$  and  $p_{\mathcal{D} \rightarrow \mathcal{D}}$  are functions of  $z'$  and  $t'$ . All these quadratures are easy to evaluate. They all reduce to a quadrature over time which could be computed numerically by Gauss-Legendre methods. In the case of a radionuclide chain, the transition probabilities between the discrete states  $j$  are given by

$$p^{j \rightarrow j}(z', t') = \frac{\int_{t'}^{T_0} dt \int_{\overline{\mathcal{D}}} d\bar{r} \tilde{K}^{j \rightarrow j}(\bar{r}', t'; j | \bar{r}, t; j)}{\int_{t'}^{T_0} dt \int_{\overline{\mathcal{D}}} d\bar{r} \tilde{K}^{j \rightarrow j}(\bar{r}', t'; j | \bar{r}, t; j) + \int_{t'}^{T_0} dt \int_{\overline{\mathcal{D}}} d\bar{r} \tilde{K}^{j \rightarrow i}(\bar{r}', t'; j | \bar{r}, t; i)} \quad (3.4)$$

$$p^{j \rightarrow i}(z', t') = \frac{\int_{t'}^{T_0} dt \int_{\overline{\mathcal{D}}} d\bar{r} \tilde{K}^{j \rightarrow i}(\bar{r}', t'; j | \bar{r}, t; i)}{\int_{t'}^{T_0} dt \int_{\overline{\mathcal{D}}} d\bar{r} \tilde{K}^{j \rightarrow j}(\bar{r}', t'; j | \bar{r}, t; j) + \int_{t'}^{T_0} dt \int_{\overline{\mathcal{D}}} d\bar{r} \tilde{K}^{j \rightarrow i}(\bar{r}', t'; j | \bar{r}, t; i)} \quad (3.5)$$

The modified kernels  $\tilde{K}^{j \rightarrow j}$  and  $\tilde{K}^{j \rightarrow i}$  are defined from (2.20) by replacing  $K_{\mathcal{D}}$  and  $K_{\mathcal{S}}$  by  $\tilde{K}_{\mathcal{D}}$  and  $\tilde{K}_{\mathcal{S}}$ , respectively.

## 3.2 Transition densities

The transitions in space and time are sampled from at most four-dimensional multivariate pdfs. One has

$$f_{Q \rightarrow \mathcal{D}}(\bar{r}, t; i) = \frac{\tilde{Q}(\bar{r}, t; i)}{\int_{t_s}^{T_0} dt \int_{\mathcal{D}} d\bar{r} \tilde{Q}(\bar{r}, t; i)} \quad (3.6)$$

$$f_{Q \rightarrow \mathcal{S}}(\bar{r}, t; i) = \frac{\tilde{Q}(\bar{r}, t; i)|_{z=z_u}}{\int_{t_s}^{T_0} dt \oint_{\mathcal{S}} d\bar{r} \tilde{Q}(\bar{r}, t; i)} \quad (3.7)$$

$$f_{\mathcal{D} \rightarrow \mathcal{D}}(\bar{r}', t'; i \rightarrow \bar{r}, t; i) = \frac{\tilde{K}_{\mathcal{D}}(\bar{r}', t'; i | \bar{r}, t; i)}{\int_{t'}^{T_0} dt \int_{\mathcal{D}} d\bar{r} \tilde{K}_{\mathcal{D}}(\bar{r}', t'; i | \bar{r}, t; i)} \quad (3.8)$$

$$f_{\mathcal{D} \rightarrow \mathcal{S}}(\bar{r}', t'; i \rightarrow \bar{r}, t; i) = \frac{\tilde{K}_{\mathcal{D}}(\bar{r}', t'; i | \bar{r}, t; i)|_{z=z_u}}{\int_{t'}^{T_0} dt \oint_{\mathcal{S}} d\bar{r} \tilde{K}_{\mathcal{D}}(\bar{r}', t'; i | \bar{r}, t; i)} \quad (3.9)$$

$$f_{\mathcal{S} \rightarrow \mathcal{D}}(\bar{r}', t'; i \rightarrow \bar{r}, t; i) = \frac{\tilde{K}_{\mathcal{S}}(\bar{r}', t'; i | \bar{r}, t; i)}{\int_{t'}^{T_0} dt \int_{\mathcal{D}} d\bar{r} \tilde{K}_{\mathcal{S}}(\bar{r}', t'; i | \bar{r}, t; i)} \quad (3.10)$$

$$f_{\mathcal{S} \rightarrow \mathcal{S}}(\bar{r}', t'; i \rightarrow \bar{r}, t; i) = \frac{\tilde{K}_{\mathcal{S}}(\bar{r}', t'; i | \bar{r}, t; i)|_{z=z_u}}{\int_{t'}^{T_0} dt \oint_{\mathcal{S}} d\bar{r} \tilde{K}_{\mathcal{S}}(\bar{r}', t'; i | \bar{r}, t; i)} \quad (3.11)$$

where  $z = z_u$  denotes the equation that defines the planar upper surface  $\mathcal{S}$ . In practice, any of the pdfs  $f(\bar{r}, \tau)$  so obtained may be rewritten as:

$$f(\bar{r}, \tau) = f_1(\tau) f_2(\bar{r} | \tau) \quad (3.12)$$

In TRACKS, the following five different expressions of  $f_1(\tau)$  are used

$$f_1(\tau) \sim \begin{cases} [1 + (T_0 - \tau) \varepsilon] e^{-\lambda\tau} \\ \frac{e^{-a\tau - \frac{b}{\tau}}}{\sqrt{\tau}} \\ (T_0 - \tau) e^{-\lambda\tau} \\ \frac{T_0 - \tau}{\sqrt{\tau}} e^{-\lambda^*\tau} \\ \frac{T_0 - \tau}{\sqrt{\tau}} e^{-a\tau - \frac{b^*}{\tau}} \end{cases} \quad (3.13)$$

where  $a, b, b^*, \lambda^*$  and  $\varepsilon$  are known constants. These one-dimensional pdfs may be sampled by inversion or rejection techniques or a combination of these two techniques [12,33]. The conditional pdf  $f_2(\bar{r}|\tau)$  is, depending on the case at hand, either a two- or a three-dimensional Gaussian distribution.

### 3.3 Random walk methodology

A combined random walk has to be performed: inside the geological medium  $\mathcal{D}$  because of the kernel  $K_{\mathcal{D}}$ , and on the boundary  $\mathcal{S}$  which accounts for the contribution from  $K_{\mathcal{S}}$ . We are interested in computing, by means of truncated Neumann series (see Eq. (2.36)), the general scores

$$J_j = \int_{t_s}^{T_0} dt \int_{\mathcal{D}} d\bar{r} \varphi(\bar{r}, t; j) A(\bar{r}, t; j) \simeq \sum_{m=0}^{N_L} \tilde{J}_{j,m} \quad (3.14)$$

where  $t_s$  is the release time of the radionuclides from the repository and  $T_0$  the final simulation time.  $\varphi(\bar{r}, t; j)$  denotes the pay-off function which defines the target physical quantity. Each partial score  $\tilde{J}_{j,m}$  is evaluated by random walks constructed from the integral equation (2.16). We proceed as follows.

1. before each random walk, a state  $j$  of radionuclide is randomly selected according to the relative intensity of the source terms  $\tilde{Q}(\bar{r}, t; j)$ . Moreover, at any step, before sampling the next position and time, one has to randomly decide whether a radioactive transition occurs ( $j \rightarrow i$ ) or not ( $j \rightarrow j$ ). The next spatial position and time are then sampled from  $\tilde{K}^{j \rightarrow j}$  or from  $\tilde{K}^{j \rightarrow i}$ , depending on the branches  $j \rightarrow j$  or  $j \rightarrow i$  chosen.
2. The sampling of a new spatial position is performed into two steps. From the transition probabilities  $p_{Q \rightarrow \mathcal{D}}$ ,  $p_{Q \rightarrow \mathcal{S}}$ , etc ..., one first decide whether the random walker falls somewhere inside the geological domain  $\mathcal{D}$  or somewhere on its outer boundary

$\mathcal{S}$ . Finally, the transitions are effectively achieved from the transition densities  $f_{Q \rightarrow \mathcal{D}}$ ,  $f_{Q \rightarrow \mathcal{S}}$ , etc ...

3. The simulation continues until steps 1-2 are repeated  $N_L$  times.

## 3.4 Activities at points and on surfaces

Assume that one is interested in assessing the radionuclide activities at  $N_P$  given points  $\bar{P}_k$  or on  $N_S$  specified planes  $\mathcal{S}_\ell$  of equation  $z = z_\ell$ . A more efficient Monte Carlo simulation may be achieved by modifying the transition probabilities and the transition densities used so far [34]. The corresponding pay-off functions are given by Eqs. (2.39)-(2.42). Obviously, for efficiency purposes, one should include  $\bar{P}_k$  and  $\mathcal{S}_\ell$  in the computation of pdfs. We have from [34], for  $\ell = 1, \dots, N_S$  and for  $k = 1, \dots, N_P$ , that

$$p_{\mathcal{D} \rightarrow \mathcal{S}_\ell}(\bar{r}', t'; i) = \frac{\int_{t'}^{T_0} dt \oint_{\mathcal{S}_\ell} d\bar{r} \tilde{K}_{\mathcal{D}}(\bar{r}', t'; i | \bar{r}, t; i)}{R_{\mathcal{D}}(\bar{r}', t'; i)} \quad (3.15)$$

$$p_{\mathcal{D} \rightarrow \bar{P}_k}(\bar{r}', t'; i) = \frac{\int_{t'}^{T_0} dt \tilde{K}_{\mathcal{D}}(\bar{r}', t'; i | \bar{P}_k, t; i)}{R_{\mathcal{D}}(\bar{r}', t'; i)} \quad (3.16)$$

$$p_{\mathcal{S} \rightarrow \mathcal{S}_\ell}(\bar{r}', t'; i) = \frac{\int_{t'}^{T_0} dt \oint_{\mathcal{S}_\ell} d\bar{r} \tilde{K}_{\mathcal{S}}(\bar{r}', t'; i | \bar{r}, t; i)}{R_{\mathcal{S}}(\bar{r}', t'; i)} \quad (3.17)$$

$$p_{\mathcal{S} \rightarrow \bar{P}_k}(\bar{r}', t'; i) = \frac{\int_{t'}^{T_0} dt \tilde{K}_{\mathcal{S}}(\bar{r}', t'; i | \bar{P}_k, t; i)}{R_{\mathcal{S}}(\bar{r}', t'; i)} \quad (3.18)$$

$$p_{Q \rightarrow \mathcal{S}_\ell}(\bar{r}', t'; i) = \frac{\int_{t_s}^{T_0} dt \oint_{\mathcal{S}_\ell} d\bar{r} \tilde{Q}(\bar{r}, t; i)}{R_Q(\bar{r}', t'; i)} \quad (3.19)$$

$$p_{Q \rightarrow \bar{P}_k}(\bar{r}', t'; i) = \frac{\int_{t_s}^{T_0} dt \tilde{Q}(\bar{P}_k, t; i)}{R_Q(\bar{r}', t'; i)} \quad (3.20)$$

where

$$\begin{aligned}
R_{\mathcal{D}}(\bar{r}', t'; i) &= \int_{t'}^{T_0} dt \int_{\mathcal{D}} d\bar{r} \tilde{K}_{\mathcal{D}}(\bar{r}', t'; i | \bar{r}, t; i) + \int_{t'}^{T_0} dt \oint_{\mathcal{S}} d\bar{r} \tilde{K}_{\mathcal{D}}(\bar{r}', t'; i | \bar{r}, t; i) \\
&+ \sum_{m=1}^{N_S} \int_{t'}^{T_0} dt \oint_{S_m} d\bar{r} \tilde{K}_{\mathcal{D}}(\bar{r}', t'; i | \bar{r}, t; i) + \sum_{n=1}^{N_P} \int_{t'}^{T_0} dt \tilde{K}_{\mathcal{D}}(\bar{r}', t'; i | \bar{P}_n, t; i) \quad (3.21)
\end{aligned}$$

$$\begin{aligned}
R_{\mathcal{S}}(\bar{r}', t'; i) &= \int_{t'}^{T_0} dt \int_{\mathcal{D}} d\bar{r} \tilde{K}_{\mathcal{S}}(\bar{r}', t'; i | \bar{r}, t; i) + \int_{t'}^{T_0} dt \oint_{\mathcal{S}} d\bar{r} \tilde{K}_{\mathcal{S}}(\bar{r}', t'; i | \bar{r}, t; i) \\
&+ \sum_{m=1}^{N_S} \int_{t'}^{T_0} dt \oint_{S_m} d\bar{r} \tilde{K}_{\mathcal{S}}(\bar{r}', t'; i | \bar{r}, t; i) + \sum_{n=1}^{N_P} \int_{t'}^{T_0} dt \tilde{K}_{\mathcal{S}}(\bar{r}', t'; i | \bar{P}_n, t; i) \quad (3.22)
\end{aligned}$$

$$\begin{aligned}
R_Q(\bar{r}', t'; i) &= \int_{t_s}^{T_0} dt \int_{\mathcal{D}} d\bar{r} \tilde{Q}(\bar{r}, t; i) + \int_{t_s}^{T_0} dt \oint_{\mathcal{S}} d\bar{r} \tilde{Q}(\bar{r}, t; i) \\
&+ \sum_{m=1}^{N_S} \int_{t_s}^{T_0} dt \oint_{S_m} d\bar{r} \tilde{Q}(\bar{r}, t; i) + \sum_{n=1}^{N_P} \int_{t_s}^{T_0} dt \tilde{Q}(\bar{P}_n, t; i) . \quad (3.23)
\end{aligned}$$

The transition probabilities defined through Eqs. (3.1)-(3.3) change to

$$p_{Q \rightarrow \mathcal{D}}(\bar{r}', t'; i) = \frac{\int_{t_s}^{T_0} dt \int_{\mathcal{D}} d\bar{r} \tilde{Q}(\bar{r}, t; i)}{R_Q(\bar{r}', t'; i)} = 1 - p_{Q \rightarrow \mathcal{S}}(\bar{r}', t'; i) \quad (3.24)$$

$$\begin{aligned}
p_{\mathcal{D} \rightarrow \mathcal{S}}(\bar{r}', t'; i) &= \frac{\int_{t'}^{T_0} dt \oint_{\mathcal{S}} d\bar{r} \tilde{K}_{\mathcal{D}}(\bar{r}', t'; i | \bar{r}, t; i)}{R_{\mathcal{D}}(\bar{r}', t'; i)} \\
&= 1 - p_{\mathcal{D} \rightarrow \mathcal{D}}(\bar{r}', t'; i) \quad (3.25)
\end{aligned}$$

$$\begin{aligned}
p_{\mathcal{S} \rightarrow \mathcal{S}}(\bar{r}', t'; i) &= \frac{\int_{t'}^{T_0} dt \oint_{\mathcal{S}} d\bar{r} \tilde{K}_{\mathcal{S}}(\bar{r}', t'; i | \bar{r}, t; i)}{R_{\mathcal{S}}(\bar{r}', t'; i)} \\
&= 1 - p_{\mathcal{S} \rightarrow \mathcal{D}}(\bar{r}', t'; i) \quad (3.26)
\end{aligned}$$

Besides (3.6)-(3.11), we have the following transition densities:

$$f_{Q \rightarrow \mathcal{S}_\ell}(\bar{r}, t; i) = \frac{\tilde{Q}(\bar{r}, t; i)|_{z=z_\ell}}{\int_{t_s}^{T_0} dt \int_{\mathcal{S}_\ell} d\bar{r} \tilde{Q}(\bar{r}, t; i)} \quad (3.27)$$

$$f_{Q \rightarrow \bar{P}_k}(\bar{r}, t; i) = \frac{\tilde{Q}(\bar{P}_k, t; i)}{\int_{t_s}^{T_0} dt \tilde{Q}(\bar{P}_k, t; i)} \quad (3.28)$$

$$f_{\mathcal{D} \rightarrow \mathcal{S}_\ell}(\bar{r}', t'; i \rightarrow \bar{r}, t; i) = \frac{\tilde{K}_{\mathcal{D}}(\bar{r}', t'; i | \bar{r}, t; i)|_{z=z_\ell}}{\int_{t'}^{T_0} dt \int_{\mathcal{S}_\ell} d\bar{r} \tilde{K}_{\mathcal{D}}(\bar{r}', t'; i | \bar{r}, t; i)} \quad (3.29)$$

$$f_{\mathcal{D} \rightarrow \bar{P}_k}(\bar{r}', t'; i \rightarrow \bar{P}_k, t; i) = \frac{\tilde{K}_{\mathcal{D}}(\bar{r}', t'; i | \bar{P}_k, t; i)}{\int_{t'}^{T_0} dt \tilde{K}_{\mathcal{D}}(\bar{r}', t'; i | \bar{P}_k, t; i)} \quad (3.30)$$

$$f_{\mathcal{S} \rightarrow \mathcal{S}_\ell}(\bar{r}', t'; i \rightarrow \bar{r}, t; i) = \frac{\tilde{K}_{\mathcal{S}}(\bar{r}', t'; i | \bar{r}, t; i)|_{z=z_\ell}}{\int_{t'}^{T_0} dt \int_{\mathcal{S}_\ell} d\bar{r} \tilde{K}_{\mathcal{S}}(\bar{r}', t'; i | \bar{r}, t; i)} \quad (3.31)$$

$$f_{\mathcal{S} \rightarrow \bar{P}_k}(\bar{r}', t'; i \rightarrow \bar{P}_k, t; i) = \frac{\tilde{K}_{\mathcal{S}}(\bar{r}', t'; i | \bar{P}_k, t; i)}{\int_{t'}^{T_0} dt \tilde{K}_{\mathcal{S}}(\bar{r}', t'; i | \bar{P}_k, t; i)} \quad (3.32)$$

These new densities add two more elementary pdfs  $f_1(\tau)$  to the five ones listed in (3.13). The additional pdfs are following:

$$f_1(\tau) \sim \begin{cases} \frac{e^{-a\tau - \frac{b}{\tau}}}{\tau^{3/2}} \\ \frac{T_0 - \tau}{\tau^{3/2}} e^{-a\tau - \frac{b^*}{\tau}} \end{cases} \quad (3.33)$$

which may be sampled by combining inversion and rejection techniques.

The generalized Monte Carlo simulation is illustrated in Fig. 3.1 for one radionuclide. We see that if a random walker falls inside  $\mathcal{D}$  which corresponds to Position 1 in the figure, the next transition will be sampled from the (modified) kernel  $\tilde{K}_{\mathcal{D}}$ . Depending on the

transition probabilities computed during the pre-processing step, the random walker may fall at the next step either in  $\mathcal{D}$ , or on the outer surface  $\mathcal{S}$ , or on any of the target surfaces  $\mathcal{S}_\ell$  ( $1 \leq \ell \leq N_S$ ), or at any of the target points  $\bar{P}_k$  ( $1 \leq k \leq N_P$ ). If the random walker reaches the outer surface  $\mathcal{S}$  (Position 2 in Fig. 3.1, the next transition will be sampled from  $\tilde{K}_\mathcal{S}$  and the same branching possibilities are available at Position 2 as at Position 1. The simulation has to be stopped if the random walker reaches one of the target surfaces or points. In this case, no contribution from these locations could be expected. In Fig. 3.2, the general Monte Carlo algorithm for the transport of a radionuclide chain is represented. There are two main loops: one over  $n$  which is the index of each pseudo-particle and one over  $m$  which is the number of transitions from the source;  $m$  coincides with the index of the terms of the Neumann series. The sampling of the initial “radioactive state”  $j$  at the source is carried out by computing the ratios

$$\frac{R_Q(\bar{r}', t'; j)}{\sum_{k=1}^{N_r} R_Q(\bar{r}', t'; k)}. \quad (3.34)$$

The state  $j$  being defined, a random sampling among  $2 + N_S + N_P$  branches is performed. After the scoring, the simulation ends for the  $N_S + N_P$  branches leading to the target surfaces or points. For the two remaining branches, a state transition is considered. Let us point out that if the random walker is on the outer surface  $\mathcal{S}$ , no score is computed for a state transition  $j$  to  $i$ . This could be mathematically explained by means of the expression of the integral equations (2.16)-(2.19) where  $K^{j \rightarrow i}$  does not contain any contribution from  $\mathcal{S}$ . That is the reason why in Fig. 3.2 indicates that “no score” is computed and the simulation is finished.

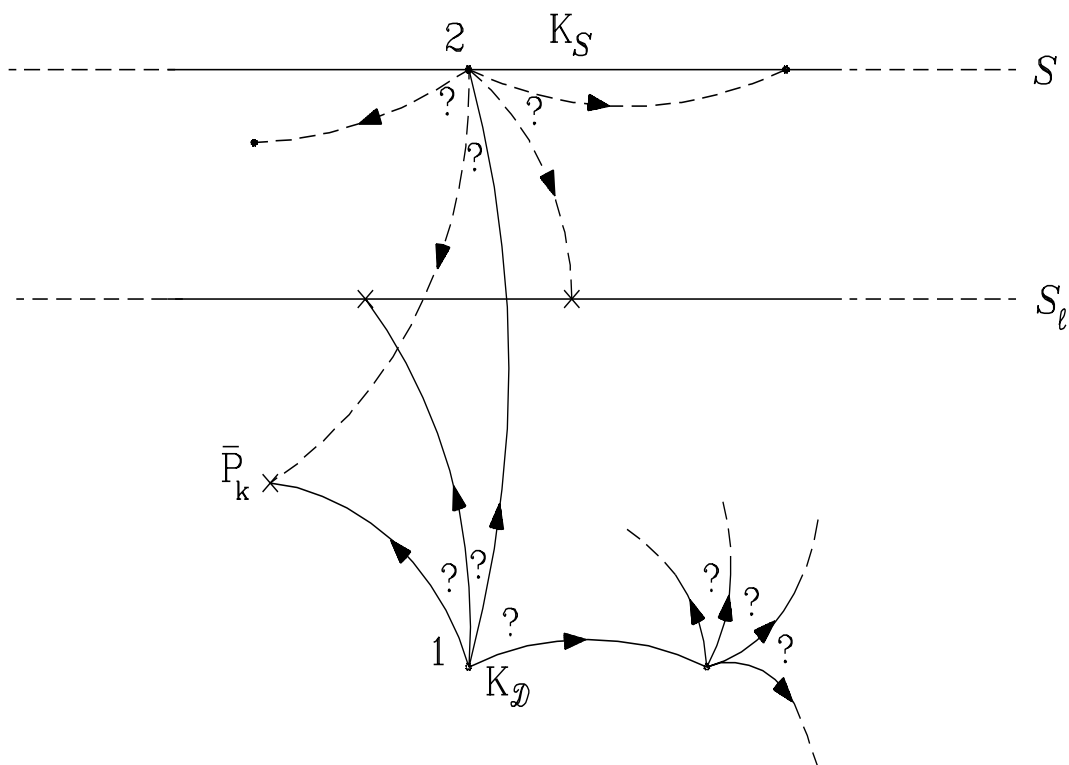


Figure 3.1: Branchings view of the random walks for one radionuclide. Transition: Position 1  $\rightarrow$  Position 2. The simulation ends at symbol “x”.

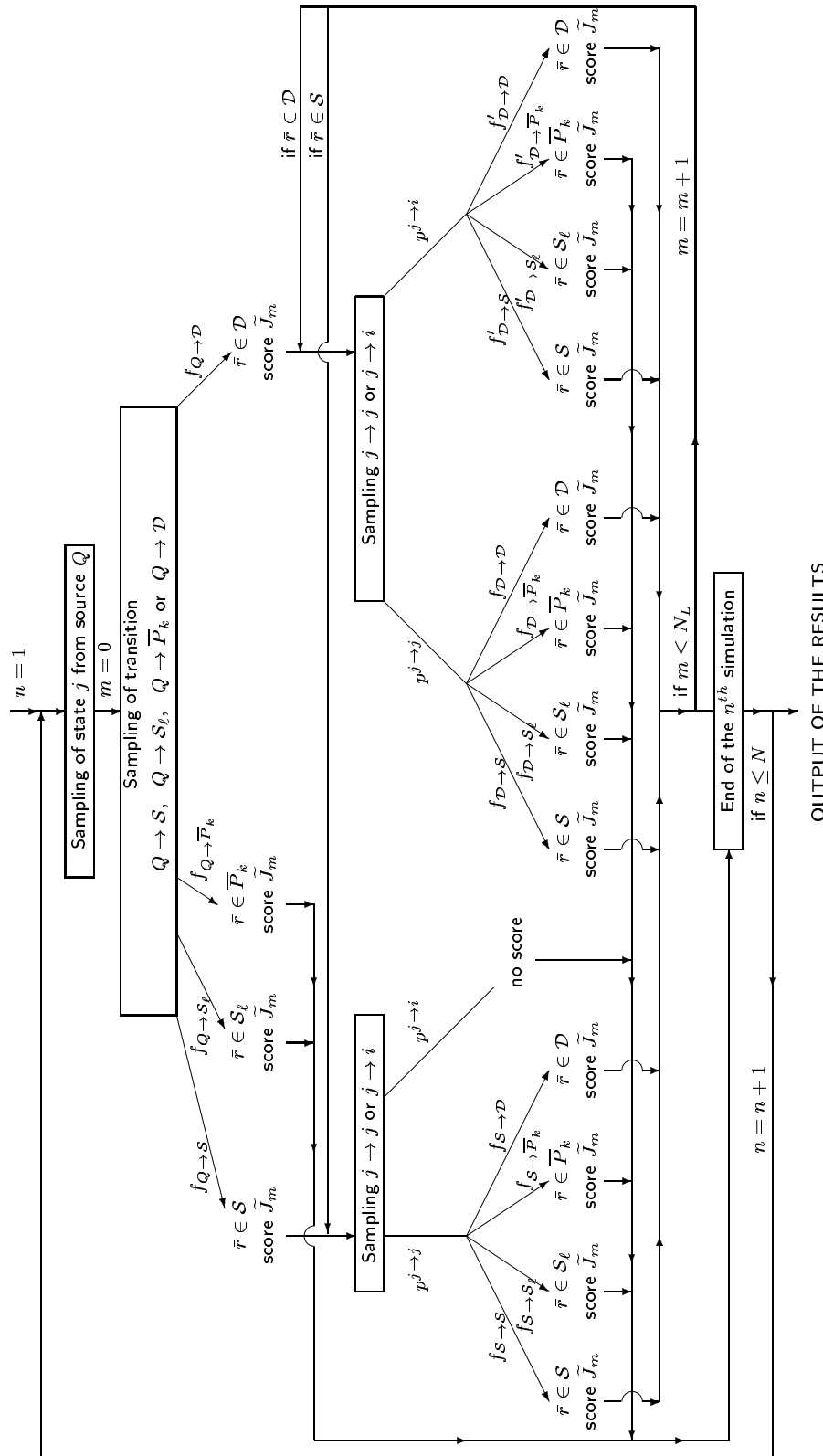


Figure 3.2: General flow-chart of the Monte Carlo simulation for the evaluation of local-wise cumulative activities



# Chapter 4

## Code Structure

---

---

### 4.1 General information

TRACKS.1.0 is written in standard FORTRAN 77 as a collection of routines grouped into modules. In order to get a self-contained code, we have included some subroutines from BLAS [7] and LAPACK [2], whose list is given in the sequel. In TRACKS.1.0 we assume that the following conditions are satisfied:

- The domain is a three-dimensional parallelepipedic static geological saturated porous medium (Fig. 4.1). It is made of a stack of layers bounded by horizontal planes.
- The domain is limited upwards by a planar surface  $\mathcal{S}$  of equation  $z = z_u$  where an impervious boundary condition is imposed: the total normal flux of radionuclides is assumed to be zero on  $\mathcal{S}$  ( $\beta = 0$  in Eq. (2.10)). This condition is assumed homogeneous, that is the interface soil-air is impervious for the migration of radionuclides. This condition is realistic if none of the elements present in the radionuclide chain are gaseous elements or if the quantity of radionuclides accumulated on the upper surface are not extracted by some means or other.
- Following the degradation of the engineered barriers, one is mainly interested in computing the quantity of radionuclides that reach the interface between the host rock and the other geological layers.
- The dispersion tensor is diagonal and constant (the longitudinal and transverse dispersivity are assumed to be identical).
- Uniform upwards and downwards advection processes.

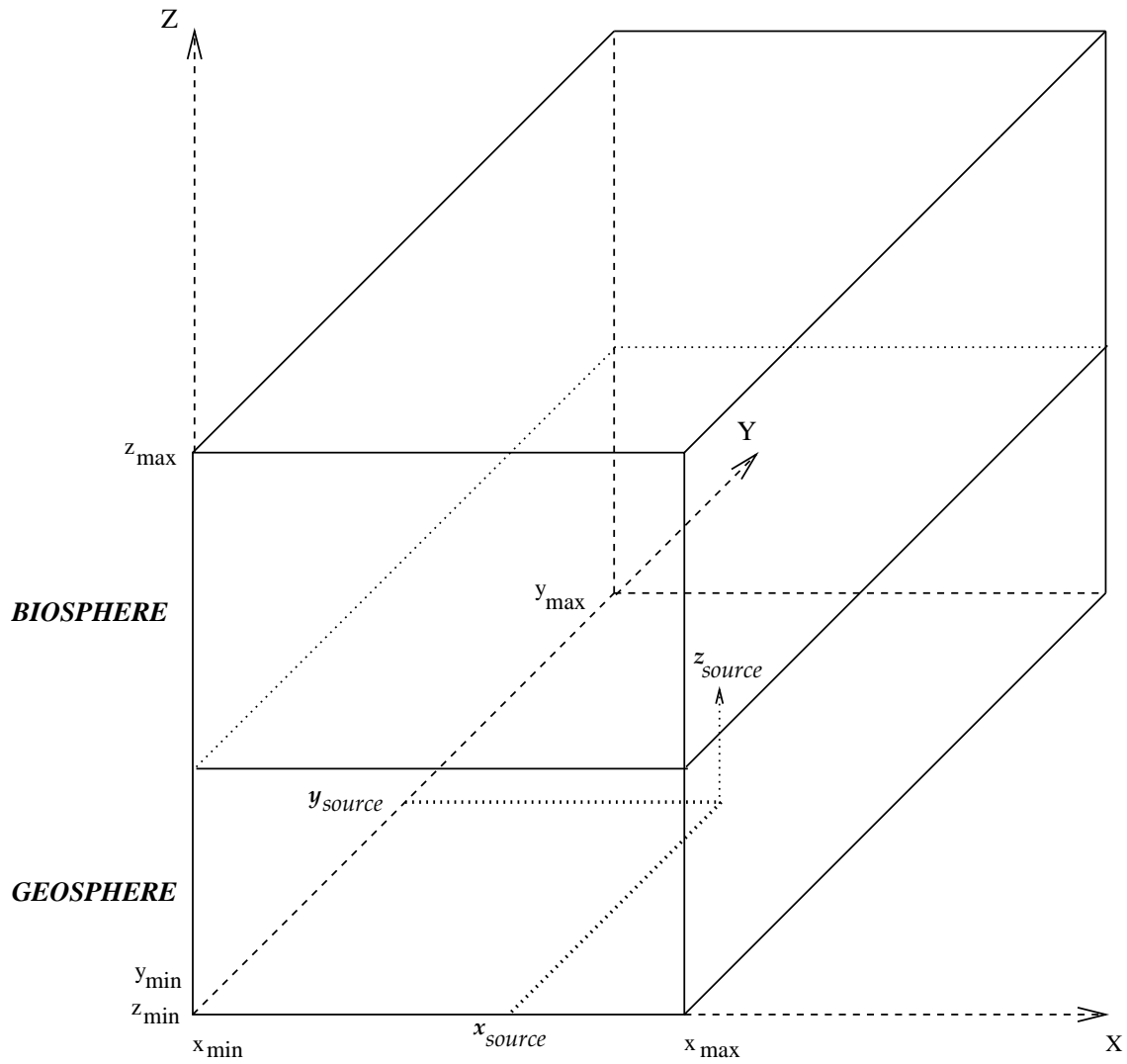


Figure 4.1: Physical domain

- No solubility limits are taken into account in the model near the source location.
- There is no multiple branchings in the radionuclide chain:  $p(j \rightarrow j) + p(j \rightarrow j+1) = 1$ . In other words, the chain is linear.
- The effects of uncertainties on the value of the concentration may be estimated for the retardation factor whose pdf is given. One may resort to the double randomization technique: random generators are globally invoked twice. Once for sampling hydrogeological parameters from given pdfs, which define the probable range of parameter values as well as their likelihood. Finally, for each selected parameter set, an appropriate number of random walks are simulated for the evaluation of mean concentration of contaminants [24,29,39]. More details are given in Appendix D.

## 4.2 TRACKS package

Tracks.1.0 package is provided as a gzipped tar file "Tracks.1.0.tar.gz". The files included may be extracted by typing either of the following:

```
gunzip -c Tracks.1.0.tar.gz | tar -xvf -
```

or

```
gtar -zxvf Tracks.1.0.tar.gz
```

This will give rise to the directory "Tracks.1.0" which contains the files and subdirectory given below. The minimum information that one needs in order to compile and run TRACKS with the test example may be found in the file Tracks.info whose content deprived of the copyright notice is following:

---

I. The directory "Tracks.1.0" contains the following files and subdirectory :

```
-----  
Main Directory  
-----
```

\*\*\* Documentation files (3 files) \*\*\*

1. Tracks.info -> this file
2. Tracksdoc.ps -> user's guide
3. Tracksdoc.pdf -> user's guide

\*\*\* Tracks routines proper (11 files) \*\*\*

4. tracks.f -> main source file
5. trinput.f -> reading of the data
6. tprepro.f -> pre-processing
7. tmcsimu.f -> Monte Carlo simulation
8. mcsimu2.f -> sampling of new positions in the phase-space
9. trsubro.f -> auxiliary subroutines
10. tfuncts.f -> auxiliary functions
11. numerec.f -> routines from "Numerical Recipes"
12. posproc.f -> post-processing of the simulation results
13. tblas.f -> auxiliary routines from BLAS and LAPACK
14. elapse.c -> auxiliary C routine for computing the elapse time

\*\*\* makefile (1 file) \*\*\*

15. Makefile -> should be updated to meet local requirements

\*\*\* input files (2 files) \*\*\*

16. tracks.dat -> main input file
17. velxyz.dat -> example of the mean velocity vector

-----  
Subdirectory "Tracksh" (12 files)  
-----

18. absc.h
29. crpar.h
20. frobrch.h
21. functs.h
22. premcs.h
23. samsou.h

```

24. scores.h
25. statw.h
26. tparams.h
27. tracom1.h
28. tracom2.h
29. velf.h

```

---

II. Tracks is a self-contained package. There is no need of any particular libraries. To run Tracks,

- (1) edit the "Makefile" and change the names of the Fortran (F77) and C (CC) compiler (e.g., g77, gcc, ...), if necessary. Specify the compilation options : FFLAGS, CFLAGS .
  - (2) type "make"
  - (3) type "tracks"
  - (4) The main output is in the file "tracks.out"
  - (5) See the user's guide for more information
- 

III. Tracks.1.0 has been successfully tested on the following platforms :

- (1) Silicon Graphics Origin 2000 (195 MHz)
- (2) SUN Enterprise 450 [Solaris]
- (3) Compaq Digital GS140 (699 MHz)
- (4) PC Server under Linux (Gnu compiler : g77, gcc)

## 4.3 Program description

TRACKS is globally made of three main parts:

1. **The pre-processing:** preliminary calculations are done before the random walks. This includes
  - The transition probabilities:  $p_{D \rightarrow S}$ ,  $p_{Q \rightarrow D}$ , ...
  - The transition probabilities between the radionuclides of a chain:  $p^{j \rightarrow j}$  and  $p^{j \rightarrow i}$ .
  - The statistical weights which account for the modified quantities  $\frac{Q}{\tilde{Q}}$ , etc ...

All the above-mentioned quantities are computed for a fixed (input) number of points. If necessary, during the simulation unknown values are interpolated from the known ones.

2. **The Monte Carlo simulation:** random walks computations.
3. **The post-processing:** the results obtained undergo appropriate treatment.

We give below, when necessary, the list of all routines contained in a file together with some explanation on its object. The flow-chart of TRACKS main modules is depicted on Fig. 4.2.

```
-----
                                tprepro
C*****
C                                                                    |
C  Computation of transition probabilities in the space "(x,y,z,t,i)" |
C  where "(x,y,z)" denotes the spatial coordinates, "t" time and "i" |
C  the radionuclide index in the chain.                               |
C  List of subroutines included : PREPROC  DICHOT  TRPROB           |
C                                                                    |
C  TRPROB -> routine for computing transition probabilities in the space |
C                                                                    |
C*****
```

```
-----
                                mcsimu2.f
C*****
C                                                                    |
C  Routines where sampling of new positions in the phase-space      |
C  "(x,y,z,t,i)" are implemented from different probability density  |
C  functions.                                                         |
C                                                                    |
C  List of subroutines involved :                                     |
C                                                                    |
C  EXPD    -> Exponential probability density function (pdf)         |
C  GAMMD   -> Gamma pdf                                              |
C  GIGD3   -> Generalized inverse Gaussian pdf (3D)                 |
C  MEXPD   -> modified Exponential pdf                              |
C  MGAMD   -> modified Gamma pdf                                     |
C  MGIGD   -> modified Generalized inverse Gaussian pdf (1D)       |
C  MGIGD3  -> modified Generalized inverse Gaussian pdf (3D)       |
C                                                                    |
C*****
```

```

-----
                                trsubro.f
C*****
C
C list of subroutines included :
C
C GENCORP -> generation of coefficients for random parameters
C GK      -> auxiliary routine for the generation of random field
C          according to the Turning Bands method [], [].
C PAINT   -> evaluation of transport parameters of the adjoint solution
C POFINST -> evaluation of instantaneous activities or concentrations
C          in local areas.
C PROCRF  -> pre-processing for random field generation
C QCAL    -> evaluation of correction coefficients derived from the
C          mean velocity field for the calculation of the general
C          integral kernel
C QCALM   -> variant of QCAL
C RFIELD  -> pre-processing of coefficients for the evaluation of random
C          retardation field.
C VFIELD  -> pre-processing of coefficients for the evaluation of random
C          velocity field.
C
C*****

```

```

-----
                                numerec.f
C*****
C
C list of portable functions and subroutines extracted and modified
C from "Numerical Recipes" :
C
C GASDEV -> standard Gaussian random generator
C GAULEG -> Gauss-Legendre abscissae and weights
C          (called in QGAUS and QGAUS2)
C GCF     -> auxiliary function used in PERF and PERFC
C GSER    -> auxiliary function used in PERF and PERFC
C INDEXX  -> sorting subroutine
C PERF    -> error function
C PERFC   -> complementary error function
C QGAUS   -> Gauss-Legendre evaluation of a 1D quadrature
C QGAUS2  -> Gauss-Legendre evaluation of a 2D quadrature
C
C*****

```

```

C*****
C                                                                 |
C AUXILIARY ROUTINES FROM BLAS AND LAPACK : LSAME  DLAMCH  DLAMC1 DLAMC2 |
C                                                                 |
C                               DLAMC3 DLAMC4  DLAMC5 DLARAN |
C                                                                 |
C DLARAN -> random generator of a number from a uniform (0,1) pdf |
C                                                                 |
C*****

```

## 4.4 Input data structure

### 4.4.1 Description of input variables

All the numbers must be entered in a **free format** in a file named **tracks.dat**. For the sake of user-friendliness, the data are introduced following the same steps as in the theoretical approach. One first provides data for the advection-dispersion equations, next data for the Monte Carlo simulation (or integral computation), and finally the data for the output.

transport equations → integral formulation → Monte Carlo simulation

Each line of *tracks.dat* which contains the symbol “\*” in its first column is interpreted as a line of comments which is ignored by TRACKS. Unless specifically otherwise stated, each number should be entered in a separate line. We now describe all the input variables in the order according to which they should be entered.

#### Title and output file specification

**TITLESP**      The first line must contain a title of no more than 80 characters. It may specify for instance the type of the transport problem considered.

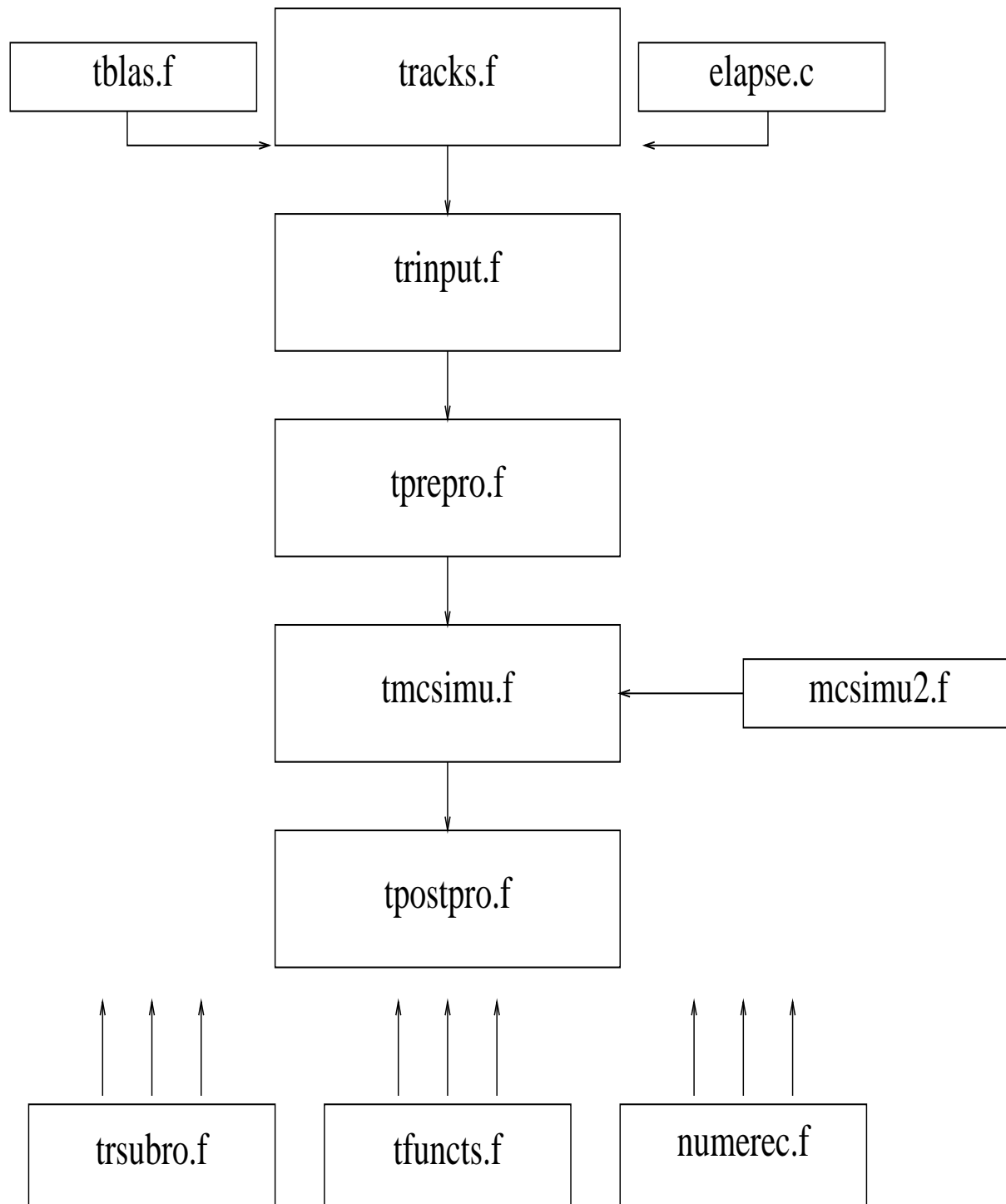


Figure 4.2: Flow-chart of TRACKS main modules

**IOUTP**

The second line must contain the output unit. If IOUTP=6 then the results of the simulation will be displayed on the screen, while with IOUTP=26 all the results will be written in the file **tracks.out**.

## Geometry of the flow domain

**DIM**

The dimension of the geological domain. DIM=1 or DIM=3 in the case of one- or three-dimensional model, respectively.

**XMIN XMAX YMIN YMAX ZMIN ZMAX**

The minimal and the maximal nodal coordinate along the x- y- and z-axis (see Fig. 4.1). The z-axis is the vertical direction. All the six coordinates must be entered in the same line. In the case of DIM=1 set XMIN=XMAX=YMIN=YMAX=0.

**NX NY NZ**

The number of grid-points along the x- y- and z-axis. All the three values must be entered in the same line. In the case of DIM=1 set NX=NY=2, otherwise a breakdown will occur.

**NLAYER**

The number of geological layers. This version of TRACKS can handle at most two layers.

**ZLAYER(2)**

The minimal coordinate of the second layer. The first layer corresponds to the deepest one, so that in the code one has automatically  $ZLAYER(1) = ZMIN$  (see Fig. 4.1). The value of ZLAYER(2) has to be entered only if NLAYER=2.

**NRADNUC**

The number of unstable elements in the radionuclide chain ( $N_r$  in the text). In other words, it denotes the number of coupled partial differential advection-dispersion equations.

## Source term and implicit boundary condition

**IACT**

If the activity  $A(\bar{r}, t; i)$  of radionuclides is sought, then IACT=1 and the source intensity should be expressed in activity. When the concentrations  $C(\bar{r}, t; i)$  of radionuclides are the working quantities then set IACT=0.

**XSOURCE YSOURCE ZSOURCE TSOURCE QSOURCE**

Coordinates  $(x_s, y_s, z_s) = \bar{r}_s$  of the repository center (source point), starting time  $(t_s)$  of the release of radionuclides, and total intensity of radionuclides  $(\sum_{i=1}^{N_r} S(\bar{r}_s, t_s; i))$  at the beginning of the simulation. The five values must be entered in the same line. In the case of DIM=1 set XSOURCE=YSOURCE=0.

**PROPSRC(I)**

Proportion (percentage) of radionuclide  $i$  in QSOURCE. One value per line. There should hold  $\sum_{i=1}^{N_r} \text{PROPSRC}(i) = 1$ .

**LAMBDA(I)**

The radioactive decay constant of radionuclide  $i$  ( $i = 1, 2, \dots, N_r$ ). One value per line.

**LAMBDA(NRADNUC+1)**

The radioactive decay constant of the stable radionuclide, if any. If this value is not available, it should be entered as  $10^{-4} * \min_{1 \leq i \leq N_r} \{\lambda_i\}$ .

**IBCOND MODRLS TRLS**

The type of boundary conditions at the upper surface (IBCOND). The release mode of radionuclides (MODRLS), and the duration of the release (time release) of radionuclides (TRLS) at the repository. All the three values must be entered in the same line.

$$\text{IBCOND} = \begin{cases} 0 \longrightarrow \text{impervious boundary condition (zero flux)} \\ 1 \longrightarrow \text{fixed value of activity or concentration} \end{cases}$$

$$\text{MODRLS} = \begin{cases} 0 \longrightarrow \text{instantaneous release (impulse injection)} \\ 1 \longrightarrow \text{band release at the upper surface} \\ 2 \longrightarrow \text{band release inside the domain} \end{cases}$$

**Parameters of advection-dispersion equations****T0**

The total simulation time.

**THETA D0 ALPHAL ALPHAT ALPHAV**

The porosity (THETA), the molecular diffusion coefficient (D0), the longitudinal (ALPHAL), the horizontal transversal (ALPHAT) and the vertical transversal (ALPHAV) dispersivity coefficient: one layer (five values) per line. The first layer is the deepest one.

**R(*i,l*)**

The (mean) retardation factor of radionuclide *i* in the layer *l*: one radionuclide (NLAYER value(s)) per line.

$R(1, 1)$	$R(1, 2)$
$R(2, 1)$	$R(2, 2)$
$R(3, 1)$	$R(3, 2)$
$\vdots$	$\vdots$

**R(NRADNUC+1,*l*)**

The (mean) retardation factor of the stable radionuclide, if any, in the layer *l*. If this value is not available, any negative value should be provided. All the NLAYER value(s) should be entered in the same line.

$R(\text{NRADNUC} + 1, 1)$      $R(\text{NRADNUC} + 1, 2)$     ...     $R(\text{NRADNUC} + 1, \text{NLAYER})$

**VELNAME**

The (advection) velocity file name: a file which contains the list of the coordinates (x,y,z) of nodal points together with the components ( $\nu_x, \nu_y, \nu_z$ ) of the mean (advection) velocity vectors on the regular grid defined by NX, NY, and NZ. No space (blank) should be left before the name of the file. If *i*, *j* and *k* stand for the index of nodal points along the x-, y- and z-axis, then the values should be entered (in free format) according to the following scheme:

```

for k = 1, NZ
  for j = 1, NY
    for i = 1, NX
      x   y   z    $\nu_x(i, j, k)$     $\nu_y(i, j, k)$     $\nu_z(i, j, k)$ 
    end_for
  end_for
end_for

```

## Uncertainty of the retardation factors

**IUNCERT**

Specify whether the uncertainty on the values of the retardation factors is taken into account.

$$\text{IUNCERT} = \begin{cases} 1 \longrightarrow \text{sampling of values, constant per layer} \\ 0 \longrightarrow \text{no sampling of values (deterministic model)} \end{cases}$$

**SLR(*i,l*)**

The standard deviation of the log-normal distribution of the random retardation factor for radionuclide *i* in the layer *l*: one radionuclide per line (NLAYER value(s)) per line. The requested values have to be provided only if IUNCERT=1.

<i>SLR</i> (1, 1)	<i>SLR</i> (1, 2)
<i>SLR</i> (2, 1)	<i>SLR</i> (2, 2)
<i>SLR</i> (3, 1)	<i>SLR</i> (3, 2)
⋮	⋮

## Data for analytical solutions

**IANASOL QANAL**

If IANASOL=1 then the analytical solution will be computed provided that: there is only one layer, there are at most three elements in the chain, and the parameters of the advection-dispersion-retention equations are constant. Otherwise set IANASOL=0. In the former case, QANAL should correspond to the value of the Darcy velocity component  $q_z$  along the z-axis. It is assumed that  $q_x = q_y = 0$ .

## Data for numerical simulations

### ITYPROC

In the case where a complete pre-processing is required set ITYPROC=1. If TYPROC=0 then TRACKS will read data from the intermediate results files generated during the pre-processing (see Subsection 4.5.1) in a previous run. This may significantly reduce the computation time in certain instances:

- during successive runs, only the spatial and/or temporal target positions (see "data for ouput) change;
- one intends to improve the accuracy of the results by increasing the total number of random walks (see below).

### NTOTSIM NBATCH NPRVSIM

The total number of random walks (NTOTSIM), the batch size (NBATCH: number of particle trackings, possibly for one random retardation factor), the number of random walks executed in a previous run. All the three values must be entered in the same line. When IUNCERT=0 (deterministic retardation factors), one should set NBATCH=1. In the case of IUNCERT=1, the quantity

$$\frac{\text{NTOTSIM} - \text{NPRVSIM}}{\text{NBATCH}}$$

gives the number of values of retardation factor sampled per layer.

## Data for output

### IVISUS

Specify whether the concentration or the activity over the upper surface is computed (IVISUS=1) or not (IVISUS=0).

### IVISPL

Number of horizontal planes (no more than 3) where the concentration or the activity is required.

### ZCOORPL(i)

If IVISPL  $\neq$  0 then ZCOORPL(i),  $i = 1, 2, \dots, \text{IVISPL}$ , should be entered as the coordinates along the z-axis of the planes where the concentration or the activity is required. All the IVISPL values must be entered in the same line. if IVISPL=0 then not any z-coordinate should be given.

**IVISPT**

Number of spatial positions (no more than 3) where concentrations or activities are sought.

**XPT(i) YPT(i) ZPT(i)**

Coordinates (x,y,z) of the IVISPT points where concentrations or activities have to be computed: one point per line. If IVISPT=0 then not any coordinate should be entered.

**INSTANT**

Number of instantaneous times (no more than 3) when concentrations or activities are sought. If INSTANT=0 then only cumulative quantities will be computed. If IDIM=3 and INSTANT≠0 then set IVISUS=0 and IVISPL=0, otherwise an error message will be issued.

**TINST(i)**

Values of the INSTANT instantaneous times when concentrations or activities are computed. All the values have to be typed in the same line. If INSTANT=0 then not any value should be entered. There should hold  $TINST(i) \leq T0$ .

**ICLASS DCLASS**

If IUNCERT=1 then DCLASS determines the class size for the histogram, while ICLASS=1 tells TRACKS that only the post-processing has to be executed in order to change the histogram, otherwise set ICLASS=0 (complete Monte Carlo simulation). In the case of IUNCERT=0 not any value should be provided for the variables ICLASS and DCLASS.

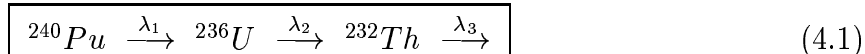
The variable DCLASS is approximately equal to the (mean) number of values (retardation factors) sampled per class. The number of classes is given by:

$$int \left( \frac{\frac{NTOTSIM - NPRVSIM}{NBATCH} - IRSIM}{DCLASS} \right) + 1$$

where *int* stands for the integer part of a real number while IRSIM denotes the number of rejected simulations (*output variable*).

## 4.4.2 Sample input file

For illustration purposes, we provide a test problem, which consists of a radionuclide chain with three elements, the last one being stable, say:



In the corresponding *tracks.dat* file, we have added explanation enough to help any user to quickly enter the data without a tedious preparation. Each line of data is preceded by one or more line(s) of comments where the parameters are listed in the way they must appear in the next line(s). The content of the sample file is following.

```
*****
*TITLE . NO MORE THAN 80 CHARACTERS
Test (3D model) : 240Pu -> 236U -> 232Th *** Time unit : year
* ioutp: OUTPUT FILE SPECIFICATION: 6-> STANDARD OUTPUT ; 26->
* tracks.out
  26
*=====
*
* ***   GEOMETRY OF THE FLOW DOMAIN   ***
*
*=====
* dim --> the dimension of the geological domain (dim = 1 or 3)
  3
*-----
* -> lower and upper bounds (in meter) along the x- y- and z-axis
* ** the z-axis is the vertical one. IF dim = 1 THEN axis = z-axis
*   xmin      xmax      ymin      ymax      zmin      zmax
0.0000E+00 1.0000E+04 0.0000E+00 1.0000E+04 -2.9000E+02 1.0000E+01
*-----
* NX   NY   NZ ---> number of grid-points along the axes x, y, z
  21   21   31
*-----
*nlayer -> number of geological layers (no more than 2).
*First layer = Lowest (deepest) layer
  2
*-----
* zlayer(2)...zlayer(nlayer) -> lower height of the layers
* all the values involved must be entered on one line
* zlayer(1) (deepest layer) is set equal to zmin
* if nlayer = 1 then delete or comment (with a '*') the next line
  -2.0000E+02
*=====
```

```

* number of unstable elements (radionuclides) in the chain
* = number of coupled Partial Differential Equations
*=====
* nradnuc
    2
*=====
*
* ***   DEFINITION OF THE SOURCE TERM ***
* ***   and implicit SPECIFICATION OF THE BOUNDARY CONDITIONS ***
*
*=====
* iact -> source intensity expressed in activity or concentration
* = 0 -> concentration
* = 1 -> activity
    1
* coordinates(x,y,z), time, intensity of the radion. point source
*   xsource      ysource      zsource      tsource      qsource
    2.5000E+03   2.5000E+03  -2.4000E+02  0.0000E+00  3.2000E+00
*-----
* propsrc(i) i=1...nradnuc : proportion of radion. i in the source
* one value per line
    0.9999E+00
    1.0000E-04
*-----
* lambda(i) i=1...nradnuc : the radioactive decay constant of
* radionuclide i.
* one value per line
    1.0250E-04
    2.8860E-08
* lambda(nradnuc+1). If this value is not available, it could be
* entered as: 10-4*min{\lambda_i}
    4.9500E-11
*-----
* ibcond -> type of boundary conditions at the upper surface
*   = 0 -> impervious boundary condition
*   = 1 -> fixed value of activity or concentration
* modrls -> release mode of radionuclides
*   = 0 -> instantaneous release at point source
*         (impulse injection)
*   = 1 -> band release at the upper (surface) boundary
*   = 2 -> band release at the point source inside the domain
* trls -> time of release (duration of the release)
* ibcond modrls      trls
    0      2  1.0000E+04

```

```

=====
*
* *** PARAMETERS OF THE ADVECTION-DISPERSION-RETENTION EQUATION
*
=====
*   t0 -> total simulation time
      3.0001E+07
* theta -> porosity (dimensionless)
* d0    -> diffusion coefficient (in m^2/year)
* alphaL -> longitudinal dispersivity coefficient (in meter)
* alphaT -> horizontal transversal dispersivity coefficient
* alphaV -> vertical transversal dispersivity coefficient
*   theta(1)      d0(1)   alphaL(1)   alphaT(1)   alphaV(1)
* l=1...nlayer. One layer per line
      0.3000E+00   1.0000E-02   0.0000E+00   0.0000E+00   0.0000E+00
      0.3000E+00   7.3000E-02   4.0000E+01   4.0000E+01   4.0000E+01
* R -> mean retardation factor per layer
*   R(i,l) ... i=1,...,nradnuc , l=1,...,nlayer
* one radionuclide per line : R(i,1) R(i,2) ... R(i,nlayer)
      1.0670E+04   1.5000E+03
      3.2000E+03   6.0000E+00
* R(nradnuc+1,1) R(nradnuc+1,2) ... R(nradnuc+1,nlayer)
      1.0670E+04   2.0000E+03
* enter the velocity file name (list of the components of the mean
* velocity vectors on the regular grid defined by NX, NY, and NZ)
* no space left (blank) before the name !
velxyz.dat
*-----
* * uncertainty of the parameters (retardation factor)
*-----
* iuncert=1 (sampling of retardation factors, constant per layer)
*   =0 (no sampling : deterministic values)
      1
* iuncert = 1 -> read slr(i,l), otherwise delete or comment the
*   line(s) involved
* slr() -> standard deviation of the log-normal distribution of
*   the random retardation factor
* distribution of R(.,.) constant over layer l
*   slr(i,l) ... i=1,...,nradnuc , l=1,...,nlayer
* one radionuclide per line : slr(i,1) slr(i,2) ... slr(i,nlayer)
      0.0500E+00   0.0000E+00
      0.0500E+00   0.0000E+00
=====
*

```

```

* *** DATA FOR AN ANALYTICAL SOLUTION ***
*           for comparison purpose
*
*=====
* ianasol -> if =1 then the analytical solution will be computed
* if there is only one layer, three elements in the chain, and
* the parameters (advection-dispersion-retention...) are constant
* qanal=value of the Darcy velocity for the analytical solution
* ianasol      qanal
*           0 0.0000E+00
*=====
*
* *** DATA FOR NUMERICAL SIMULATION ***
*
*=====
* ityproc -> type of pre-processing
*   = 0 -> no pre-processing
*   = 1 -> complete pre-processing
*           1
* ntotsim -> total number of random walks
* nbatch  -> batch size (number of particle trackings)
*           possibly for one random parameter)
* nprvsim -> number of random walks executed in a previous
*           simulation
* ntotsim  nbatch  nprvsim
* 34250000 13700   0
* In the case of iuncert=1 (uncertain values of retardation factors)
* the quantity ' (ntotsim - nprvsim)/nbatch ' gives the number of
* values sampled (per layer). When iuncert=0 (deterministic values)
* <nbatch> MUST BE SET TO 1.
*=====
*
* *** DATA FOR OUTPUT ***
*
*=====
* ivisUS -> if =1 then the concentration (or the activity) over
* the upper surface is computed, otherwise set it to 0.
*           0
* ivisPL -> number of planes (no more than 3) where
* concentrations or activities are sought.
*           1
* zcoorpl(i) i=1,2,...,ivisPL -> z-coordinates of the planes.
* All the <ivisPL> values in the same line.
* if ivisPL=0 then not any 'z-coordinates' should be given.

```

```

-2.1000E+02
* ivisPT -> number of points (no more than 3) where
* concentrations or activities are sought.
    0
* xpt(i) ypt(i) zpt(i) i=1,2,...,ivisPT -> coordinates
* of the points at which concentrations or activities have to
* be computed on condition that ivisPT is different from 0.
* One point per line.
* 0.0000E+00 0.0000E+00 -1.7000E+02
* instant -> number of instantaneous times (no more than 3) at
* which concentrations or activities are computed. If instant=0
* then only cumulative quantities are computed. If idim = 3 and
* instant > 0 then ivisUS and ivisPL must be set to zero.
    0
* tinst(i) -> instantaneous times (< or = t0) considered above.
* All the <instant> values in the same line.
* 2.0000E+07 3.0000E+07 3.0001E+07
*-----
* dclass -> determine the class size for the histogram in the case
* of iuncert=1 (otherwise no data should be entered). The larger
* dclass the larger the classes.
*iclass = 0 -> complete Monte Carlo simulation
*         = 1 -> only post-processing for changing the histogram
* iclass      dclass
    0 2.0000E+01

*=====

```

## 4.5 Output structure

The output issued by TRACKS is easy to read. The number of each radionuclide in the chain is reported together with:

- the coordinates of each target point or plane;
- the Monte Carlo score computed by TRACKS;
- the estimation of the absolute (or statistical) error;
- the relative error, say, the absolute error divided by the score;
- the variance of the score;
- the analytical solution, if any.

The statistical quantities (error and variance) are defined in Appendix D. Output examples are sketched on Figs. 4.3 and 4.4.

At the end of the Monte Carlo simulation, the times spent in the pre-processing and in the simulation are displayed. Moreover, during the computations, it is possible to estimate the remaining computation time on the basis of the information reported either on the screen or in the file *tracks.out*: every multiple of 10% of simulations, the elapse time is displayed. More specific illustrative examples are given in Chapter 5.

Besides *tracks.out*, which contains the main results of the Monte Carlo simulation(s), two types of output files in ASCII format are generated by TRACKS:

1. the *intermediate results files* (*filename.irs*): storage of temporary results of the simulations. These results are used later on in the TRACKS particle trackings, possibly in subsequent runs.
2. the *results files* (*filename.res*): storage of the final numerical results of the simulations. These results may be used for graphical purposes post-processing when a stochastic uncertainty analysis is required.

We now briefly describe each of the files involved.

### 4.5.1 The intermediate results files

The files generated and used by the TRACKS program during the pre-processing are the following:

**statws.irs:** results of numerical quadratures giving the values of statistical weights associated to random walkers sampled from the source of radionuclides. The file is also read in subsequent runs if the pre-processing is unchanged.

**tranps.irs:** results of the calculations of transition probabilities from the source to all the specified local regions of the domain.

**statwd.irs:** results of numerical quadratures giving the values of statistical weights associated to random walkers inside the domain. The file is also read in subsequent runs if the pre-processing is unchanged.

**tranpd.irs:** results of the calculations of transition probabilities at equidistant time and height from inside the domain to all the specified local regions of the domain.

**statwg.irs:** results of numerical quadratures giving the values of statistical weights associated to random walkers over the boundaries, i.e. the upper surface of the domain. The file is also read in subsequent runs if the pre-processing is unchanged.

```

=== The Activity of Radionuclides ===

=====
***** Radionuclide number : ... *****
=====

-----
** Cumulative score over plane 1 of coordinate z = ...
-----
* TRACKS score : ...
* Absolute error : ...
* Relative error : ...
* Variance ..... : ...

-----
** Cumulative score over plane 2 of coordinate z = ...
-----
* TRACKS score : ...
* Absolute error : ...
* Relative error : ...
* Variance ..... : ...

-----
** Cumulative score over plane 3 of coordinate z = ...
-----
* TRACKS score : ...
* Absolute error : ...
* Relative error : ...
* Variance ..... : ...

-----
** Scores at point 1 of coordinates
x = ... y = ... z = ...
-----
** Cumulative score **
-----
* TRACKS score : ...
* Absolute error : ...
* Relative error : ...
* Variance ..... : ...

-----
** Scores at point 2 of coordinates
x = ... y = ... z = ...
-----
** Cumulative score **
-----
* TRACKS score : ...
* Absolute error : ...
* Relative error : ...
* Variance ..... : ...

-----
** Scores at point 3 of coordinates
x = ... y = ... z = ...
-----
** Cumulative score **
-----
* TRACKS score : ...
* Absolute error : ...
* Relative error : ...
* Variance ..... : ...

```

Figure 4.3: Output structure.  $ivisUS = 0$ ,  $ivisPL = 3$ ,  $ivisPT = 3$ , and  $instant = 0$ .

```

=== The Activity of Radionuclides ===

=====
***** Radionuclide number : 1 *****
=====

-----
** Scores at point 1 of coordinates
x = ...          y = ...          z = ...
-----
** Cumulative score **
-----
* TRACKS score   : ...
* Absolute error : ...
* Relative error : ...
* Variance ..... : ...

-----
** Instantaneous score at time 1 t = ...
-----
* TRACKS score   : ...
* Absolute error : ...
* Relative error : ...
* Variance ..... : ...

-----
** Instantaneous score at time 2 t = ...
-----
* TRACKS score   : ...
* Absolute error : ...
* Relative error : ...
* Variance ..... : ...

-----
** Instantaneous score at time 3 t = ...
-----
* TRACKS score   : ...
* Absolute error : ...
* Relative error : ...
* Variance ..... : ...

-----
** Scores at point 2 of coordinates
x = ...          y = ...          z = ...
-----
** Cumulative score **
-----
* TRACKS score   : ...
* Absolute error : ...
* Relative error : ...
* Variance ..... : ...

-----
** Instantaneous score at time 1 t = ...
-----
* TRACKS score   : ...
* Absolute error : ...
* Relative error : ...
* Variance ..... : ...

...

```

Figure 4.4: Output structure.  $ivisUS = 0$ ,  $ivisPL = 0$ ,  $ivisPT = 3$ , and  $instant = 3$ .

**tranpg.irs:** results of the calculations of transition probabilities at equidistant time from the upper surface of the domain to all the specified local regions of the domain.

**randfc.irs:** list of preliminary data necessary for the generation of random fields. The file is also read in subsequent runs if the characteristics of the random fields are unchanged.

The files generated during the simulation are listed below:

**rwalks.irs:** this file lists among all the random walks some trajectories in the space phase. It contains the successive spatial positions, times and radionuclide states of the random walkers along their paths. This listing gives a general overview of how the contaminant plume spreads.

**psimul.irs:** the necessary informations about the seeds reached by the random generators in the previous simulations are memorized in this file. If an improvement in the accuracy of the scores is sought in a subsequent run, this file will be read at the beginning of the new run.

**scores.irs:** the evolution of the scores during the run is listed in this file. It allows to follow the decrease of the error committed on the score.

**scrاند.irs:** the intermediate scores after each simulation with a given set of random parameters are stored in this file. The informations derived from this file are used to generate histograms and complementary cumulative distribution functions (see the results files).

## 4.5.2 The results files

The results files are in general derived from intermediate results files after a post-processing. We have:

**scores.res:** this file is constructed from **scores.irs**. It presents the evolution of the scores in a convenient way for graphical purposes. In the case of a deterministic medium (say, with fixed parameters), this file contains the evolution, with respect to the number of random walks, of the scores and the estimations of scores errors. We give below the

content of each column of this file.

Number of random walks	Analytical solution	TRACKS score	Error	Relative error	...
------------------------	---------------------	--------------	-------	----------------	-----

From the second column, the succession (with respect to planes, spatial points and times) of the analytical solutions and the “TRACKS scores and errors are the same as the main results shown on Figs. 4.3 and 4.4.

**schist.res:** it is derived from **scrand.irs**. Appropriate values are calculated and the results are recorded for graphical (histograms) purposes. This file is constructed only for a simulation with random (uncertain) parameters. It allows to draw histograms of the scores. The intervals between the maximum and minimum value of the scores are divided in sub-intervals. The scores are classified in increasing values order. We give below the content of each column of this file.

Value of the score	Relative frequency of the score in the simulation	...
--------------------	---	-----

The succession (with respect to planes, spatial points and times) of the columns after the first two columns is the same as on Figs. 4.3 and 4.4.

**scccdf.res:** complementary cumulative distribution functions are generated from the file **scrand.irs** and stored in this file. As for the previous file, **scccdf.res** is constructed only for a simulation with random (uncertain) parameters. The content of each column of this file is:

Value of the score	Value of the (approximate) complementary cumulative function	...
--------------------	--	-----

The succession (with respect to planes, spatial points and times) of the columns after the first two columns is the same as on Figs. 4.3 and 4.4.

## Chapter 5

# Examples of application

---

---

By way of illustration, we will discuss transport of radionuclides in three-dimensional (3D) and in one-dimensional (1D) medium. As for the parameters, we will consider both stochastic values and deterministic values constant per layer for the retardation factors. For some simple transport conditions, that is to say, when

1. there is only one layer;
2. there are at most three elements in the chain;
3. the parameters of the advection-dispersion-retention equation are constant;

an analytical solution could be obtained. Such a solution has been derived in [19] for the migration in a 3D porous medium, and used in [35, pp. 466-467] and [36, pp. 232-235] in order to validate an earlier version of the code TRACKS. We will report only the results validated on a 1D semi-infinite model whose analytical solution may be found in [14]. The experiments were conducted on a COMPAQ-DIGITAL Alpha GS160 with 1001 MHz, 2 Gflops, 8 Mbytes Cache and 16 Gbytes RAM. The operating system is Compaq Tru64 UNIX 5.1A.

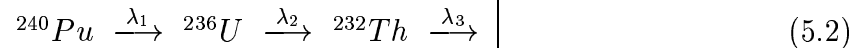
## 5.1 A 3D clay-sand geological model

We investigate the contamination problem of an aquifer made of sand, which is located above a clay layer where a radioactive waste disposal has been buried. The sand layer extends from  $z = -200\text{ m}$  to the upper surface which is modeled as a plane of equation  $z = 10\text{ m}$  where an impervious boundary condition (zero flux) is imposed. In the clay layer, which ranges from  $z = -200\text{ m}$  to  $z = -290$ , the groundwater flow (velocity) is assumed to be zero. The domain extends horizontally from  $x = 0\text{ m}$  and  $y = 0\text{ m}$  to

$x = 10\,000\text{ m}$  and  $y = 10\,000\text{ m}$ . The radioactive source is horizontally centered in the clay layer at  $x = 2500\text{ m}$ ,  $y = 2500\text{ m}$  and  $z = -240\text{ m}$ . We have opted for “ $10^{23}\text{ dpy}$ ” as measure unit for the activity of radionuclides. It is of worth noting that

$$\boxed{10^{23}\text{ dpy} \approx 3 \times 10^{15}\text{ Bq}} \quad (5.1)$$

We assume a band release of radionuclides from the source whose total activity is  $3.2 \times 10^{23}\text{ dpy}$ , which is written as 3.2 in the file *tracks.dat*. We are interested in the migration of the three-member radionuclide chain



considered in Section 4.4. The last element  ${}^{232}\text{Th}$  is assumed to be stable. Thus only the first two elements of the chain are considered in the migration. The activity proportions of  ${}^{240}\text{Pu}$  and  ${}^{236}\text{U}$  in the source are 0.9999 and  $10^{-4}$ , respectively. The values of the remaining advection-dispersion-retardation parameters are given as in the file *tracks.dat* in Section 4.4.

### 5.1.1 A simplified probabilistic risk assessment (PRA)

We consider the effects of the uncertainty on the value of the retardation factor  $R_i$  which is assumed to be constant per geological layer. This uncertainty is represented by a log-normal pdf from which random values are sampled (see Appendix D for detailed information). Such an approach has been followed in some PRA studies (see, e.g., [27]) in order to analyze the effects of uncertainty on the radiological consequences. The content of the file *tracks.out* is as follows:

```
.*****.
| <<<<<<>>>>> |
| Copyright 2003 Universite Libre de Bruxelles |
| <<<<<<>>>>> Service de Metrologie Nucleaire |
| |
|           T R A C K S   1 . 0 |
| |
| Transport of RAdionuclide Chains by non-analog |
| particle trackings in Stochastic media ..... |
| ----- |
| A non-analog Monte Carlo transport code for the |
| risk assessment of radioactive repository sites |
|*****.
```

```

*** Epsilon machine = 1.1102230246251565E-16
*** Safe minimum    = 2.2250738585072014-308

```

```

-----
*** Test (3D model) : 240Pu -> 236U -> 232Th *** Time unit : year ***
-----

```

```

*** No analytical solution for zero velocity ***
*** velocity file name :velxyz.dat ***

```

```

==> PRE-PROCESSING : <===

```

```

--> Computing statistical weights AND
    transition probabilities .....

```

```

--> Computing data for random fields ***

```

```

--> End of the pre-processing <---

```

```

==> SIMULATION : <===

```

```

*** total number of simulations .. : 34250000
*** number of previous simulations :      0
*** batch size ..... : 13700
*** number of parameter samplings : 2500

```

```

i = 3425001 --> 10% of simulations --> time = 0h 3min 32sec
i = 6850001 --> 20% of simulations --> time = 0h 7min 12sec
i = 10275001 --> 30% of simulations --> time = 0h 9min 58sec
i = 13700001 --> 40% of simulations --> time = 0h 13min 52sec
i = 17125001 --> 50% of simulations --> time = 0h 17min 30sec
i = 20550001 --> 60% of simulations --> time = 0h 21min 14sec
i = 23975001 --> 70% of simulations --> time = 0h 24min 49sec
i = 27400001 --> 80% of simulations --> time = 0h 27min 59sec
i = 30825001 --> 90% of simulations --> time = 0h 30min 53sec

```

```

*** Number of rejected simulations ..... :      0

```

```

--> End of the simulations <---

```

```

idomb =          508 Lower exit(s) from domain

```

```
-----
*** RESULTS ***
-----
```

```
=== The Activity of Radionuclides ===
```

```
=====
***** Radionuclide number : 1 *****
=====
```

```
-----
** Cumulative score over plane 1 of coordinate z = -0.21000E+03
-----
```

```
* TRACKS score      : 0.00000000E+00
* Absolute error    : 0.00000000E+00
* Relative error    : 0.00000000E+00
* Variance         : 0.00000000E+00
```

```
=====
***** Radionuclide number : 2 *****
=====
```

```
-----
** Cumulative score over plane 1 of coordinate z = -0.21000E+03
-----
```

```
* TRACKS score      : 0.14624207E+03
* Absolute error    : 0.19874226E+01
* Relative error    : 0.13589951E-01
* Variance         : 0.36714091E+04
```

```
* Effective number of parameter samplings :          2500
```

```
=====
* EXECUTION TIMES (IN SECONDS) *
=====
PRE-PROCESSING (COMPUTATION) ..: 0h  6min 56sec
MONTE CARLO SIMULATION ..... : 0h 34min 32sec

=====
T O T A L ..... : 0h 41min 28sec
```

From the information gathered in columns 3 and 4 of the files *schist.res* and *scccdf.res* histograms and complementary cumulative distribution function of the scores are generated and shown in Figs. 5.1-5.3.

The complementary cumulative distribution function, which is frequently encountered in risk assessment studies [43,44], is an efficient tool to check whether regulatory requirements are satisfied. It allows to estimate the probability of exceeding a given consequence threshold. In the case of Fig. 5.3, at 90% confidence, the probability that the cumulative activity on the plane of equation  $z = -210 m$  goes beyond, for instance,  $300 \times 10^{23} dpy$  after  $3.0001 \times 10^7$  years is approximately equal to 1.15%. How to cheaply increase the accuracy of the needed quantities is a topic under investigation (see, e.g., [39]).

## 5.1.2 A deterministic analysis

Here, we do not take into account any uncertainty. As already mentioned, it is mandatory to set *iuncert* = 0 and *nbatch* = 1. Note however that the effective batch size is *nbatch* = *ntotsim*. Of course, not any standard deviation has to be entered in the file *tracks.dat*. We have run TRACKS with *ntotsim* = 34 250 000 as in the stochastic analysis, which gives rise to the following results:

...

```
-----
*** CAS TEST : 240Pu -> 236U -> 232Th *** Time unit : year (3D) ***
-----
```

```
*** No analytical solution for zero velocity ***
*** velocity file name :velxyz.dat ***
```

```
==> PRE-PROCESSING : <==
```

```
---> Computing statistical weights AND
      transition probabilities .....
```

```
---> End of the pre-processing <---
```

```
==> SIMULATION : <==
```

```
*** total number of simulations ..... : 34250000
*** number of previous simulations .. : 0
*** batch size ..... : 34250000
*** number of parameter samplings ... : 0
*** deterministic values of parameters ***
```

```
-----  
Chain : 240Pu -> 236U -> 232Th (3D Model)  
Time Unit : year  
total simulation time : 3.0001E+07  
-----
```

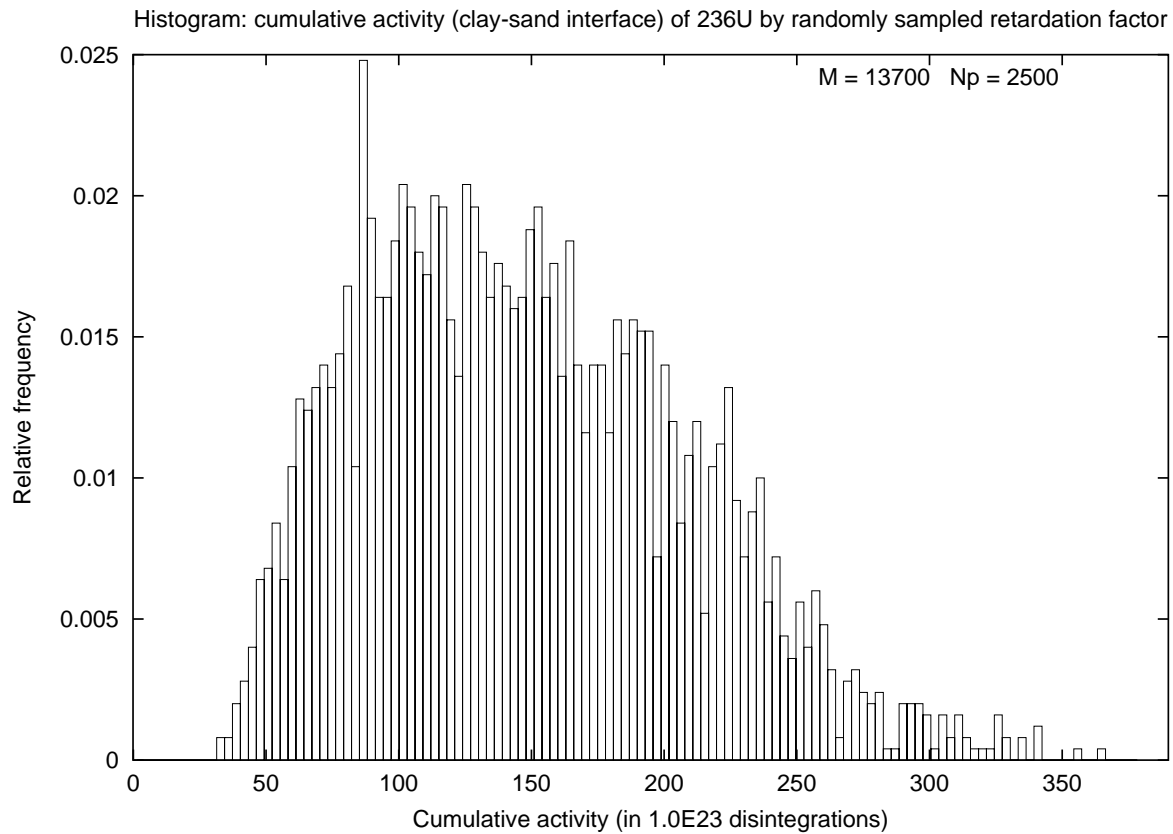


Figure 5.1: Relative frequency of cumulative activity near the interface between clay and sand layers.  $N_p$  values of retardation factors are sampled from log-normal pdfs. Here,  $iclass = 0$  and  $dclass = 20$ .  $M$  denotes the batch size.

```
-----  
Chain : 240Pu -> 236U -> 232Th (3D Model)  
Time Unit : year  
total simulation time : 3.0001E+07  
-----
```

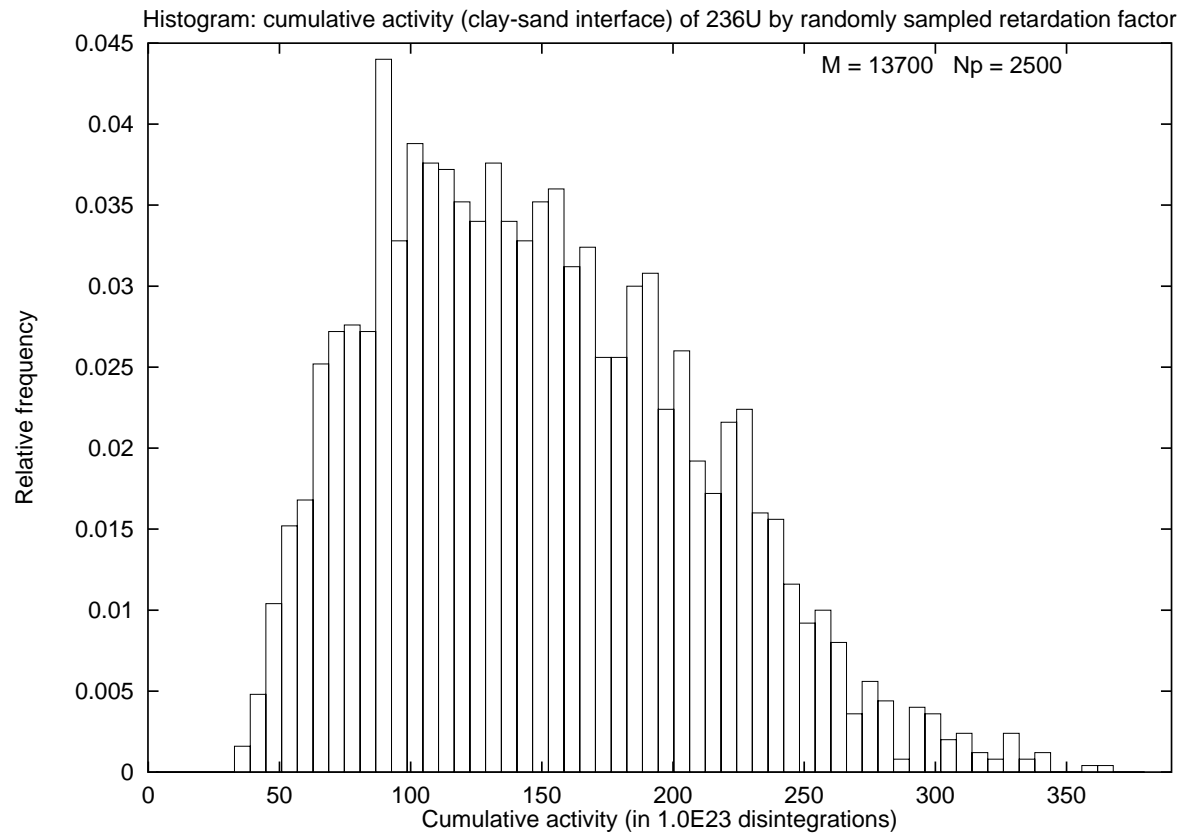


Figure 5.2: Relative frequency of cumulative activity near the interface between clay and sand layers.  $N_p$  values of retardation factors are sampled from log-normal pdfs. Here,  $iclass = 0$  and  $dclass = 40$ .  $M$  denotes the batch size.

$$CCDF(x) = 1 - \int_0^x pdf(u)du$$

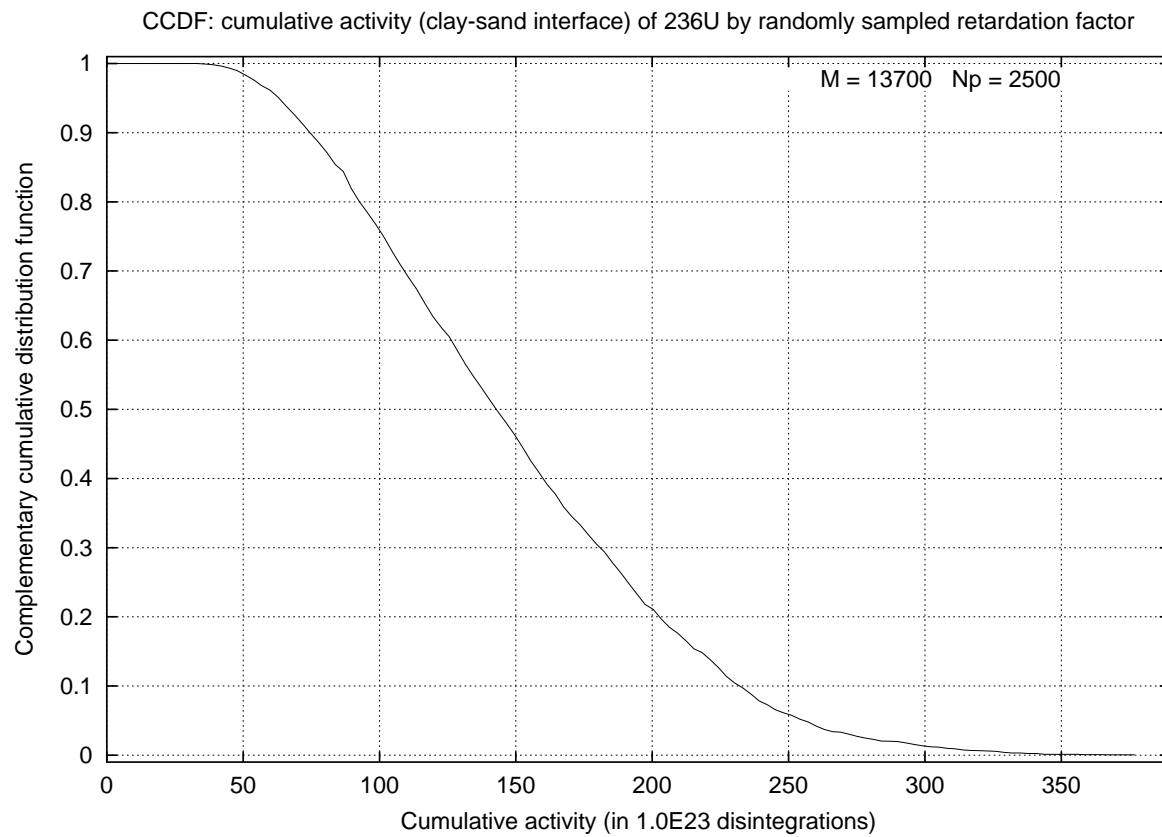


Figure 5.3: Complementary cumulative (activity) distribution function near the interface between clay and sand layers.  $N_p$  values of retardation factors are sampled from log-normal pdfs.  $M$  denotes the batch size.

```

i = 3425001 --> 10% of simulations --> time = 0h 1min 19sec
i = 6850001 --> 20% of simulations --> time = 0h 2min 43sec
i = 10275001 --> 30% of simulations --> time = 0h 4min 27sec
i = 13700001 --> 40% of simulations --> time = 0h 5min 50sec
i = 17125001 --> 50% of simulations --> time = 0h 7min 16sec
i = 20550001 --> 60% of simulations --> time = 0h 8min 36sec
i = 23975001 --> 70% of simulations --> time = 0h 9min 55sec
i = 27400001 --> 80% of simulations --> time = 0h 11min 14sec
i = 30825001 --> 90% of simulations --> time = 0h 12min 35sec

```

```

*** Number of rejected simulations ..... :          0

```

```

---> End of the simulations <---

```

```

idomb =          346 Lower exit(s) from domain

```

```

-----
*** RESULTS ***
-----

```

```

=== The Activity of Radionuclides ===

```

```

=====
***** Radionuclide number : 1 *****
=====

```

```

-----
** Cumulative score over plane 1 of coordinate z = -0.21000E+03
-----

```

```

* TRACKS score      : 0.00000000E+00
* Absolute error    : 0.00000000E+00
* Relative error    : 0.00000000E+00
* Variance .....   : 0.00000000E+00

```

```

=====
***** Radionuclide number : 2 *****
=====

```

```

-----
** Cumulative score over plane 1 of coordinate z = -0.21000E+03
-----

```

```

* TRACKS score      : 0.12825378E+03
* Absolute error    : 0.86220406E+00
* Relative error    : 0.67226407E-02

```

```
* Variance ..... : 0.94665777E+07
```

```
=====
```

```
* EXECUTION TIMES (IN SECONDS) *
```

```
=====
```

```
PRE-PROCESSING (COMPUTATION) ..: 0h  1min 33sec
```

```
MONTE CARLO SIMULATION ..... : 0h 14min 12sec
```

```
=====
```

```
T O T A L ..... : 0h 15min 46sec
```

Observe that, after  $3.0001 \times 10^7$  years, only the radionuclide  $^{236}\text{U}$  reaches the clay-sand interface. This could be explained by its long half-life time and its small retardation factor, compared to  $^{240}\text{Pu}$  (see Table 5.1). Because of its rather high retardation factor and its relatively small half-life time, the radionuclide  $^{240}\text{Pu}$  has completely decayed before going out of the clay layer. As for  $^{236}\text{U}$ , a transport simulation without parameter uncertainty indicates that, at 90 % confidence, the cumulative activity over the target plane is equal to  $(128.25 \pm 0.86) \times 10^{23}$  dpy, while a stochastic analysis (see Subsection 5.1.1) yields a mean value equal to  $(146.24 \pm 1.99) \times 10^{23}$  dpy.

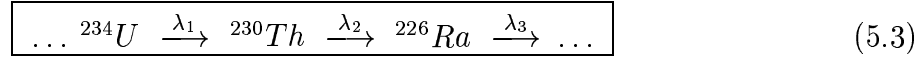
Table 5.1: Half-life times ( $T_{\frac{1}{2}}$ ) in years and retardation factors ( $R_i$ ) of  $^{240}\text{Pu}$  and  $^{236}\text{U}$  in the clay and the sand layer.

radionuclide	$T_{\frac{1}{2}}$	$R_i$	
		clay	sand
$^{240}\text{Pu}$	6 762	10 670	1 500
$^{236}\text{U}$	$2\,402 \times 10^4$	3 200	6

## 5.2 A deterministic 1D transport model

### 5.2.1 Description of the problem

We aim at computing the concentration  $C(z', t'; i)$  of radionuclides for the three-member radionuclide chain



in the infinite 1D medium  $\mathcal{R}_0^+ = \{z' ; 0 \leq z' < \infty\}$ . The PDEs (2.1)-(2.7) reduce to

$$\mathcal{L}_i C(z', t'; i) = \tilde{\mathcal{S}}(z', t'; i) \quad \text{in } \mathcal{R}_0^+ \quad \text{for } i=1, 2, 3 \quad (5.4)$$

with

$$\mathcal{L}_i = \left\{ \frac{\partial}{\partial t'} [\omega_i(z') \cdot] + \frac{\partial}{\partial z'} [q(z') \cdot] - \frac{\partial}{\partial z'} \left[ D(z') \frac{\partial}{\partial z'} \cdot \right] + \lambda_i \omega_i(z') \cdot \right\} \quad (5.5)$$

$$\tilde{\mathcal{S}}(z', t'; i) = S(z', t'; i) + \lambda_{i-1} \omega_{i-1}(z') C(z', t'; i-1) \quad (5.6)$$

$$\omega_i(z') = \theta(z') R_i(z') \quad (5.7)$$

$$D(z') = \theta(z') D_H(z') = \theta(z') (D_m(z') + \alpha \nu(z')) \quad (5.8)$$

where  $\lambda_0 = 0$ , while  $\nu$ ,  $D_m$  and  $\alpha$  denote the advection velocity, the molecular diffusion coefficient and the dispersivity, respectively. We assume that the porosity ( $\theta$ ), the retardation factors ( $R_i$ ) and the advection velocity ( $\nu$ ) are constant. Eqs. (5.4)-(5.6) may be written as:

$$\left\{ R_i \frac{\partial \cdot}{\partial t'} + \nu \frac{\partial \cdot}{\partial z'} - D_H \frac{\partial^2 \cdot}{\partial z'^2} + \lambda_i R_i \right\} C(z', t'; i) = \frac{1}{\theta} S(z', t'; i) + \lambda_{i-1} R_{i-1} C(z', t'; i-1) . \quad (5.9)$$

The initial and the boundary conditions are given by:

$$\begin{cases} C(z', 0; i) = 0 & \forall z' \geq 0, \quad \text{for } i = 2, 3 \\ C(z', 0; 1) = 0 & \forall z' > 0 \\ C(0, 0; 1) = C_1^0 & \text{arbitrarily chosen} \\ C(\infty, t'; i) = 0 & \forall t' > 0, \quad \text{for } i = 1, 2, 3 \end{cases} \quad (5.10)$$

We consider a pure  ${}^{234}\text{U}$  band release source located at  $z_s = 0$ , while  $t_s = 0$  and  $T = 10^4 \text{ yr}$ . Eq. (2.11) reads now

$$\begin{aligned} S(0, t'; i) &= C(0, t'; i) \\ &= B_i(t') [H(t') - H(t' - T)] \quad \forall t' \geq 0 \end{aligned} \quad (5.11)$$

where the coefficients  $b_{ji}$  of the Bateman equations (2.12) reduce to:

$$\left\{ \begin{array}{l} b_{11} = C_1^0 \\ b_{12} = \frac{\lambda_1 C_1^0}{\lambda_2 - \lambda_1} \\ b_{13} = \frac{\lambda_1 \lambda_2 C_1^0}{(\lambda_3 - \lambda_1)(\lambda_2 - \lambda_1)} \\ b_{22} = -\frac{\lambda_1 C_1^0}{\lambda_2 - \lambda_1} \\ b_{23} = -\frac{\lambda_1 \lambda_2 C_1^0}{(\lambda_3 - \lambda_2)(\lambda_2 - \lambda_1)} \\ b_{33} = -\frac{\lambda_1 \lambda_2 C_1^0}{(\lambda_3 - \lambda_1)(\lambda_2 - \lambda_3)} \end{array} \right. \quad (5.12)$$

The other transport parameters are specified in Table 5.2. The analytical solution of the problem under consideration has been obtained in [14]. The somewhat intricate formulas involved may also be found in [37, pp. 129-138].

Table 5.2: Half-life times ( $T_{\frac{1}{2}}$ , in *yr*), radioactive decay rates ( $\lambda_i$ , in  $yr^{-1}$ ), and retardation factors ( $R_i$ ) of radionuclides  $^{234}U$ ,  $^{230}Th$ , and  $^{226}Ra$ . Darcy velocity, porosity, molecular diffusion and dispersivity.

radionuclide	$T_{\frac{1}{2}}$	$\lambda_i$	$R_i$
$^{234}U$	$2.45 \times 10^5$	$2.83 \times 10^{-6}$	5
$^{230}Th$	$7.7 \times 10^4$	$9. \times 10^{-6}$	50
$^{226}Ra$	$1.6 \times 10^3$	$4.33 \times 10^{-4}$	20
groundwater Darcy velocity	$q = 2.27 \text{ m/yr}$		
porosity	$\theta = 0.35$		
molecular diffusion	$D_m = 0 \text{ m}^2/\text{yr}$		
dipersivity	$\alpha = 100 \text{ m}$		

The boundary condition (2.10) simplifies to

$$\left\{ -D(z') \frac{\partial}{\partial z'} C(z', t'; i) + q(z') C(z', t'; i) \right\}_{z'=z_u} = \beta(z_u, t'; i) \quad (5.13)$$

where the expressions of the radionuclide fluxes  $\beta(z_u, t'; i)$  are derived by substituting in (5.13) the analytical solutions for the concentrations  $C(z', t'; i)$ .

## 5.2.2 Numerical results

In all the experiments, the total number of simulations (*ntotsim*) is equal to  $10^6$ . We will report the normalized concentrations  $C(z', t'; i)/C_1^0$  and the integrated normalized concentrations  $\int_0^t (C(z', t'; i)/C_1^0) dt'$ , at three selected locations:

$$\left\{ \begin{array}{l} z = 100 \text{ m} \\ z = 1\,000 \text{ m} \\ z = 10\,000 \text{ m} \end{array} \right. \quad (5.14)$$

Three specific times have been defined:  $t_{0.1}$ ,  $t_{0.5}$  and  $t_{0.9}$ . They correspond to the times when the concentration of radionuclide  $^{234}\text{U}$  at  $z = 1\,000 \text{ m}$  reaches, respectively, 10 %, 50 % and 90 % of the initial boundary concentration. In other words,  $t_{0.1}$ ,  $t_{0.5}$  and  $t_{0.9}$  are defined by:

$$\left\{ \begin{array}{l} C(1, 0, t_{0.1}; 1)/C_1^0 = 0.1 \\ C(1, 0, t_{0.5}; 1)/C_1^0 = 0.5 \\ C(1, 0, t_{0.9}; 1)/C_1^0 = 0.9 \end{array} \right. \quad (5.15)$$

To get significant values for the daughter radionuclides, which are delayed strongly than the parent radionuclide  $^{234}\text{U}$ , normalized concentrations and time-integrated normalized concentrations at the selected locations have been compared for:

$$\left\{ \begin{array}{l} t_1 = 10 \times t_{0.1} = 4\,056.9 \\ t_2 = 10 \times t_{0.5} = 7\,024.7 \\ t_3 = 10 \times t_{0.9} = 12\,341.0 \end{array} \right. \quad (5.16)$$

We have observed that the results produced by TRACKS are in quite agreement with the analytical solutions. This will be displayed in the graphical representations to come. We

first give in Table 5.3 some numerical values of concentration and cumulative concentration at position  $z = 1\,000\,m$  and time  $t = t_2$ .

Table 5.3: 1D deterministic model. Comparison between TRACKS scores and analytical solutions (ANASOL) at  $z = 1\,000\,m$  and  $t = t_2$ . Instantaneous concentrations and cumulative concentrations.

	ANASOL		TRACKS	
	Cum. Conc.	Inst. Conc.	Cum. Conc.	Inst. Conc.
$^{234}\text{U}$	6185.4	0.9803	$6156.6 \pm 51.5$	$0.9775 \pm 0.0031$
$^{230}\text{Th}$	8.9451	$4.1312 \times 10^{-3}$	$9.01 \pm 0.91$	$4.117 \times 10^{-3} \pm 3.7 \times 10^{-5}$
$^{226}\text{Ra}$	0.4773	$2.439 \times 10^{-4}$	$0.4624 \pm 0.012$	$2.438 \times 10^{-4} \pm 3.1 \times 10^{-6}$

We show in Figs. 5.4-5.9 the normalized, instantaneous and cumulative, concentration profiles of radionuclides  $^{234}\text{U}$ ,  $^{230}\text{Th}$  and  $^{226}\text{Ra}$  at  $z = 10\,000\,m$  versus the time. As already mentioned, there is an excellent agreement between the TRACKS scores and the analytical solution. Figs 5.10-5.16 compare TRACKS scores with the analytical solution at positions  $z = 1\,000\,m$  and  $z = 100\,m$ . Now, for some values of time larger than the release time  $T = 10\,000$  years, there is a discrepancy between TRACKS results and the analytical values. TRACKS overestimates the concentrations. As we approach the source (compare  $z = 100\,m$  to  $z = 1\,000\,m$ ), the discrepancy increases but the general trend is correct. This overestimation, which is due to the treatment of the boundary condition (5.13), is discussed at length in [37, pp. 151-156]: after the band release time  $T = 10\,000$  years, an amount of radionuclides larger than predicted by the analytical solution is present and in the vicinity of the source. Observe that in the case of cumulative concentrations (Fig. 5.16), there is not any significant discrepancy. The (additional) amount of radionuclides accumulated after  $T = 10\,000$  years is small in comparison with the (additional) amount of radionuclides accumulated from  $t_s = 0$  year to  $T = 10\,000$  years.

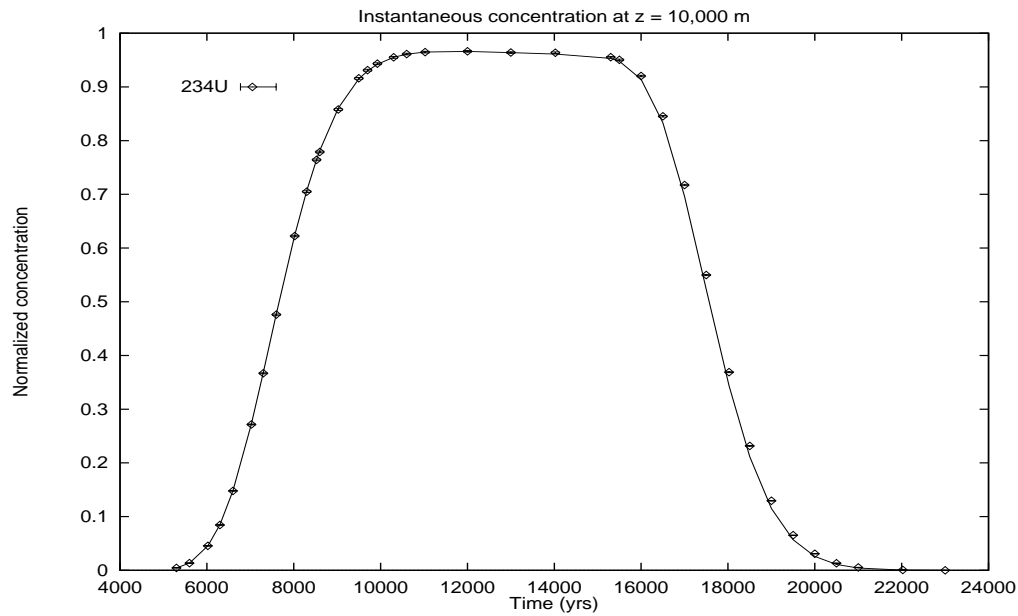


Figure 5.4: 1D deterministic model. Concentration profile for  $^{234}\text{U}$  at  $z = 10\,000\text{ m}$ . Diamonds ( $\diamond$ ) represent TRACKS results and error-bars denote the 90 % confidence interval. The solid line (—) displays the analytical solution.

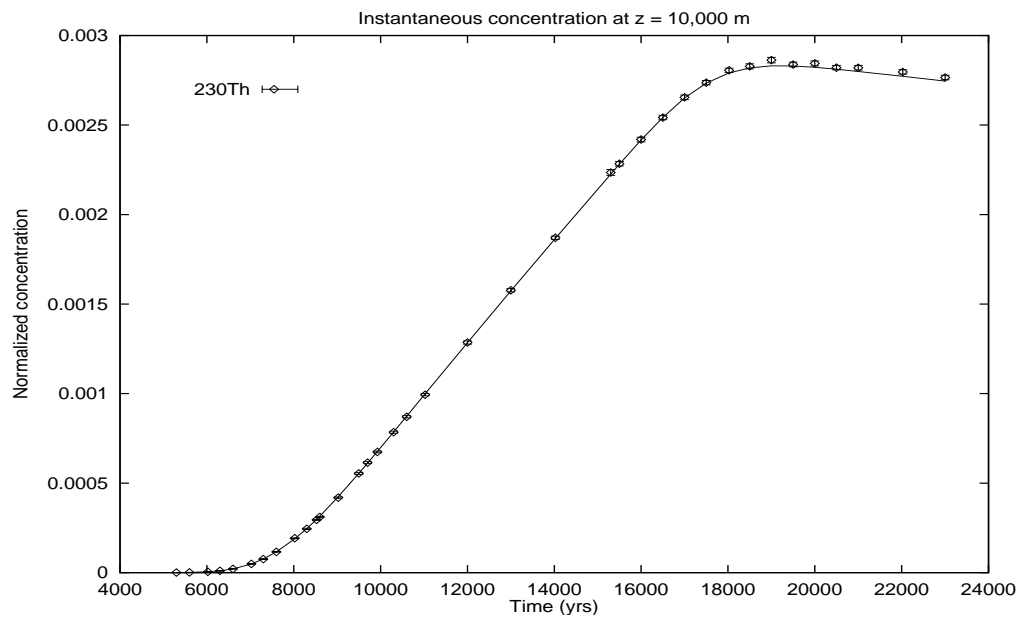


Figure 5.5: 1D deterministic model. Concentration profile for  $^{230}\text{Th}$  at  $z = 10\,000\text{ m}$ . Diamonds ( $\diamond$ ) represent TRACKS results and error-bars denote the 90 % confidence interval. The solid line (—) displays the analytical solution.

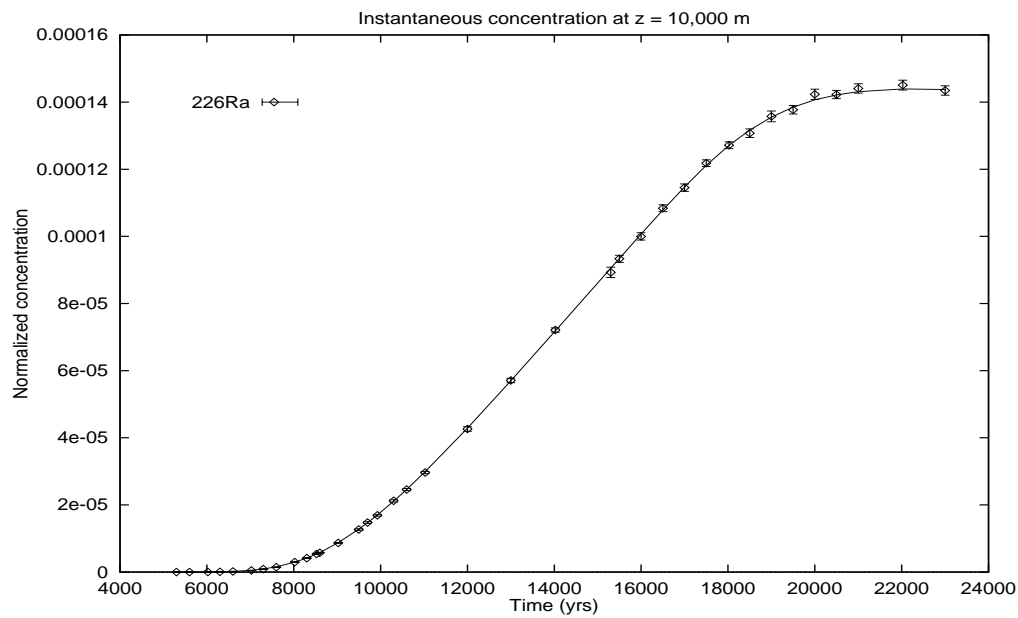


Figure 5.6: 1D deterministic model. Concentration profile for  $^{226}\text{Ra}$  at  $z = 10\,000\text{ m}$ . Diamonds ( $\diamond$ ) represent TRACKS results and error-bars denote the 90% confidence interval. The solid line (—) displays the analytical solution.

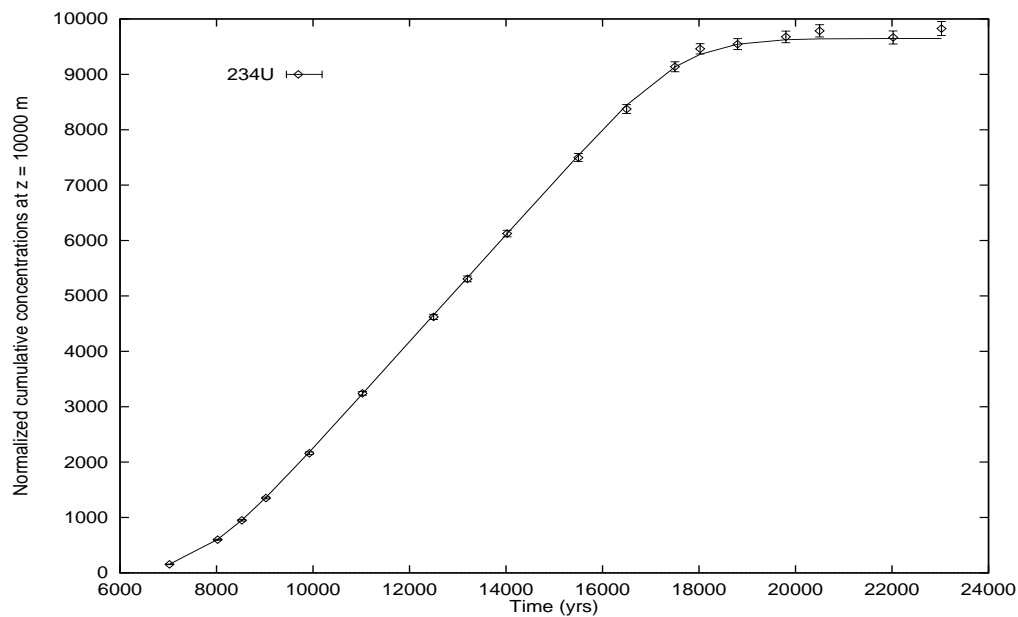


Figure 5.7: 1D deterministic model. Cumulative concentration profile for  $^{234}\text{U}$  at  $z = 10\,000\text{ m}$ . Diamonds ( $\diamond$ ) represent TRACKS results and error-bars denote the 90% confidence interval. The solid line (—) displays the analytical solution.

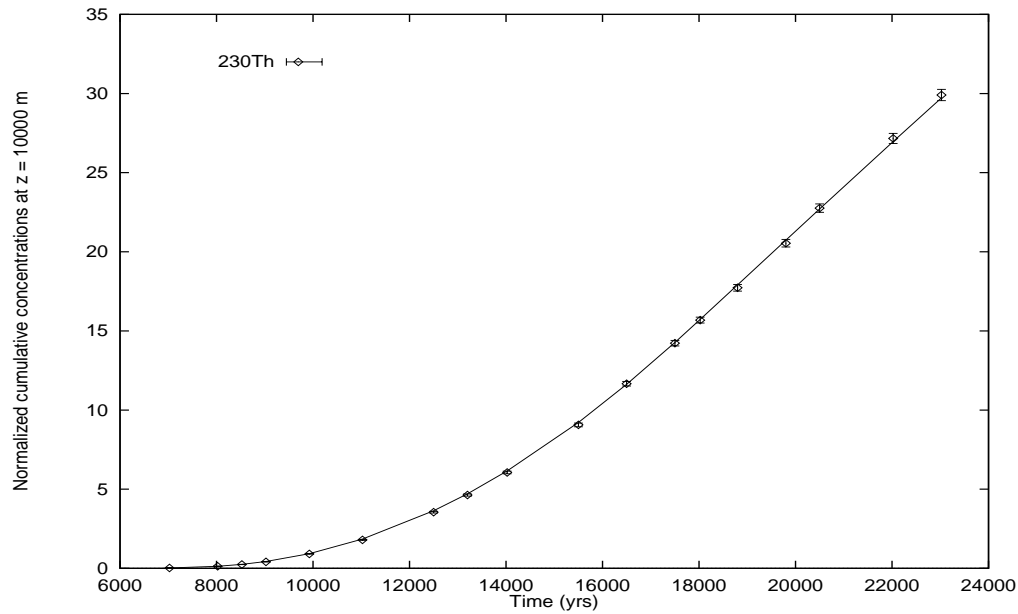


Figure 5.8: 1D deterministic model. Cumulative concentration profile for  $^{230}\text{Th}$  at  $z = 10000\text{ m}$ . Diamonds ( $\diamond$ ) represent TRACKS results and error-bars denote the 90 % confidence interval. The solid line (—) displays the analytical solution.

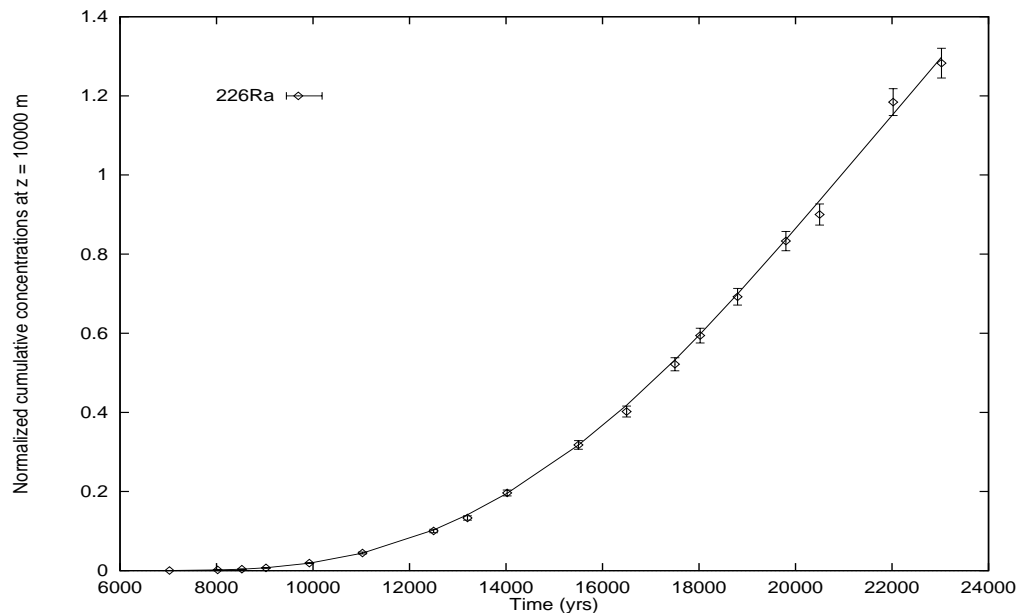


Figure 5.9: 1D deterministic model. Cumulative concentration profile for  $^{226}\text{Ra}$  at  $z = 10000\text{ m}$ . Diamonds ( $\diamond$ ) represent TRACKS results and error-bars denote the 90 % confidence interval. The solid line (—) displays the analytical solution.

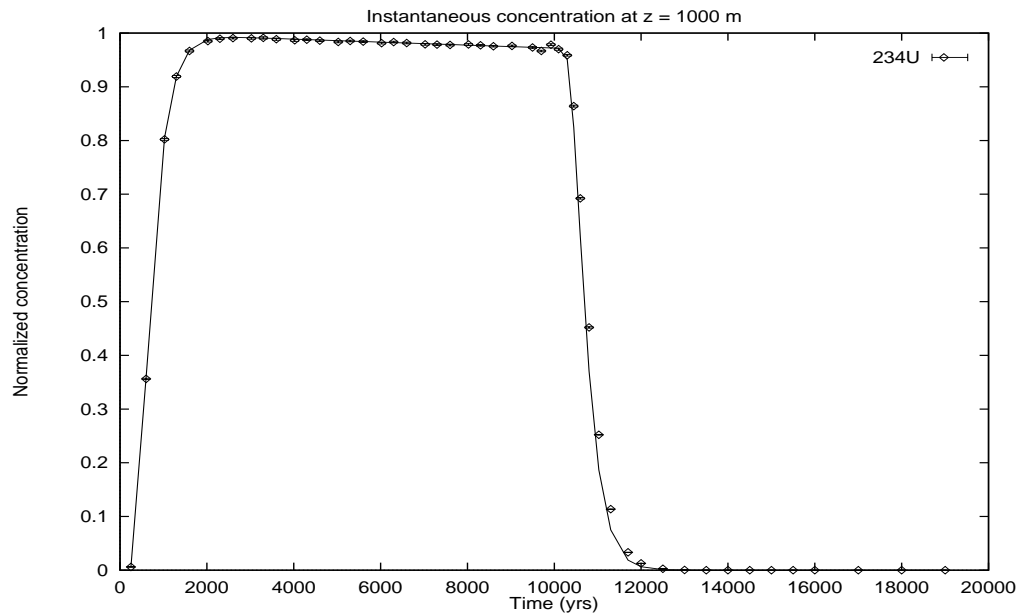


Figure 5.10: 1D deterministic model. Concentration profile for  $^{234}\text{U}$  at  $z = 1000 \text{ m}$ . Diamonds (◇) represent TRACKS results and error-bars denote the 90% confidence interval. The solid line (—) displays the analytical solution.

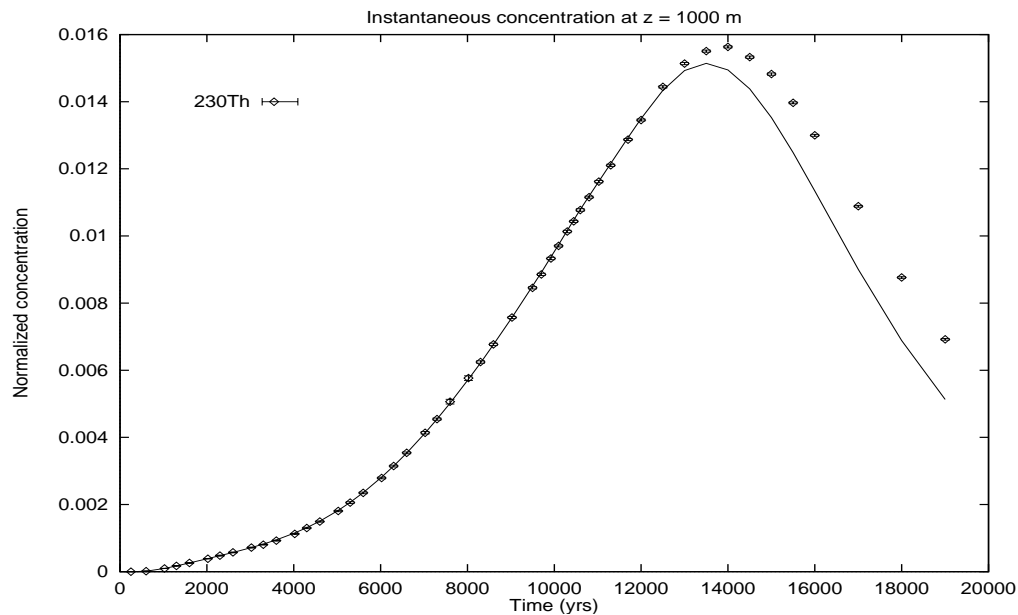


Figure 5.11: 1D deterministic model. Concentration profile for  $^{230}\text{Th}$  at  $z = 1000 \text{ m}$ . Diamonds (◇) represent TRACKS results and error-bars denote the 90% confidence interval. The solid line (—) displays the analytical solution.

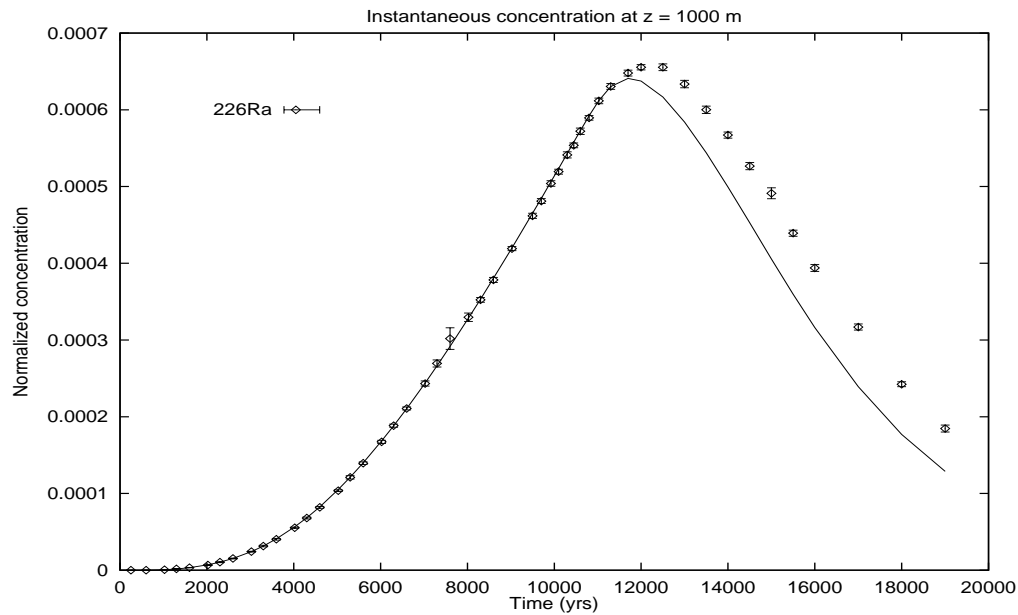


Figure 5.12: 1D deterministic model. Concentration profile for  $^{226}\text{Ra}$  at  $z = 1000\text{ m}$ . Diamonds ( $\diamond$ ) represent TRACKS results and error-bars denote the 90 % confidence interval. The solid line (—) displays the analytical solution.

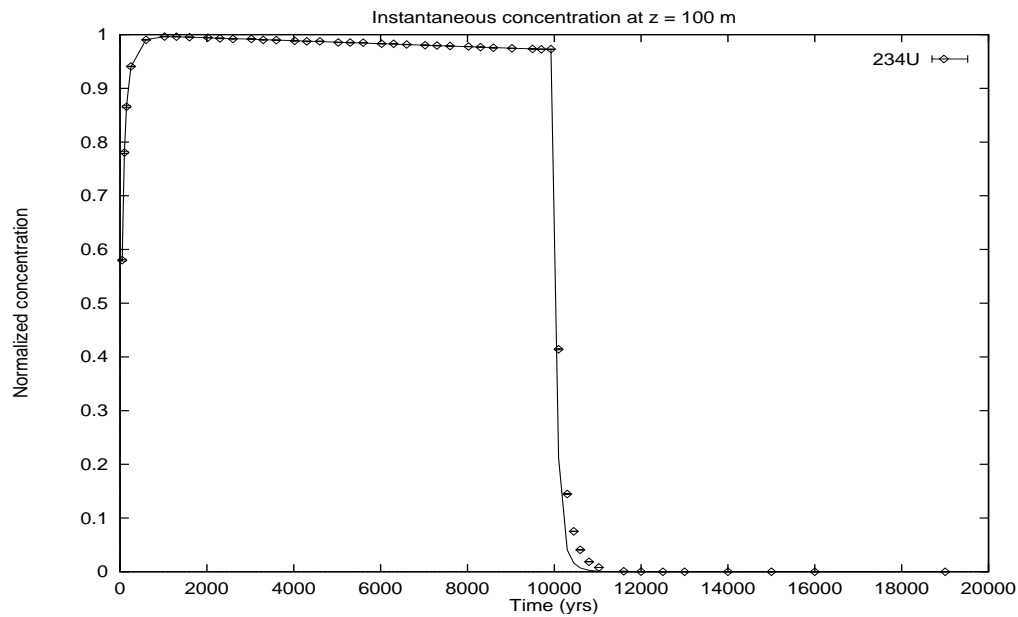


Figure 5.13: 1D deterministic model. Concentration profile for  $^{234}\text{U}$  at  $z = 100\text{ m}$ . Diamonds ( $\diamond$ ) represent TRACKS results and error-bars denote the 90 % confidence interval. The solid line (—) displays the analytical solution.

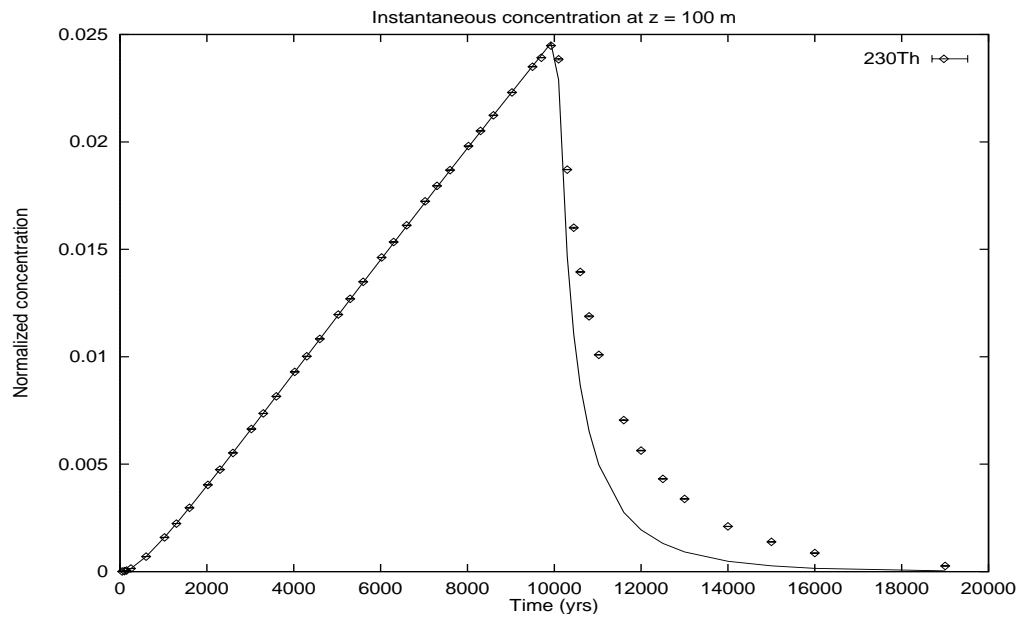


Figure 5.14: 1D deterministic model. Concentration profile for  $^{230}\text{Th}$  at  $z = 100$  m. Diamonds ( $\diamond$ ) represent TRACKS results and error-bars denote the 90% confidence interval. The solid line (—) displays the analytical solution.

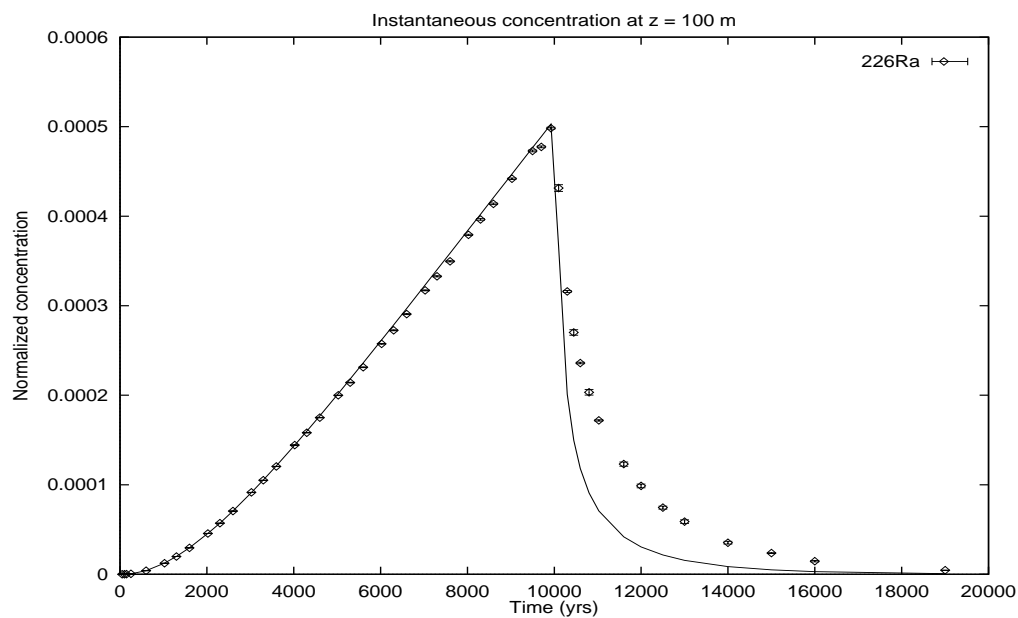


Figure 5.15: 1D deterministic model. Concentration profile for  $^{226}\text{Ra}$  at  $z = 100$  m. Diamonds ( $\diamond$ ) represent TRACKS results and error-bars denote the 90% confidence interval. The solid line (—) displays the analytical solution.

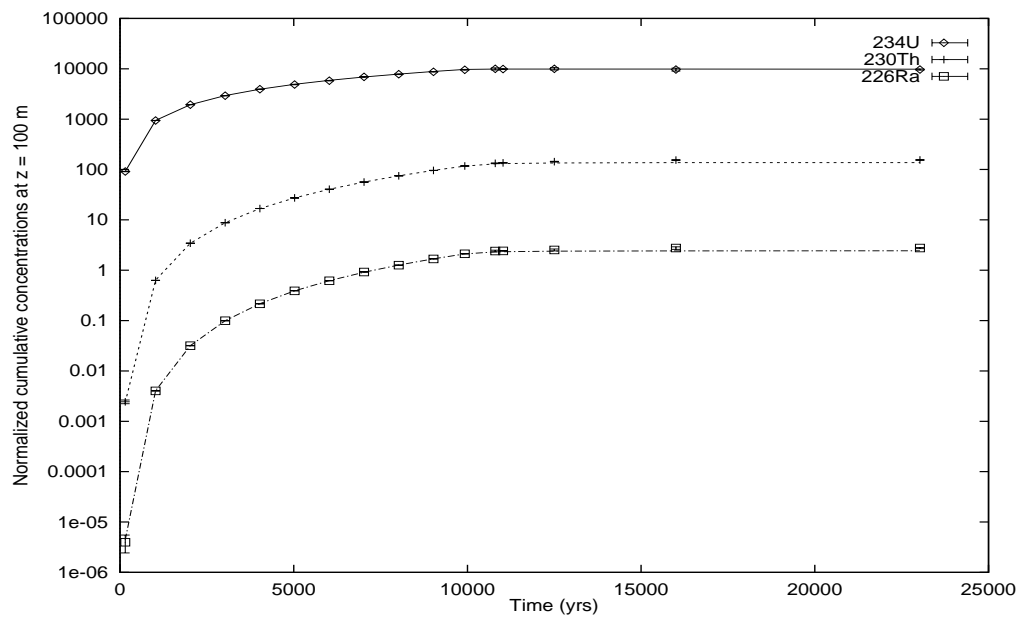


Figure 5.16: 1D deterministic model. Cumulative concentration profiles for  $^{234}\text{U}$ ,  $^{230}\text{Th}$  and  $^{226}\text{Ra}$  at  $z = 100\text{ m}$ . Comparison between TRACKS scores and the analytical solutions (solid line).

## Chapter 6

# Concluding remarks and Perspectives

---

---

The transport code TRACKS.1.0 has a modular structure as other modern packages like PORFLOW [1] and MT3DMS [45]. It is portable. It has been successfully tested on various platforms running under very different operating system:

- Silicon Graphics Origin 2000,
- SUN Enterprise 450 (Solaris),
- Compaq Digital GS140,
- PC Server under Linux (Gnu compiler: g77, gcc).

TRACKS uses some standard routines from BLAS and LAPACK. The elapse time could be estimated independently of the platform. Compared to earlier versions [34,32,37], the number of input variables is considerably limited. This has been made possible in exchange for intensive computations in order to select the “best” values of some parameters [37, pp. 175–199]. Moreover, the data are now introduced following the same steps as in the theoretical approach. One first provides data for the advection-dispersion equations, next data for the Monte Carlo simulation (or integral computation), and finally the data for the output. A sample input data file commented is provided. The presentation is made easier in such a way that one should not be an expert in transport modeling in order to run the code. TRACKS.1.0 has been validated in a series of deterministic test problems.

In transport calculations computer memory and computation time are very often a severe limitation for realistic three-dimensional simulations. Especially when the uncertainty of parameters enters into consideration. The theoretical approach followed in TRACKS allows to estimate the quantity of contaminants at selected physical and temporal positions, which considerably reduce the computation time, in comparison with classical

methods that handle all the nodal points in the whole geological domain. TRACKS.1.0 is able to compute in a reasonable time:

- In the case of one-dimensional models
  - cumulative concentration at selected points, until given times,
  - instantaneous concentration at selected points and times,
- In the case of three-dimensional models
  - cumulative concentration on selected planes, until given times,
  - cumulative concentration at selected points, until given times,
  - instantaneous concentration at selected points and times.

By cumulative concentration, we understand concentration integrated over a specified simulation time. The double randomization method implemented in TRACKS provides a flexible cheap tool for the treatment of uncertainty of parameters (here the retardation factor constant per layer).

Nevertheless, there are a few points that await further investigation.

- In subsequent versions of TRACKS, the solubility limits of radionuclides should be taken into account during the simulation as in PORFLOW [1].
- With TRACKS.1.0 the number of radionuclides in chains is limited to three. The treatment of more elements requires to generalize the source term: Eqs. (2.11)-(2.13).
- The present version of TRACKS works well only if all the three dispersivity constants ( $\alpha_L$ ,  $\alpha_{TH}$  and  $\alpha_{TV}$ ) coincide. In the case of anisotropic dispersion, an appropriate adjoint reference solution has been found and will be implemented in the future.
- Strong discontinuities in the variation of the transport parameters: this challenge requires to improve the theory initiated in [29].
- The treatment of more complex geometries in the geological medium.

---

# References

---

1. ACRI. PORFLOW: A software tool for multiphase fluid flow, heat and mass transport in fractured porous media. User's manual, Version 5.0. Analytic & Computational Research, Inc., California, 2002.
2. E. Anderson, Z. Bai, C. Bischof, S. Blackford, J. Demmel, J. Dongarra, J. Du Croz, A. Greenbaum, S. Hammarling, A. McKenney, and D. Sorensen. LAPACK Users' Guide, Third Edition, SIAM Publication, 1999.
3. K. Andersson and D. Galson, editors. *Safety Assessment of Radioactive Waste Repositories: GEOVAL-1990; Symposium on Validation of Geosphere Flow and Transport Models*. OECD/NEA/SKI, 1991.
4. J. Bear. *Dynamics of Fluids in Porous Media*. American Elsevier, New York, 1972.
5. J. Bear. *Hydraulics of Groundwater*. Mc Graw-Hill Series in Water Resources and Environmental Engineering, Mc Graw-Hill, 1979.
6. D.H. Bennett, A.L. James, T.E. McKone, and C.M. Oldenburg. On uncertainty in remediation analysis: variance propagation from subsurface transport to exposure modeling. *Reliability Engineering & System Safety*, 62(1-2):117-129, 1998.
7. L.S. Blackford, J. Demmel, J. Dongarra, I. Duff, S. Hammarling, G. Henry, M. Heroux, L. Kaufman, A. Lumsdaine, A. Petitet, R. Pozo, K. Remington, and R.C. Whaley. An updated set of Basic Linear Algebra Subprograms (BLAS). *ACM Transactions on Mathematical Software (TOMS)*, 28(2):135-151, June 2002.
8. R.D. Burnett and E.O. Frind. Simulation of contaminant transport in three dimensions. 2. Dimensionality effects. *Water Resources Research*, 23(4):695-705, April 1987.
9. G. Christakos. *Random field Models in Earth Sciences*. Academic Press, San Diego, London, 1992.
10. J.H. Cushman. *Dynamics of Fluids in Hierarchical Porous Media*. Academic Press, 1990.

11. G. Dagan. *Flow and Transport in Porous Formations*. Springer-Verlag, New York, 1989.
12. L. Devroye. *Non-Uniform Random Variate Generation*. Springer-Verlag, New York, 1986.
13. A. Erdélyi, W. Magnus, F. Oberhettinger, and F.G. Triconi. *Tables of Integral Transforms, Bateman Manuscript Project*. Mc Graw-Hill, 1954.
14. M. Foglia, F. Iwamoto, M. Harada, P.L. Chambré, and T.H. Pigford. The superposition solution of the transport of a radionuclide chain through a sorbing medium. *American Nuclear Society Transactions*, 33:384–386, 1979.
15. R.A. Freeze. A stochastic-conceptual analysis of one-dimensional groundwater flow in nonuniform homogeneous media. *Water Resources Research*, 11(5):725–741, 1975.
16. L.W. Gelhar. *Stochastic Subsurface Hydrology*. Prentice Hall, New Jersey, 1993.
17. L. Hardy and J. Marivoet. Sensitivity study on the local transport model of the neogene aquifer. Technical Report R-3468, SCK/CEN, October 2000.
18. M.H. Kalos and P.A. Whitlock. *Monte Carlo Methods, Volume 1: Basics*. John Wiley and sons, New-York, 1986.
19. F.J. Leij, T.H. Skaggs, and M.T. van Genuchten. Analytical solution for solute transport in three-dimensional semi-infinite porous media. *Water Resources Research*, 27(10):2719–2733, 1991.
20. I. Lux and L. Koblinger. *Monte Carlo Particle Transport Methods : Neutron and Photon Calculations*. CRC Press, 1991.
21. A. Mantoglou and J.L. Wilson. The turning band method for simulation of random fields using line generation by a spectral method. *Water Resources Research*, 18(5):1379–1394, 1982.
22. J. Marivoet. Updating of the Performance Assessment of Geological Disposal of High - Level and Medium Level wastes in the Boom clay formation. Technical Report BLG 634, SCK/CEN - NIRAS/ONDRAF, 1990.
23. Y. Meyus. Long-term performance studies of the geological disposal of conditioned high-level and long-lived radioactive waste. Technical Report R-3251, SCK/CEN - NIRAS/ONDRAF, February 1998.
24. G.A. Mikhaïlov. *Minimization of computational costs of non-analogue Monte Carlo methods*. World Scientific, Singapore, 1991.
25. OECD, editor. *Safety Assessment of Radioactive Waste Repositories: GEOVAL-94; Validation through model testing*, 1995.
26. PAGIS. Performance assessment of geological isolation systems for radioactive waste - disposal in clay formations. Technical Report CEN-EUR 11776 EN, Nuclear Science and Technology, Joint Research Center, 1988.
27. PAGIS. Performance assessment of geological isolation systems for radioactive waste - summary. Technical Report EUR 11775 EN, Nuclear Science and Technology, Joint Research Center, 1988.

28. W.H. Press, B.P. Flannery, S.A. Teukolsky, and W.T. Vetterling. *Numerical recipes, the art of scientific computing*. Cambridge university press, 1989.
29. K.K. Sabelfeld. *Monte Carlo Methods in Boundary Value Problems*. Springer Series in Computational Physics. Springer-Verlag, Berlin, 1991.
30. Safety Assessment and Feasibility Interim Report (SAFIR) 2. Technical Report, NIRAS/ONDRAF, December 2001.
31. M. Sahimi. *Flow and transport in porous media and fractured rock*. From classical methods to modern approaches. VCH, Weinheim, 1995.
32. X. Sillen, Y. Meyus, and J. Marivoet. Benchmark exercises project for the TRACKS code - Partial report - 1D tests, uniform parameter. Technical report, SCK/CEN, 1998.
33. O.F. Smidts. *Analyse probabiliste du risque du stockage de déchets radioactifs par la méthode des arbres d'événements continus*. PhD thesis, Université Libre de Bruxelles, Brussels, 1997.
34. O.F. Smidts. Point and surface estimations by a non-analog Monte Carlo simulation for the transport of radionuclide chains in porous media, *Monte Carlo Methods and Applications* 4:4 (1998), 289–318.
35. O.F. Smidts and J. Devooght. Analysis of the transport of radionuclide chains in a stochastic geological medium by a biased Monte Carlo simulation. *Nuclear Science and Engineering*, 129:224–245 + corrigendum, 130:164, 1998.
36. O.F. Smidts and J. Devooght. A non-analog Monte Carlo simulation of transport of radionuclides in a porous medium. *Mathematics and Computers in Simulation*, 47(2–5):461–472, 1998.
37. O.F. Smidts and J. Devooght. The TRACKS project - Activity report 1997 - 1999, Université Libre de Bruxelles, Brussels, 1999.
38. O.F. Smidts, J. Devooght, Y. Meyus, and J. Marivoet. Benchmark exercices project. Technical Report, Université Libre de Bruxelles, April 1998.
39. O.F. Smidts, and M. Magolu monga Made. Transport of radionuclides in porous media: A double randomization technique for the uncertainty analysis. Communication presented at the 3rd IMACS Seminar on Monte Carlo Methods (MCM-2001, Salzburg).
40. B.G.J. Thompson and B. Sagar. The development and application of integrated procedures for post-closure assessment, based upon Monte Carlo simulation: the probabilistic systems assessment (PSA) approach. *Reliability Engineering & System Safety*, 42:125–160, 1993.
41. A.F.B. Tompson. Numerical simulation of chemical migration in physically and chemically heterogeneous porous media. *Water Resources Research*, 29(11):3709–3726, 1993.
42. A.F.B. Tompson, R. Ababou, and L.W. Gelhar. Implementation of the three-dimensional turning bands random field generator. *Water Resources Research*, 25(10):2227–2243, 1989.

43. WIPP (Waste Isolation Pilot Plant). Preliminary performance assessment for the waste isolation pilot plant. Technical Report SAND92-0700, Sandia National Laboratories, 1992.
44. Yucca Mountain Project. Viability assessment of a repository at Yucca Mountain. Technical Report USDOE/RW-0508, US Department of Energy, USA, 1998.
45. C. Zheng and P.P. Wang. MT3DMS: A modular three-dimensional multispecies transport model for simulation of advection, dispersion, and chemical reactions of contaminants in groundwater systems. Documentation and user's guide. Contract Report SERDP-99-1, U.S. Army Engineer Research and Development Center, Vicksburg, MS, 1999.

## Appendix A

# The adjoint reference equation parameters

---

The choice of the adjoint reference equations (2.14)-(2.15) strongly influence the convergence of Neumann series of the form (2.30)-(2.31) or the truncated form (2.36). A bad choice may even lead to divergent series [29]. For the purposes of efficiency of the Monte Carlo simulation, the values of the parameters  $\omega_j^*(\bar{r}')$ ,  $\bar{q}^*(\bar{r}')$  and  $\bar{D}^*(\bar{r}')$ , should be chosen with care. The ideal would be that the selected values coincide with the true values of the geological medium. In such a situation the correction terms (see Eq. 2.23)

$$\begin{cases} \Delta\omega_j &= \omega_j(\bar{r}') - \omega_j^* \\ \Delta\bar{q} &= \bar{q}(\bar{r}') - \bar{q}^* \\ \Delta\bar{D} &= \bar{D}(\bar{r}') - \bar{D}^* \end{cases} \quad (\text{A.1})$$

vanish. The more the parameters  $\omega_j^*(\bar{r}')$ ,  $\bar{q}^*(\bar{r}')$  and  $\bar{D}^*(\bar{r}')$  are close to the parameters  $\omega_j(\bar{r}')$ ,  $\bar{q}(\bar{r}')$  and  $\bar{D}(\bar{r}')$ , respectively, the faster the convergence (if any) of the Neumann series involved. The other side of the coin is that the corresponding adjoint reference problem could be very difficult, if not impossible, to solve analytically. A compromise has been proposed in [33,35,36]:

1. Define the trajectory  $\bar{g}(|t' - t|, \bar{r})$  of a radionuclide located at  $\bar{r}$  at time  $t$ , moving with the stream in a velocity field  $\bar{v}$  by

$$\begin{cases} \frac{d\bar{g}(|t' - t|, \bar{r})}{dt'} = \bar{v}(\bar{g}(|t' - t|, \bar{r})) \\ \bar{g}(0, \bar{r}) = \bar{r} \end{cases} \quad (\text{A.2})$$

with

$$\bar{v}(\bar{r}'') = -\frac{\langle \bar{q}(\bar{r}'') \rangle}{\omega_j(\bar{r}'')} \quad (\text{A.3})$$

where  $\langle \bar{q}(\bar{r}'') \rangle$  denotes the mean Darcy velocity at position  $\bar{r}''$ .

2. Solve (A.2)-(A.3) for  $\bar{g}(|t' - t|, \bar{r})$ .

3. Set

$$\begin{cases} \omega_j^*(\bar{r}') &= \omega_j(\bar{g}(|t' - t|, \bar{r})) \\ \bar{q}^*(\bar{r}') &= \bar{q}(\bar{g}(|t' - t|, \bar{r})) \\ \bar{D}^*(\bar{r}') &= \bar{D}(\bar{g}(|t' - t|, \bar{r})) \end{cases} \quad (\text{A.4})$$

The minus sign in Eq. (A.3) reflects the simulation strategy. In the integral formulation, the particle goes from  $\bar{r}'$  at time  $t'$  to  $\bar{r}$  at time  $t$ . The trajectory defined by (A.2) starts from  $\bar{r}$  and tries to go back to  $\bar{r}'$  (the ideal backward position).

At each step of the simulation, the correction terms take into account the differences between the trajectory followed by the random walker and the approximate mean displacement foreseen by  $\bar{g}(|t' - t|, \bar{r})$ .

## Remark

It emerges from numerical experiments that, if the total number of simulations is large enough, it is efficient to simply set the values of the reference equations parameters equal to the mean values of the parameters involved, in each layer, especially when the parameters of the original equations are constant per layer.

## Appendix B

# Examples of adjoint reference solution

---

The source term  $Q$  and the kernels  $K_{\mathcal{D}}$ ,  $K_{\mathcal{S}}$ ,  $K^{j \rightarrow i}$ , and  $K^{j \rightarrow j}$  involved in the integral formulation of the transport problem depend on the explicit expression of the adjoint reference solution  $C^*(\bar{r}', t'; j | \bar{r}, t; j)$ . In TRACKS, simple analytical adjoint reference solutions are obtained by assuming that:

- (a) the transport parameters are constant in the whole domain,
- (b)  $\bar{D}$  is a constant diagonal tensor, say  $\bar{D} = D \bar{I}$  where  $\bar{I}$  stands for the identity tensor,
- (c)  $\bar{q} = q \bar{I}_z$  where  $\bar{I}_z$  denotes the unit vector along the z-axis.

This gives:

$$C^*(\bar{r}', t'; j | \bar{r}, t; j) = \begin{cases} \frac{\exp\{-A - \lambda_j(t - t')\}}{\omega_j(\bar{r}) \left(4\pi \int_0^{t-t'} D_{e_j} [g(s, \bar{r})] ds\right)^{\frac{3}{2}}} & t > t' \\ 0 & t \leq t' \end{cases} \quad (\text{B.1})$$

with

$$A = \frac{(x' - x)^2 + (y' - y)^2 + \left(z' - z + \int_0^{t-t'} q_{e_j} [g(s, \bar{r})] ds\right)^2}{4 \int_0^{t-t'} D_{e_j} [g(s, \bar{r})] ds} \quad (\text{B.2})$$

where  $\bar{r} = (x, y, z)$ ,  $\bar{r}' = (x', y', z')$ , while

$$\begin{cases} q_{e_j} [g(s, \bar{r})] &= \frac{q [g(s, \bar{r})]}{\omega_j [g(s, \bar{r})]} \\ D_{e_j} [g(s, \bar{r})] &= \frac{D [g(s, \bar{r})]}{\omega_j [g(s, \bar{r})]} \end{cases} \quad (\text{B.3})$$

From the definition of  $Q$ ,  $K_{\mathcal{D}}$ ,  $K_S$ , and  $K^{j \rightarrow i}$  (see Section 2.2), the following simple nonnegative kernels  $\tilde{K}_{\mathcal{D}}$ ,  $\tilde{K}_S$ ,  $\tilde{K}^{j \rightarrow i}$ , and source term  $\tilde{Q}$  have been proposed in [33,35] and are used in TRACKS:

$$\tilde{Q}(\bar{r}, t; j) = \frac{s_j}{T_0} (T_0 - \tau_s) \frac{e^{-\lambda_j \tau_s}}{\tilde{\omega}_j (4\pi \tilde{D}_{e_j} \tau_s)^{\frac{3}{2}}} \exp \left\{ -\frac{(x - x_s)^2 + (y - y_s)^2 + (z_s - z + \tilde{q}_{e_j} \tau_s)^2}{4 \tilde{D}_{e_j} \tau_s} \right\}$$

$$\tilde{K}_{\mathcal{D}}(\bar{r}', t'; j | \bar{r}, t; j) = \frac{1}{T_0} \frac{e^{-\lambda_j \tau}}{(4\pi \tilde{D}_{e_j} \tau)^{\frac{3}{2}}} \exp \left\{ -\frac{(x' - x)^2 + (y' - y)^2 + (z' - z + \tilde{q}_{e_j} \tau)^2}{4 \tilde{D}_{e_j} \tau} \right\}$$

$$\tilde{K}_S(\bar{r}', t'; j | \bar{r}, t; j) = \frac{T_0 - \tau}{T_0} |\hat{q}_{e_j}| \frac{e^{-\lambda_j \tau}}{(4\pi \hat{D}_{e_j} \tau)^{\frac{3}{2}}} \exp \left\{ -\frac{(x' - x)^2 + (y' - y)^2 + (z_u - z + \hat{q}_{e_j} \tau)^2}{4 \hat{D}_{e_j} \tau} \right\}$$

$$\tilde{K}^{j \rightarrow i}(\bar{r}', t'; j | \bar{r}, t; i) = \frac{\tilde{\omega}_j \lambda_i}{\tilde{\omega}_i T_0} (T_0 - \tau) \frac{e^{-\lambda_i \tau}}{(4\pi \tilde{D}_{e_i} \tau)^{\frac{3}{2}}} \exp \left\{ -\frac{(x' - x)^2 + (y' - y)^2 + (z' - z + \tilde{q}_{e_i} \tau)^2}{4 \tilde{D}_{e_i} \tau} \right\}$$

with

$$\begin{cases} \tau &= t - t' \\ \tau_s &= t - t_s \\ s_j &= \text{intensity of radionuclide } j \text{ in the source term} \end{cases}$$

while

- $\bar{r}_s = (x_s, y_s, z_s)$  denotes (the center of) a, possibly auxiliary, source

$$S(\bar{r}', t'; j) = s_j \delta(\bar{r}' - \bar{r}_s) \delta(t' - t_s) ;$$

- $\tilde{K}^{j \rightarrow i}$  has been obtained by assuming a linear radionuclide chain, say,  $j = i - 1$  and  $p(j \rightarrow i) = \lambda_j$ ;

- $\tilde{\omega}_j$ ,  $\tilde{q}$  and  $\tilde{D}$  stand for the mean value of, respectively,  $\omega_j(\bar{r}')$ ,  $q(\bar{r}')$  and  $D(\bar{r}')$  in the layer involved, while  $\tilde{q}_{e_j} = \tilde{q}/\tilde{\omega}_j$  and  $\tilde{D}_{e_j} = \tilde{D}/\tilde{\omega}_j$ ;
- $\hat{D}_{e_j} = \tilde{D}_{e_j}$ ,  $\hat{q}_{e_j} = \hat{q}_j/\tilde{\omega}_j$  where, for efficiency purposes,  $\hat{q}_{e_j}$  is chosen according to the following rule of thumb [33, pp. 289-297]:

$$\min \left\{ z_u; z_s + \tilde{q}_{e_j} T_0 - \sqrt{6 \tilde{D}_{e_j} T_0} \right\} \leq z_u - |\hat{q}_{e_j}| T_0 \leq \min \left\{ z_u; z_s + \tilde{q}_{e_j} T_0 + \sqrt{6 \tilde{D}_{e_j} T_0} \right\}$$

where  $z = z_u$  is the coordinate of the upper surface along the z-axis. Once  $\hat{q}_{e_j}$  is determined, it is easy to compute  $\hat{q}_j$  from the relation  $\hat{q}_{e_j} = \hat{q}_j/\tilde{\omega}_j$ .

## Appendix C

# Monte Carlo calculation of integrals

Let  $\Omega$  denote a given domain in a  $d$ -dimensional space,  $g(\vec{r})$  stand for a nonnegative function defined in  $\Omega$ , while  $p(\vec{r})$  denote a probability density function, say:

$$\begin{cases} p(\vec{r}) \geq 0 & \forall \vec{r} \in \Omega \\ \int_{\Omega} p(\vec{r}') d\vec{r}' = 1 \end{cases} \quad (\text{C.1})$$

The integral

$$J = \int_{\Omega} g(\vec{r}') d\vec{r}' \quad (\text{C.2})$$

may be rewritten as:

$$J = \int_{\Omega} f(\vec{r}') p(\vec{r}') d\vec{r}' \quad (\text{C.3})$$

with

$$f(\vec{r}') = \begin{cases} \frac{g(\vec{r}')}{p(\vec{r}')} & \forall \vec{r}' \text{ such that } p(\vec{r}') > 0 \\ 0 & \text{otherwise} \end{cases} \quad (\text{C.4})$$

Assume that the points  $\bar{r}_i$ ,  $i = 1, 2, \dots, N$ , are sampled in  $\Omega$  from the probability density function  $p(\bar{r})$ . Define

$$\tilde{J}_N = \frac{1}{N} \sum_{i=1}^N f(\bar{r}_i) \quad (\text{C.5})$$

Then from the Strong Law of Large Numbers it follows that

$$\lim_{N \rightarrow \infty} P \left( J - \varepsilon \leq \tilde{J}_N \leq J + \varepsilon \right) = 1 \quad \forall \varepsilon > 0, \quad (\text{C.6})$$

say, the probability that the sample average  $\tilde{J}_N$  is close to the target integral  $J$  can be made arbitrarily close to 1 provided that one takes sufficiently large samples (see, e.g., [18]):  $\tilde{J}_N$  is an unbiased estimate of  $J$ . The Central Limit Theorem gives

$$\lim_{N \rightarrow \infty} P \left( \left| \tilde{J}_N - J \right| \leq \alpha \frac{\sigma_J}{\sqrt{N}} \right) = \frac{1}{\sqrt{2\pi}} \int_{-\alpha}^{+\alpha} e^{-\frac{u^2}{2}} du \quad (\text{C.7})$$

where the standard deviation (square root of the variance)

$$\sigma_J = \int_{\Omega} (f(\bar{r}') - J)^2 p(\bar{r}') d\bar{r}' = \int_{\Omega} (f(\bar{r}'))^2 p(\bar{r}') d\bar{r}' - J^2 \quad (\text{C.8})$$

is replaced in practice by the following unbiased estimate:

$$s_N = \sqrt{\frac{1}{N-1} \left[ \sum_{i=1}^N (f(\bar{r}_i))^2 - \frac{1}{N} \left( \sum_{i=1}^N f(\bar{r}_i) \right)^2 \right]} \quad (\text{C.9})$$

The quantity

$$\boxed{\frac{s_N}{\sqrt{N}} \approx \frac{\sigma_J}{\sqrt{N}}} \quad (\text{C.10})$$

is defined as the *statistical uncertainty*. By means of statistical tables, (C.7) with  $\alpha = 1.645$  tells us that, at 90% level of probability, the actual value of  $J$  belongs to the interval

$$\boxed{\left[ \tilde{J}_N - \frac{1.645 s_N}{\sqrt{N}}, \tilde{J}_N + \frac{1.645 s_N}{\sqrt{N}} \right]} \quad (\text{C.11})$$

In order to reduce the error, which is  $\mathcal{O}(N^{-1/2})$ , one can either increase  $N$  or resort to some appropriate variance reduction technique [18,20]. The outstanding advantage of Monte Carlo method over classical numerical methods is that its rate of convergence is independent of the space dimension  $d$ .

## Appendix D

# Double randomization technique

---

## D.1 Brief description

Any particle tracking method could be combined with the random sampling of uncertain parameters according to given pdfs. Such an analysis which consists in using two types of random sampling (one for the parameters and one for the transport simulation) in an efficient way is known as the *double randomization technique*. In practice, pdfs are deduced in PRA studies by experts judgments and/or by extrapolation from available experimental data [22,26,43]. In TRACKS, only the effects of the uncertainties on the value of the retardation factor are considered:

- $N_v$  values of the retardation factor are sampled;
- for each sampling, the corresponding Monte Carlo score  $\tilde{J}_N$  is computed;
- the mean  $\hat{J}_{N_v}$  of the  $N_v$  Monte Carlo scores  $\tilde{J}_N$  is computed, say,

$$\hat{J}_{N_v} = \frac{1}{N_v} \sum_{i=1}^{N_v} \tilde{J}_N(\bar{R}^{(i)}) \quad (\text{D.1})$$

with

$$\begin{aligned}\bar{R}^{(i)} &= \left( \bar{R}_1^{(i)}, \bar{R}_2^{(i)}, \dots, \bar{R}_{N_r}^{(i)} \right) \\ \bar{R}_j^{(i)} &= \left\{ R_{j,l}^{(i)} \right\}_{l=1, 2, \dots, \text{nlayer}}\end{aligned}\tag{D.2}$$

where  $R_{j,l}^{(i)}$  denotes the  $i$ th sampled retardation factor of radionuclide  $j$  in the layer  $l$ .

- the distribution of the Monte Carlo scores  $\tilde{J}_N(\bar{R}^{(i)})$  observed as well as their frequency is presented in the form of a histogram.

The variance  $\sigma_{\hat{J}}$  associated to the mean score  $\hat{J}_{N_v}$  is given by the relation:

$$\sigma_{\hat{J}} = \frac{\sigma_{p.t.}^2}{N} + \sigma_{u.p.}^2\tag{D.3}$$

where  $\sigma_{p.t.}^2$  is the variance associated to the particle trackings while  $\sigma_{u.p.}^2$  denotes the variance associated to the uncertainty on the score due to the uncertainty on the value of the parameters sampled. The batch size  $N$ , which denotes the number of particle trackings per sampling of the uncertain parameter, should be chosen in such a way that  $\sigma_{p.t.}^2/N$  is negligible in comparison with  $\sigma_{u.p.}^2$ . The optimal value of  $N$  could be estimated by increasing the value of  $N$  until  $\sigma_{\hat{J}}$  is no more affected by the value of  $N$ . In the case where the analytical solution of the transport problem is available, it is easy to compute  $\sigma_{u.p.}^2$  because  $\sigma_{p.t.}^2 = 0$ .

## D.2 Implementation in TRACKS

During the pre-processing step, the transition probabilities of the random walkers from different parts of the geological domain are computed. These values are stored for different values of time  $t'$  and depth  $z'$ . In the case where uncertainties of retardation factors are taken into consideration, the transition probabilities are also computed for three values of the retardation factor:

1.  $\langle R \rangle$ , the mean retardation factor,
2.  $\langle R \rangle - \sigma_R$ ,
3.  $\langle R \rangle + \sigma_R$ ,

where  $\sigma_R$  denotes the standard deviation of the retardation factor distribution. During the simulation, the transition probabilities associated to a sampled retardation factor are interpolated from the transition probabilities associated to  $\langle R \rangle$ ,  $\langle R \rangle - \sigma_R$  and  $\langle R \rangle + \sigma_R$ .

### D.3 Sampling of retardation factors

Our analysis is restricted to the model where the retardation factor  $R$  is constant per geological layer. The uncertainty on  $R$  is represented by a pdf from which random values are sampled. By definition of the retardation factor, we have for the  $j$ th element of a radionuclide chain:

$$\boxed{R_j = 1 + \frac{\rho_b}{\theta} K_d^{(j)}} \quad (\text{D.4})$$

where

$$\left\{ \begin{array}{l} \theta \quad : \quad \text{the porosity} \\ \rho_b \quad : \quad \text{the bulk density of the solid phase} \\ K_d^{(j)} \quad : \quad \text{the distribution (or partition) coefficient} \end{array} \right. \quad (\text{D.5})$$

$K_d^{(j)}$  is highly dependent on the composition of the porous medium, the type of the radionuclide and on a series of chemical conditions like pH, ... The coefficient  $K_d^{(j)}$  is mainly responsible for the uncertainty on the retardation factor. Some measurements of  $K_d^{(j)}$  for specific sites could be found in the literature, see, e.g., [26,22]. In TRACKS, we assume a log-normal (natural logarithm) distributions for  $K_d^{(j)}$ . The following pdf is used:

$$\boxed{f(R_j) = \frac{1}{\sqrt{2\pi} \sigma_j R_j} \exp\left(-\frac{(\ln R_j - \mu_j)^2}{2 \sigma_j^2}\right)} \quad (\text{D.6})$$

where  $\mu_j$  and  $\sigma_j$  stand for the mean and the standard deviation of the log-normal pdf involved. In Table D.1, we report values of the statistical parameters  $\mu_i$  and  $\sigma_i$  for a geological medium made of clay and sand.

Table D.1: Means ( $\mu$ ) and standard deviations ( $\sigma$ ) of the log-normal pdfs for the retardation factors of  $^{240}\text{Pu}$  and  $^{236}\text{U}$  in clay and sand.

	clay		sand	
	$\mu$	$\sigma$	$\mu$	$\sigma$
$^{240}\text{Pu}$	9.19	0.4	6.99	0.8
$^{236}\text{U}$	7.99	0.4	1.48	0.8

The mean values of the retardation factors are given by:

$$\boxed{\langle R \rangle = \exp\left(\mu + \frac{\sigma^2}{2}\right)} \quad (\text{D.7})$$